The effect of geometrical presplit blast parameters on presplit quality at Kuusilampi open pit mine

Matti Islander

School of Engineering

Thesis submitted for examination for the degree of Master of Science in Technology.

Espoo 24.9.2021

Supervisor

Prof. Mikael Rinne

Advisor

M.Sc. (Tech.) Juho Torvi

Aalto University
School of Engineering

Aalto University
School of Engineering

Aalto University, P.O. BOX 11000, 00076 AALTO
www.aalto.fi
Abstract of the master's thesis

Author Matti Islander

Title The effect of geometrical presplit blast parameters on presplit quality at Kuusilampi open pit mine

Degree programme Master's Programme in European Mining, Minerals and Environmental Programme (EMMEP)

Major European mining course (EMC) **Code of major** ENG3077

Supervisor Prof. Mikael Rinne

Advisor M.Sc. (Tech.) Juho Torvi

Date 24.9.2021 **Number of pages** 81+7 **Language** English

Abstract

In open pit mines, controlled blasting methods are used to reduce blast damage on the remaining rock mass, which increases the safety and economy of the operation. Presplitting is one of the most common controlled blasting methods used to achieve stable pit walls. The aim of this thesis is to discover suitable presplitting designs for the different areas of the Kuusilampi open pit mine. Furthermore, this thesis studied the connection between a geotechnical block model's rock mass quality estimates and the result of presplit blasting. This study has been conducted to improve the slope stability at the mine by improving the presplit blasting practices.

This thesis consists of a historical review of presplitting practice at Kuusilampi open pit and presplitting tests. Presplitting tests were conducted with smaller diameter explosive cartridge than previously used and different borehole diameters, inclinations and spacings. The results were estimated based on visual inspection of the presplit faces and by calculating the half core factor, and over- and underbreak in cubic meters per square meter of presplit face.

In this thesis, no major differences were found in the presplit results with the different presplit parameters. Furthermore, it was concluded that the greatest improvements to the slope stability at the Kuusilampi open pit could be achieved with modifications to the buffer row. Additionally, no connection was found between the rock mass quality estimate of the geotechnical block model and presplitting results, because the geotechnical block model was found to lack sufficient accuracy and resolution to represent the rock mass quality accurately.

Keywords Presplitting, Presplit blasting, Controlled blasting, Pit slope stability

Preface

First of all, I want to thank Juho Torvi and Terrafame for giving me this thesis opportunity despite of the challenges created by the Covid-19 pandemic. Furthermore, I want to thank Professor Mikael Rinne and my instructor Juho Torvi for their guidance on this thesis. I also want to thank Aki Ullgren and Pentti Vihanto on their valuable insight they provided me during this thesis work. I would also like to thank Raphael Yorke, Annika Korhonen and other personnel on the mine site that answered my questions and educated me on the practices used at the site. Finally, I want to thank my family for supporting me in various ways throughout my studies.

Otaniemi, 24.9.2021

Matti I. Islander

Contents

Symbols and abbreviations

Symbols

v	Peak value of peak particle velocity, mm/s
R	Distance from the blast source, m
Q_{max}	Mass of explosives detonated simultaneously, kg
I_{BD}	Index of blast damage
V_{max}	Peak vector sum of ground vibration, mm/s
ρ_r	Rock mass density, kg/m^3
v_p	Weighted p-wave velocity of rock, m/s
k	Strength of rock obtained from rock mass rating (RMR)
σ_{td}	Dynamic tensile strength of rock, MPa
ρ_e	Explosive Density, kg/m^3
c	Velocity of sound in rock, m/s
K_{lc}	Fracture toughness of rock, $Pa\sqrt{m}$
γ	Adiabatic expansion coefficient
P_b	Borehole pressure, Pa
$P_{b,crack}$	Experimental value of critical borehole pressure, Pa
d_e	Explosive diameter, m
d_h	Borehole diameter, m
Q	Explosive heat, J/kg
q	Powder factor, kg/m^2
m_e	Mass of explosives, kg
H	Height of presplit, m
S	Spacing of boreholes, m
σ_t	Tensile strength, Pa

Abbreviations

GSD	Ground Sample Distance
VOD	Velocity of detonation, m/s
RMC	Rock mass classification
PPV	Peak particle velocity, mm/s
HCF	Half core factor, %
MWD	Measured while drilling

List of Figures

List of Tables

1 Introduction

1.1 Background

Pit wall stability is crucial for the safety and economy of an open pit mine. The slope geometry is planned according to the rock mass quality and the geotechnical features of the area and with a certain factor of safety to ensure the safety of the operation. However, the stability of the pit walls can be compromised by careless blasting. Controlled blasting methods have been developed to reduce the amount of blasting damage done to the pit walls and to produce a smooth pit wall.

Presplitting is one of the most common controlled blasting methods used. In presplitting a discontinuity plane is created in between the production blast field and the pit wall by blasting a row of tightly spaced boreholes simultaneously. The boreholes are charged with decoupled explosives and the presplit line is detonated before the production holes.

Presplitting has been observed to function well in hard and massive rock mass but in jointed rock mass presplitting has difficulties in producing a clean and stable pit wall. This is also the case at Kuusilampi open pit. Presplitting has been used in Kuusilampi open pit since the beginning and it has functioned well in good quality black schist. However, in some areas of the open pit, where the rock quality is lower or discontinuities are located and oriented very unfavourably, achieving stable pit walls through presplitting has proven to be challenging and bench scale failures have been observed.

As the mining extends deeper at Kuusilampi open pit, the importance of wall stability and achieving the planned safety berms and pit walls are increasing. The mine has planned presplitting tests with smaller explosive cartridge, different hole diameters, spacings and inclinations in different areas of the mine. Furthermore, the mine is extending to a mica schist area where presplitting has not been done previously. Presplitting tests will also be conducted in this area. This thesis is conducted as a part of these tests.

This thesis will start by introducing blast damage theory. After that the theory behind presplitting and relevant previous literature will be discussed. Then, the structural geology of the Kuusilampi open pit will be discussed based on previous studies. Then, the previous experience on presplitting at Kuusilampi open pit will be examined. After which the test procedure and the data gathered are introduced. Then the results of the tests are discussed. Next, the relevance of the results and recommendations for further improvements are discussed. Finally, a summary of this thesis and its main findings are provided in the conclusion chapter.

1.2 Research problems

This thesis will seek to answer the following questions:

- What are the optimal hole diameter, spacing and inclination for the different design sections of the open pit?
- How should the presplitting parameters be changed to react to changing rock mass quality to achieve stable pit slopes?

The optimality of the presplit parameters is considered only based on the quality of the resulting bench faces and amount of blast damage the remaining rock mass is subjected to.

1.3 Aim of the thesis

The main objective of this thesis is to discover suitable presplitting parameters for the different areas of the mine. The presplitting parameters that will be focused on are the borehole diameter, spacing and inclination. A secondary objective is to study if and how the presplitting parameters should be changed to counter changes in the rock mass quality. The rock mass quality is evaluated based on a geotechnical block model that includes Q', RQD and GSI values and have been interpolated from core logging data.

1.4 Delimitation

The condition of the final bench face is dependent on the rock mass quality, presplitting and production blasting. This thesis will not study the effects of the production blast. However, the effect of the buffer row will be discussed as it has a substantial effect on the observed final bench face. Furthermore, this thesis focuses on three presplitting parameters: hole diameter, spacing and inclination. The effect of other presplitting parameters will be introduced in the theory part and their effect on the final result will be discussed.

The optimality of the studied presplit parameters is considered mainly based on the resulting slope stability. The costs of different presplit parameters are not considered in this thesis. Although, the costs are a very important aspect when considering the optimality of the presplit parameters.

2 Blasting theory

This chapter starts by introducing general blast damage theory and bench blasting with the focus on achieving stable pit walls and limiting unwanted blast damage. Then, the theory behind presplitting will be discussed. After, which the objectives of presplitting will be introduced. Finally, the presplit design parameters and the effects of geotechnical features on presplitting will be examined.

2.1 Blast damage theory

Blasting damages the rock mass by two mechanisms: wave motion and gas expansion. The stress waves cause dynamic loading whereas the gas expansion is considered to be quasi-static loading. This is relevant to blast damage as the dynamic strength of rocks is significantly higher than the static strength.

Detonation of an explosive in a borehole creates a compressive shock wave which creates a crushed zone around the borehole. The shock wave is quickly attenuated into stress waves due to the intense fracturing of the rock mass. There are two types of stress waves created by an explosion: P-wave and S-wave. P-wave or the primary wave is a longitudinal stress wave which can be compressive or tensile but blasting creates a compressive wave. S-wave or secondary wave is a shear wave. Blasting damage theories focus mainly on the primary wave, which is also done here.

The compressive P-wave does not exceed the dynamic compressive strength of the rock and thus does not damage the rock through compression. However, the compressive stress creates a tangential tensile stress component which is responsible for creating radial fractures around the borehole as the tensile strength of rock is significantly lower than the compressive strength. The blast damage done to rock mass by shock and stress waves in single hole blasting is illustrated in figure 1. The behaviour of stress waves when propagating to an interface is discussed later in chapter 2.6.2.

Finally, the gas expansion starts fracturing the rock mass after the stress waves. The speed of gas expansion is between 160–240 m/s which is a lot lower than the wave speed (Zhang, 2016). The gas expansion drives the fractures further by protruding into the fractures around the borehole which causes high tensile stress in the existing fracture tips.

Stress wave attenuation is caused by four elements in rock mass: geometrical, cracking, internal friction and fractures. Geometrical attenuation is due to the dispersion of the stress wave in three dimensional space as it propagates. The second element causes attenuation because the stress wave creates cracks in the rock mass which consumes energy. Internal friction causes some of the stress wave's energy to be lost in the rock mass as heat. Finally, fractures, cracks or discontinuities cause some

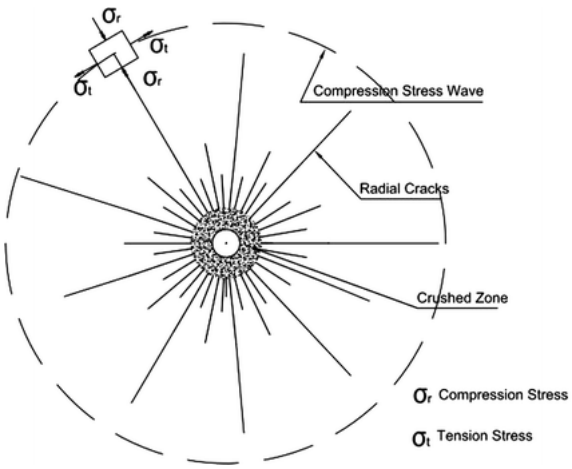

Figure 1: Blasting damage created by compressive stress and shock wave in single hole blasting (Zou, 2017).

energy losses as the stress wave comes into contact with them.

2.2 Bench blasting

There are three ways bench blasting can damage the pit walls: vibrations, gas penetration and bulk movement (Blair, 2018). Blast vibrations is the damage mechanism that is considered to have the most far reaching damage effects. Peak particle velocity (PPV) is used as a measure to evaluate the potential vibration damage a blast has. PPV can be estimated with equation 1, where k and b are site specific constants, R is the distance from the blast, and Q_{max} is the mass of explosives detonating simultaneously or within the same delay window meaning that the explosives can be detonated simultaneously due to delay element inaccuracy. The vibration damage is then typically controlled with delay times, and explosive charge per hole and hole diameter.

$$v = k \left(\frac{R}{\sqrt{Q_{max}}} \right)^{-b} \tag{1}$$

Where:

v = Peak value of peak particle velocity in mm/s

k and b = site specific constants

R = distance from the blast in m

Q_{max} = mass of explosives detonating simultaneously in kg

Gas penetration can damage the rock mass in the pit wall by protruding into the bench face and driving fractures forward in the remaining rock mass. This damage mechanism is typically controlled with borehole placement (i.e. burden and spacing). This damage mechanism is also largely affected by structures in the rock mass, which typically cause underbreak by offering a path of least resistance for the gas pressure to escape. In jointed rock masses, if the blasting result is controlled by structures in the rock mass, reducing the spacing and burden should improve the blasting result. The gas penetration damage can also be controlled with explosive charging methods, such as decking, air decking and stemming. Decking and air decking is used to remove the explosive charge from a specific part of a blast hole which can be used to reduce the explosive damage at a weaker rock mass area of the borehole. Stemming is used to increase the duration of the gas pressure in the borehole and typically overbreak occuring at the bench crest can be reduced by increasing the stemming length.

Bulk movement damage is created by the blasted rock mass impacting the bench face. This can be reduced with blast designs that provide sufficient throw distance and time to the blasted rock mass, with blast direction normal to the bench's dip direction and initiation sequence. Sufficient throw distance and time ensure that there is enough swell space for the liberated rock mass to expand to. If the swell space is not provided the confinement increases for the back rows of the blast, which can increase the force exerted by the blasted rock mass at the bench face. However, if confinement is further increased, this can cause underbreak but this also increases the seismic energy (i.e. the vibrations) created by the blast, which can cause further unwanted damage (Zhang, 2016).

However, Blair (2018) questions the effect of the two mechanisms: gas penetration and bulk movement. He argues that because these two mechanisms have not been detected by any vibration measurements close to the pit wall, these have no effect on blast damage to the pit wall. Thus, these mechanisms would have to damage the rock mass without creating vibrations in the rock mass.

In bench blasting, buffer row or rows are typically used close to the remaining rock mass to limit the blast damage from vibrations and gas penetration. The buffer row closest to the remaining rock mass is sometimes also referred to as the trim row, but here it will be referred to as a buffer row. Figure 2 illustrates the different components of a bench blast with a presplit at the planned bench face. The buffer row or rows typically have smaller diameter boreholes than the production blast holes, which reduces the vibrations. Although equation 1 does not account for this variable, Singh et.al. (2006), found that dividing the same amount of explosives detonating simultaneously into several holes reduces the created vibrations. Furthermore, smaller spacing and burden is used in the buffer row(s) which increases the control in the blasting result. Large blast holes, spacing and burden are more influenced by geological structures in the blasting result.

Blast damage or back break is also influenced by hole inclination. Zhang (2016) shows through P-wave reflection that inclined holes result in less back break at the

crest of the bench than vertical holes. Inclined holes also help decrease underbreak at the toe of the bench by reducing the shear force at the bottom of the hole (Zhang 2016).

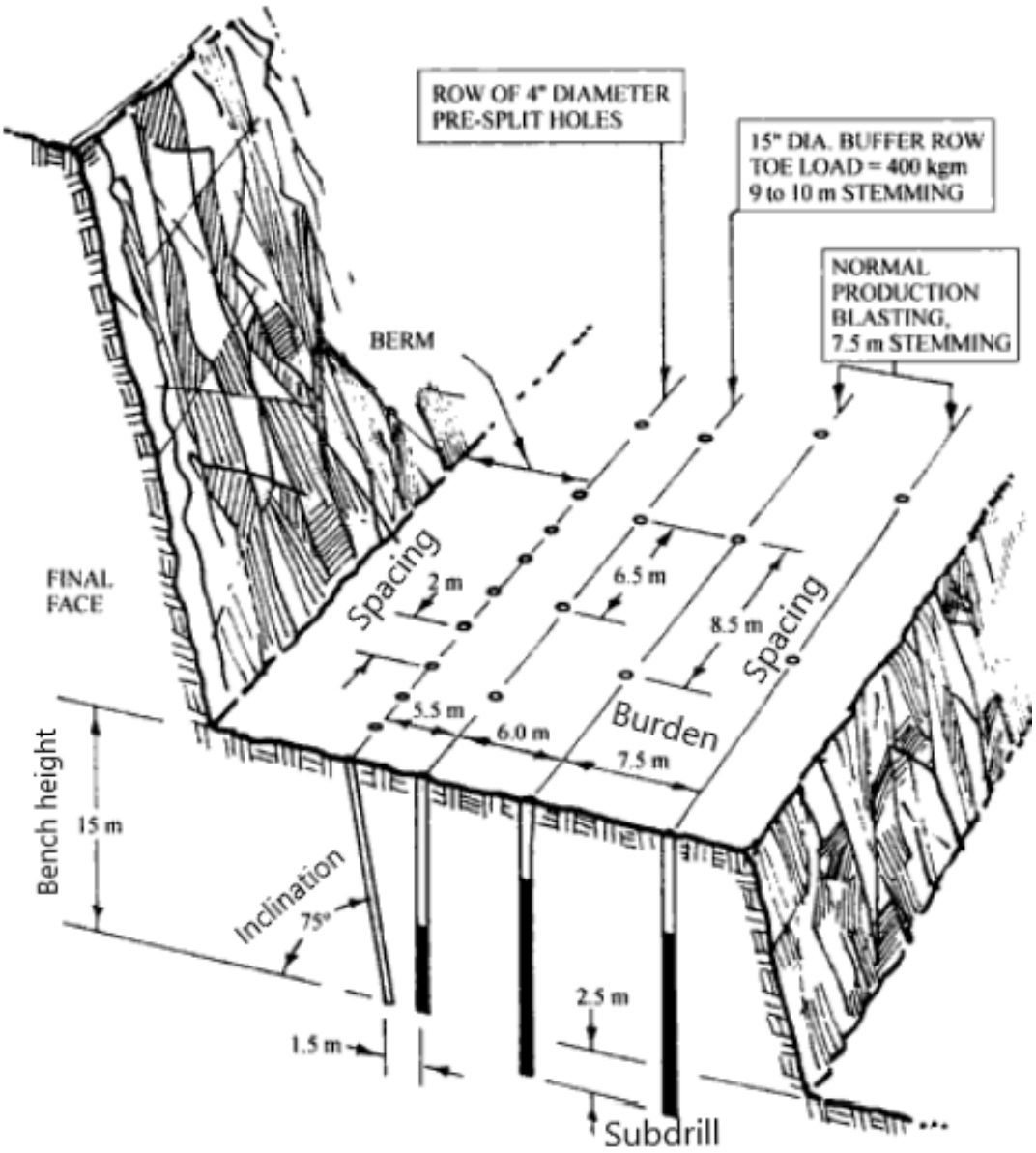

Figure 2: An example of the components of bench blasting (Bauer, 1982 in Hustrulid, 1999 modified by Islander).

2.3 Presplitting theory

The general consensus is that in presplitting the discontinuity plane is created between the boreholes by the interaction of explosive force of adjacent boreholes. This interaction creates stress concentrations between the boreholes which results in

preferential fracturing in between the boreholes. For this interaction to occur it is essential that the boreholes are sufficiently closely spaced and that the detonation of the boreholes is near-simultaneous.

The fracturing of the rock mass is enabled further in between the boreholes than in other directions by stress wave superposition. This is illustrated in figure 3. In this figure the peak of tangential tensile stress created by the radial compressive stress wave is assumed to follow the front of the P-wave. The figure shows that the resulting tensile stress is the highest on the line AB in between the boreholes.

Furthermore, Hustrulid (1999) states that there is a crack suppression effect with adjacent simultaneously detonated boreholes. This is based on the fact that the P-wave from O1 (figure 3) will apply compressive force on the cracks propagating in the direction of the dashed line from O2 which can have a suppressive effect on the crack propagation.

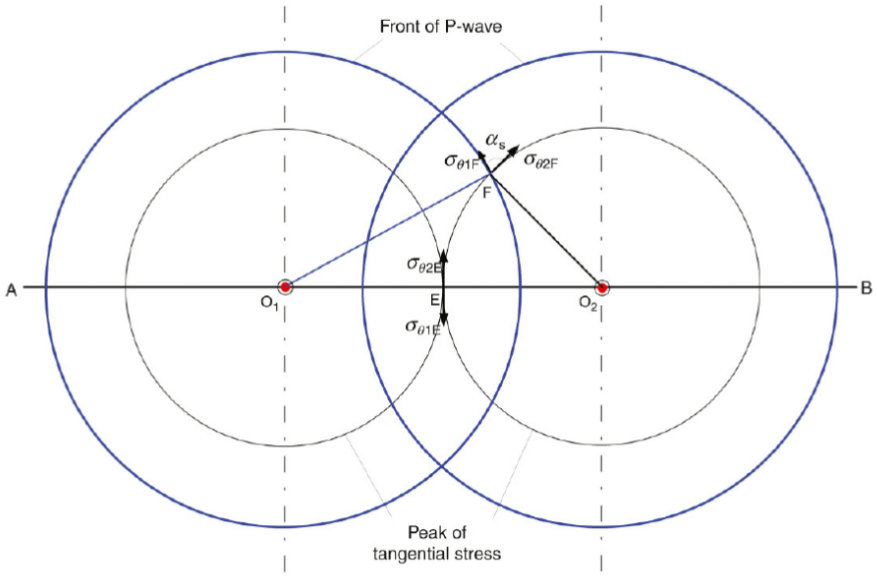

Figure 3: Stress wave interaction around simultaneously detonated boreholes (Zhang, 2016).

After the stress wave has passed, the gas expansion from the boreholes creates further stress concentration on the presplit line and the initial fractures made by the stress waves help the explosive gas to expand towards the adjacent boreholes which results in the creation of a discontinuity plane between the boreholes.

There have been multiple theories about the mechanics behind presplitting. Worsey (1981) describes three different theories that attempt to explain the crack propagation between simultaneously detonated boreholes. Two of these theories suggested that the stress waves are wholly responsible for the crack growth and one of the theories tried to explain the crack growth by gas expansion only. Worsey (1981) concludes

that the stress wave cannot be entirely responsible for the crack growth because the crack propagation speed is a lot lower than the wave speed in the rock mass. Worsey also concludes that gas expansion is the main component behind the crack propagation between simultaneously detonated boreholes. Recent studies described by Yang et al. (2020) suggest that the stress wave is responsible for micro cracking between the boreholes and the explosive gas is responsible for the major crack created in between the boreholes.

However, Zou (2017) states that there is a lot of practical evidence that a presplit plane can still be created even if the holes have delay times in the excess of 25 ms. Ouchterlony (1997) found in his tests that delay times of over 1 ms between holes results in fracturing that resembles single hole blasting. This suggests that the mechanics behind presplitting are not concerned with explosive interaction between adjacent boreholes. Zou (2017) also describes an alternative theory for presplitting created by Langefors and Kihlström (1978), where the preferential cracking between the boreholes is created by stress concentrations around empty circular holes.

Although, a presplit line can be created with non simultaneous detonation, this may increase the created fracture lengths in the remaining rock mass as Ouchterlony (1997) found in his tests that simultaneous detonation results in shorter crack lengths.

2.4 Objective of presplitting

Generally, the objective of presplitting has been to reduce the damage from blasting to the remaining rock mass and thus enable steeper pit slopes in open pit mining. A succesful presplit protects the remaining rock mass by venting the expanding gases from a production blast before they protrude into the bench face. A succesful presplit will also attenuate some of the stress waves created by the production blast. However, the presplit plane will only affect the stress waves in its close proximity (Adamson, 2012). In addition, Adamson (2012) suggests two other objectives for presplitting, which are the creation of a smooth wall for the loaders to dig back to and aiding fragmentation by creating a discontinuity surface for the buffer row to act on.

Typically, the success of presplitting has been measured by visual observation. From the visual observations two figures are calculated: deviation of the final face from the planned and half-cast factor (HCF). HCF is a measure where the visible presplit borehole half cores will be measured and divided by the meters of holes drilled. Furthermore, the presplit success can be estimated by considering the ease of loading and scaling time required. These measures quantify well some of the objectives presplitting has. However, these measures are poor in quantifying the actual damage done to the remaining rock mass.

Peak particle velocity (PPV) is a widely accepted parameter for measuring the extent of blast damage. For example Birhane (2014) introduces a site scaling law that

is used at Aitik mine that uses measured PPV values from blasts to estimate the damage extent of the bench face and the required amount of scaling. Raina (2019) also introduces a measure, that utilises the vector sum of PPV values, for presplitting success, which is the index of blast damage created by Yu and Vongpaisal (1996). This is shown in equation 2. The numerator of this equation represents the stress induced to the rock mass by blasting and the denominator represents the rock mass' strength.

$$I_{BD} = \frac{V_{max} * \rho_r * v_p}{k * \sigma_{td}} \tag{2}$$

Where:

I_{BD} = Index of blast damage

V_{max} = Peak vector sum of ground vibration in mm/s

ρ_r = Rock mass density in kg/m^3

v_p = p-wave velocity of rock in m/s

k = Strength of rock from Rock mass rating

σ_{td} = Dynamic tensile strength of rock in MPa

PPV is a better measure for estimating the blast damage further away. However, determining the damage ranges for certain PPV values is difficult due to the heterogeneous nature of rock mass. Thus it cannot accurately evaluate if the blast has damaged or activated some discontinuities behind the bench face which will cause failure later.

However, Rajmeny and Shrimali (2019) used a slope stability radar to detect sliding movements in large scale structures after blasting and calculated the PPVs' of the blasts with equation 1 to determine PPV ranges that will cause sliding movement in three previously distinguished faults in the pit walls. Similar studies could be used to determine site specific PPV ranges for blasting damage. Although suggestions for universal PPV ranges exist, they cannot accurately determine the ranges where blast vibrations cause damage due to the heterogeneous nature of rock mass.

In case presplitting does not result in a smooth bench face or some failure occurs after blasting, it is very difficult to establish the extent of damage done by presplitting, because the rock mass quality can only be estimated and because the production blast can also have unexpected consequences. Even if the presplit results in a clean bench face, some discontinuity can be activated behind the bench face which can cause water to enter the discontinuity and failure will occur after some time.

2.5 Presplit design parameters

As described in the previous chapter, the key factors in succesful presplitting are borehole spacing and delay times between boreholes. In addition, a key factor is also decoupling of explosives and the borehole. Furthermore, there are multiple design factors that affect the result of presplitting, which will be further discussed next.

Simultaneous detonation of boreholes seeks to maximize the fracture length in the preferred direction. Concurrently, the fracturing of the rock mass in other directions is minimized by using decoupled explosives meaning that the hole diameter is larger than the explosive diameter. This leaves an air gap between the borehole wall and the explosive, which consumes some of the explosive energy as the air is compressed after the detonation. Decoupled charge results in a much lower borehole pressure, which reduces the crushed zone around it. For succesful presplitting it is essential that a decoupling ratio which minimizes the damage done to the pit wall while producing the presplit plane between the boreholes, is found. Finding a suitable decoupling ratio is about matching the borehole diameter with the explosive and the rock mass quality

Spacing of the presplit holes define how the explosive energy is distributed in the rock mass. As discussed earlier, a sufficiently low spacing ensures that there is sufficient explosive pressure interaction with adjacent boreholes. However, a too low borehole spacing will result in overbreak as the rock mass is subjected to too high explosive energy. A widely used empirical method for defining a suitable spacing for presplitting is powder factor. In presplitting the powder factor is defined as mass of explosives per square meter of rock mass to be presplit (equation 3). Generally in mining, previous experience is used to select a suitable range for the powder factor and then tests are conducted within this range to find a sufficient powder factor and spacing.

$$q = \frac{m_e}{H * S} \tag{3}$$

Where:

q = Powder factor in kg/m^2

m_e = Mass of explosives in kg

H = Height of presplit in m

S = Spacing of presplit holes in m

The drawback of powder factor is that it disregards many key factors for presplitting. Another method for defining suitable presplit parameters is by estimating the explosive pressure on the borehole wall and linking this to rock strength. Ouchterlony (1996) derived equations 4, 5, 6 and 7 for estimating the crack length in cautious blasting

based on tests done in granite. Equation 4 estimates the explosive pressure subjected to the walls of the borehole, equation 5 is used to estimate the adiabatic expansion coefficient of the explosive, equation 6 is used to estimate the required pressure to fracture the rock mass and equation 7 estimates the fracture radius created by the explosive in a given rock type. Several other sources, such as Dindarloo et al. (2015) and Mckenzie (2013), have used a similar equation for approximating the borehole pressure as equation 4 with the exception of not using the adiabatic expansion coefficient (γ).

Ouchterlony's equations account for explosive parameters, coupling ratio, rock strength and partly even the rock mass quality with the sonic velocity of the rock mass. However, Ouchterlony (1997) states that equation 6 should be used with caution in practical applications and that fracture toughness might not be the correct rock strength parameter for estimating the required pressure to fracture the rock, because these equations have been created and tested on limited data. Furthermore, the purpose of Ouchterlony's study (1997) was to improve contour blasting in mainly tunnels which is why these equations might not be accurate in an open pit mining operation.

Furthermore, other sources have estimated the spacing using the tensile strength of rock as in equation 8 with slightly different variations. Equation 8 was created by Sanden (1974), Calder (1977) and Chiapetta (1991) in Danell et al. (1997) through theoretical examination of the interaction between rock strength and stress waves and does not consider the effect of gas expansion which was concluded to be the main contributor in presplitting in the previous chapter. Thus, these empirical equations are highly limited in their ability to predict suitable presplitting designs. However, they can be used as a starting point for presplitting tests.

$$P_b = \frac{\gamma^\gamma}{(\gamma+1)^{\gamma+1}} * \rho_e * (VOD)^2 * (\frac{d_e}{d_h})^{2.2} \tag{4}$$

$$\gamma = \sqrt{1 + \frac{VOD^2}{2 * Q}} \tag{5}$$

$$P_{b,crack} = 3.30 * \frac{K_{1C}}{\sqrt{d_h}} \tag{6}$$

$$\frac{2R_c}{d_h} = (\frac{P_b}{P_{b,crack}})^{2/[3(VOD/c)^{0.25}-1}} \tag{7}$$

$$S = \frac{d_h * (P_b + \sigma_t)}{\sigma_t} \tag{8}$$

Where:

P_b = Borehole pressure in Pa

γ = Adiabatic expansion coefficient

ρ_e = Explosive density in kg/m^3

VOD = Velocity of detonation in m/s

d_e = Explosive diameter in m

d_h = Borehole diameter in m

Q = Explosive heat of the explosive in J/kg

$P_{b,crack}$ = Experimental value of critical borehole pressure in Pa

K_{lc} = Fracture toughness of rock in $Pa\sqrt{m}$

R_c = Crack radius in m

c = Velocity of sound in rock in m/s

S = Spacing of presplit holes in m

σ_t = tensile strenght of rock in Pa

Ouchterlony's equations 4, 5 and 7 show which explosive parameters are mainly of interest in presplitting. VOD is probably the most important factor affecting presplitting as it defines how fast the energy is released and how the energy release is divided between gas pressure and shock wave. From equation 4 it can be seen that the borehole pressure increases with increasing VOD which should result in longer fractures in the rock. However, as can be seen from equation 7 if a high VOD is used relative to the sonic velocity of the rock mass, the resulting cracks will be shorter.

This effect is partly utilised in presplitting by using high VOD explosives the crack lengths in undesired directions are reduced. As Singh (2005) also found an inverse relation between overbreak and VOD meaning that an increase in VOD results in reduced overbreak. Explosive's manufacturers', such as Maxam and Orica, also provide special charges for presplitting that have high VODs.

Other important explosive parameters are density, energy and charge diameter. Density and energy define how much energy can be produced by the explosive upon detonation. The charge diameter defines the coupling ratio together with the borehole diameter, which was discussed previously in this chapter. The charge diameter also defines the mass of explosives per borehole meter together with the density.

Bench height is a blasting parameter that is typically chosen based on the slope stability, ore type and production rate. Zhang (2016) introduces two empirical formulas that link the drill hole diameter and bench height for production blasting. However, there is very limited information on the effect of bench height to presplitting. When powder factor is utilised in designing a presplit, bench height is an influencing

parameter. Increasing the bench height reduces the powder factor which suggests that a shorter spacing should be used with a larger bench height.

However, bench height might not be the correct parameter to be considered for presplit designs. Birhane (2014) uses the height ratio between the presplit and the production blast instead. The effect of the height ratio or single and double benching is illustrated in figure 4. The figure illustrates that the degree of overbreak is higher in single benching than in double benching as crest failure is prevented in the lower bench in double benching by the weight of the overlying wall. Rorke (2011) in Birhane (2014) also suggests that if single benching is utilised instead of double or triple benching the spacing in the presplit should be reduced.

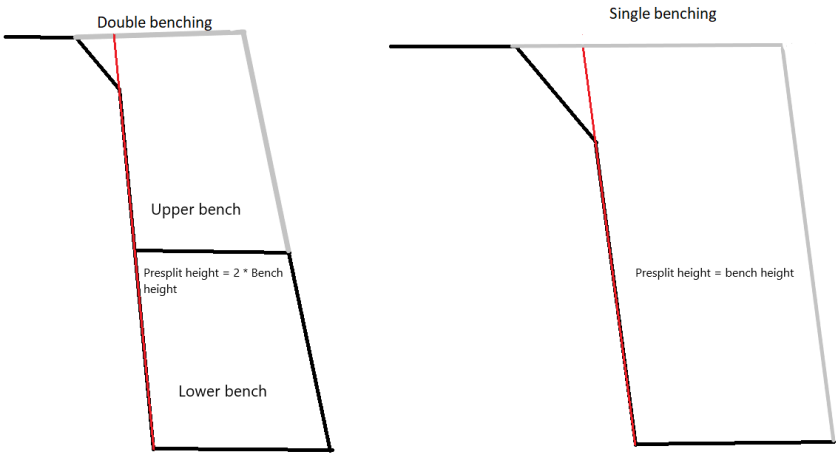

Figure 4: Single versus double benching. Red line illustrates the presplit plane. In double benching the presplit height is twice the bench height while in single benching the bench height equals the presplit height.

The use of stemming in presplitting should be considered carefully as stemming can cause cratering of the holes which results in increased backbreak. However, stemming only increases the duration of the borehole pressure (Zhang, 2016). If cratering occurs with stemming, the explosive charge is too high in the top part of the hole and can be reduced by leaving longer part uncharged from the top of the hole. If no stemming is used, a higher explosive charge can be used instead.

In presplitting and production blasting the hole inclination is usually vertical or near vertical because drilling vertical holes has a few advantages compared to drilling inclined holes, such as drilling vertical holes is more efficient, accurate and has a lower wear on the drill bits (Zou, 2017). Inclined boreholes also have a higher possibility of collapsing especially in highly jointed rock mass.

However, considering blasting results inclined boreholes generally have a few advantages to vertical boreholes. If the presplit line is vertical, shear force is induced in the presplit plane, which is illustrated in figure 5. The production blast will also create a force normal to the presplit line. This combined with the shear force can weaken the discontinuities (B in figure 5) behind the presplit line and cause a failure

along the discontinuity. Birhane (2014) argues that inclining the presplit line by 10° to 80° can eliminate this shear force.

The optimum hole inclination in regard to wall stability mainly depends on the dip of the main discontinuities in the rock mass according to Singh et al. (2014). Discontinuities offer explosive gases a path to expand to which can cause failure of the rock mass along the discontinuity. Using the same borehole inclination as the main discontinuity dip will reduce the probability of a borehole crossing paths with the discontinuity and thus reducing the probability of gases venting into the discontinuity. However, with increasing hole depth the borehole deviation may become the controlling factor in what inclination should be used. If borehole depth cannot be reduced, the inclination should be kept closer to vertical to achieve higher drilling accuracy.

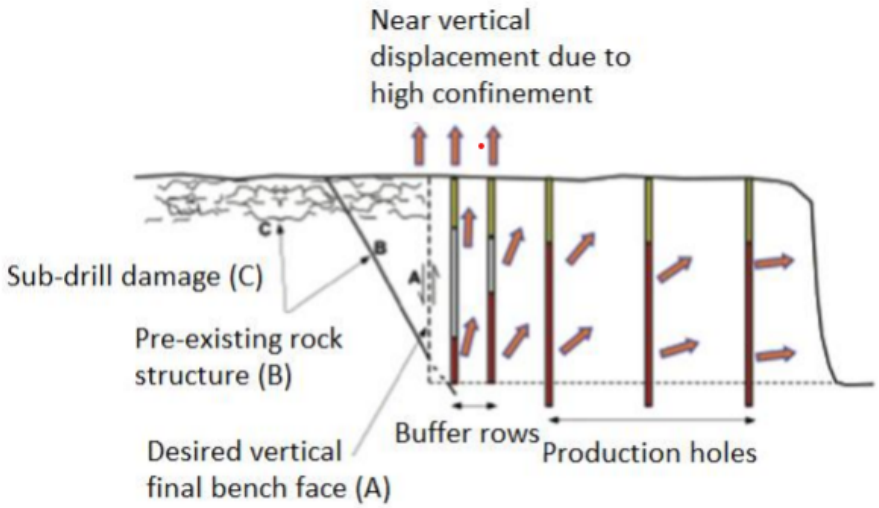

Figure 5: Effect of borehole inclination on presplitting (Rorke, 2011 in Birhane, 2014).

2.6 Geotechnical features affecting presplitting

This chapter discusses the effects of the most influential geotechnical properties of rock mass that affect presplitting. These being the rock strength, discontinuities, weathering, and water. Worsey (1981) also discussed the effects of texture and grain size of rock which he concluded have no significant effect on presplitting. In-situ stress of the rock mass also has some effects on presplitting. However, as this study focuses on open pit mining the magnitude of horizontal stresses is ignorable. Thus, these parameters will not be discussed further here.

2.6.1 Rock strength

Rock strength affects presplitting by defining the force that is required to fracture the rock. As discussed in the previous chapter and shown in equations 4 and 8, the tensile or compressive strength can be used to estimate the required explosive charge and spacing to create a presplit plane in continuous rock mass. Some rock types, such as mica schist, have anisotropical strength parameters meaning that the strength of the rock depends on the direction it is loaded.

The strength anisotropy can be expected to result in longer fracturing in the weaker direction and shorter fractures in the higher strength direction. This may cause higher damage towards the final pit wall in presplitting if the rock's weaker direction is perpendicular to the presplit line. However, Worsey (1981) found in his tests that no significant damage was observed in the presplit face, when presplitting was done in these conditions.

Weathering of the rock mass mainly affects the strength of the rock mass. Thus, it has the same principal effects as the rock strenght. However, highly weathered rock mass can even behave as soil. In such conditions the rock mass can be excavated without blasting entirely.

2.6.2 Discontinuities

Discontinuities are the most important geotechnical feature affecting presplitting. The discontinuity parameters that are of importance in presplitting are frequency, orientation, dip and aperture or surface of the discontinuity. First, the effects of discontinuity parameters on stress waves and gas expansion will be examined. Then, the effects of discontinuities on presplitting results will be discussed.

Stress waves are attenuated, reflected and refracted when they meet a discontinuity surface. The degree of attenuation over discontinuities depend on the frequency, orientation and surface condition. Danell et al. (1997) states that the attenuation is the greatest when the angle between the presplit line and discontinuity is between 15° and 45°. The attenuation is also increased with increasing discontinuity frequency between the boreholes. Furthermore, Danell et al. (1997) states that the attenuation of stress waves increase with discontinuities that have lower friction. Increased wave attenuation in the presplit line can impair the micro cracking caused by the stress waves and thus reduce the quality of the presplit.

The reflection and refraction behaviour of stress waves when meeting a discontinuity surface depends on the surface condition and the orientation of the discontinuity. The type of wave also has some influence, such as a compressive P-wave will be reflected as a tensile stress wave but the refracted wave is still compressive. The surface condition or the shear and normal stiffness of the joint define how a stress

wave behaves when it reaches the joint interface. When the shear and normal stiffness are zero, the discontinuity acts as a free surface, which means that wave refraction does not occur and only a reflected wave is produced. Tarique et al. (1996) in Singh (2005) found that a discontinuity with an aperture of at least 3 mm functions as a free surface. If the joint has a certain shear and normal stiffness both a reflected and a refracted waves are produced. When the joint stiffness approaches infinity (e.g. a tightly cemented joint), no reflection of the wave will occur. (Ma, 2010).

The discontinuity orientation affects the angles and types of waves that are created during the interaction between the joint and the incident wave. If a stress wave propagates at a normal angle to a discontinuity, only a reflected and refracted wave will be produced. However, when a wave reaches a discontinuity surface at an oblique angle, four waves are created a reflected P-wave and S-wave, and a refracted P-wave and S-wave, which is illustrated in figure 6. Although, figure 6 shows an incident P-wave, the same principle applies for an incident S-wave.

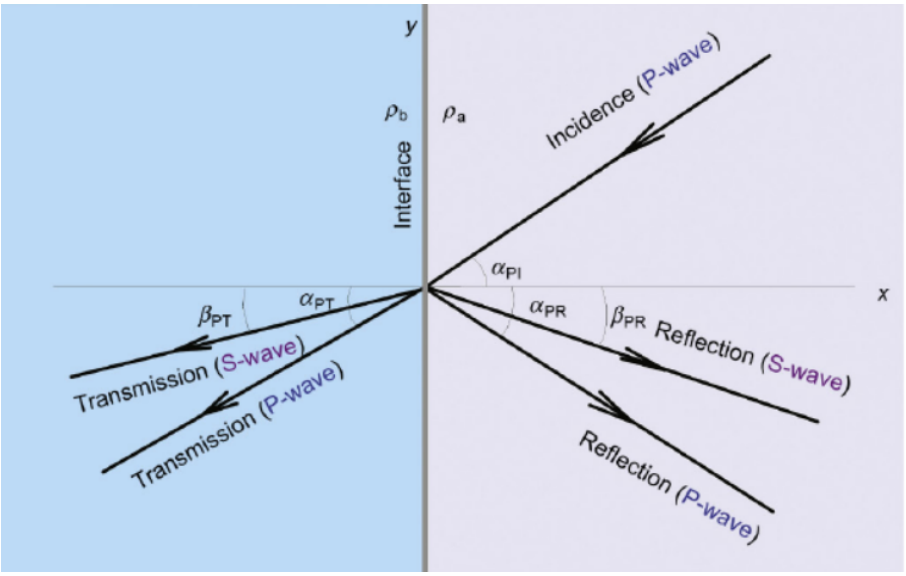

Figure 6: Reflection and refraction (transmission) of a P-wave reaching a joint surface (Zhang, 2016).

If a discontinuity is located relatively far away from the presplit line, its effect depends on the wave behaviour at the interface. Predicting this effect to presplitting is very complicated as it is mainly concerned with predicting the magnitude of the reflected P-wave. This prediction is further complicated by the wave interaction from adjacent boreholes. In case the magnitude of the reflected P-wave exceeds the dynamic tensile strength of the rock mass, spalling will occur and high degree of overbreak is expected. Otherwise, the discontinuity will most likely have no effect on the slope stability. Although, the stress wave can activate or weaken the discontinuity which may cause failure at a later date.

Discontinuities affect the gas expansion by offering a path of lower resistance for the gases to escape. Whether the explosive gases protrude into the discontinuities

depends on the type and dip of the discontinuity. Discontinuities, that are tightly closed, affect the gas expansion very little. However, joints, that are open or have some infilling, are very likely to vent the gases from the blasthole. The effect of discontinuity dip on gas expansion is illustrated in figure 7. The figure shows that when the blasthole is normal to the major joint orientation the main pressure created by the explosive is parallel to the joints. In this case, the gases are more likely to expand into the joints (Raina, 2019). Worsey (1981) also stated that a discontinuity with a dip of less than 30° from the horizontal can allow the gases to protrude into the discontinuity.

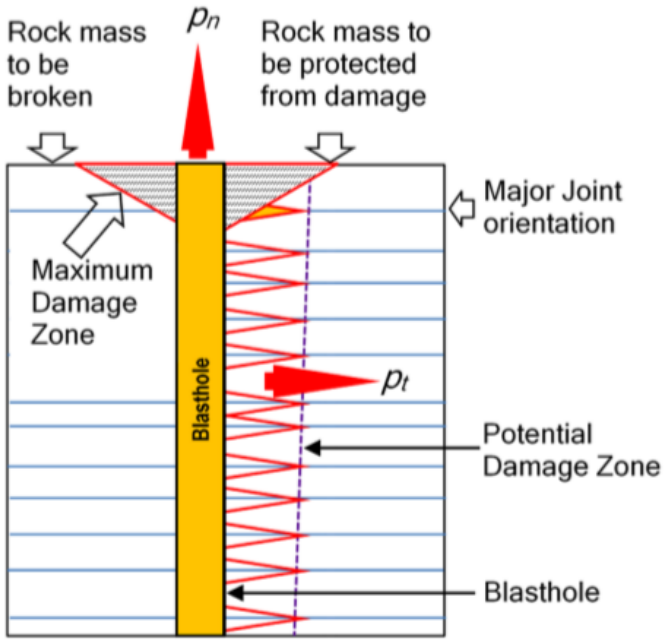

Figure 7: The effect of discontinuity orientation on gas expansion (Raina, 2019).

Worsey (1981) suggests based on his tests that one dominant fracture will be created in presplitting and that fracturing around a presplit hole occurs in an elliptical shape, which is illustrated in figure 8. In case a discontinuity is within a presplit hole's ellipse, the dominant fracture tends to form normal to the discontinuity. Thus, a persistent discontinuity within the ellipse and parallel to the presplit will result in the highest degree of overbreak. Worsey (1981) and Singh (2005) both stated that a discontinuity with an angle less than or equal to 15° towards the presplit line will result in high degree of overbreak and presplitting can fail completely. Figure 9 illustrates the effect of discontinuity orientation on overbreak when the angle between the presplit and discontinuity is greater than 15°. Singh (2005) constructed the graph shown in figure 9 based on small scale presplit tests made with concrete.

As discussed previously, the frequency of discontinuities largely affect the stress wave propagation and its ability to fracture the rock mass which may affect presplitting effectiveness. On this basis, Workman and Calder (1991) in Danell et al. (1997) recommended that joints per borehole spacing should be less than 2–3. Singh (2005)

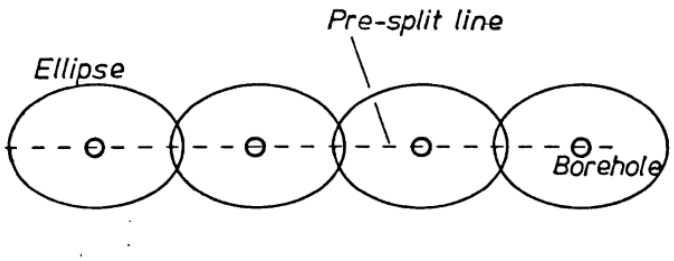

Figure 8: Fracture extension in a presplit line (Worsey, 1981).

also recommended that borehole spacing should be less than two times the joint spacing. However, Worsey (1981) found in his tests that joint frequency did not affect presplitting functionality adversely because the fractures extended over the discontinuities effectively. Singh (2005) also stated that tight and cemented joints have no significant effect on overbreak. Thus the joint frequency is not as significant rock mass parameter as discontinuity orientation and type of discontinuity.

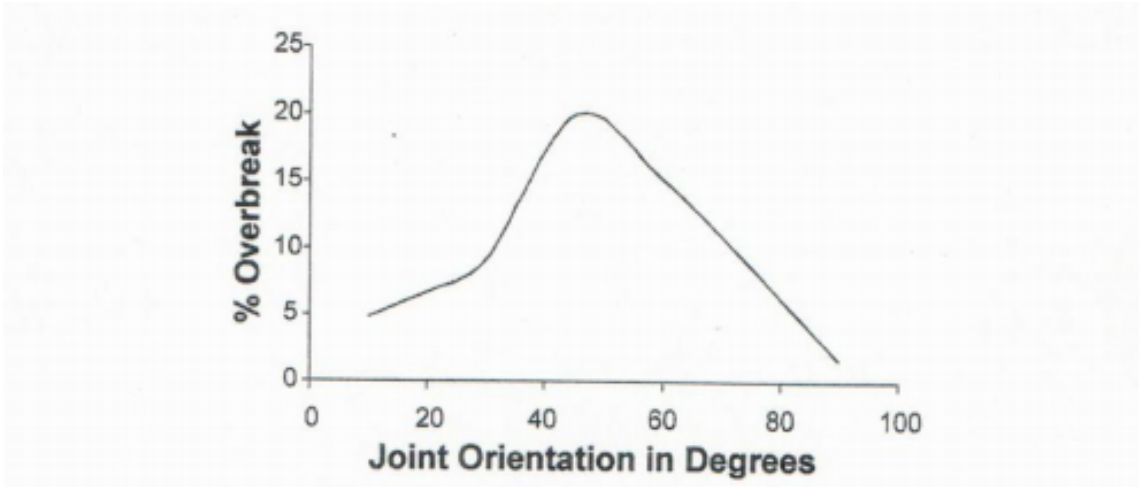

Figure 9: The effect of discontinuity orientation to presplitting, (Singh, 2005).

2.6.3 Water

Water can affect presplitting in two ways if we assume that water resistant explosives are used. The first case that is considered is that there is water in the boreholes. In this case, the decoupling does not function as intended because where as air is compressible, water can be considered as incompressible. It can also be considered that water's impedance is closer to the explosive's and rock mass' (Worsey, 1981). Anyway in this case the shock wave from the explosive is transferred to the rock mass more efficiently which results in a more highly fractured zone around the borehole. This suggests that presplitting with water filled holes results in higher damage to the final pit wall.

If the boreholes are filled water, the gas expansion of the explosive would force the water in to the fractures. Worsey (1981) argues that this would reduce the fracture lengths created by the gas expansion because water has high surface tension and higher molecular size than air and thus would not drive the fractures further as efficiently. However, Zhang (2016) states that decoupled charge with water creates longer fractures and better fragmentation compared to air decoupled charges. Thus water is only expected to increase overbreak and blast damage in presplitting.

In the second case that is considered is that the discontinuities are filled with water. Generally, this reduces the slope stability as the shear strengths of discontinuities are reduced. For presplitting however, the stress wave created by the explosion is also transmitted over discontinuities more efficiently and the magnitude of a reflected P-wave is reduced which reduces the probability of spalling failure. Singh (2007) also stated that water filled joints allow shock waves to travel without internal spalling but when the rock mass is in tension the water is mobilized which may cause overbreak.

3 Geology of Kuusilampi Open pit

This chapter describes the geology and the geotechnical features of the Kuusilampi open pit. First, the main rock types at Kuusilampi open pit and their strength and structural properties will be introduced. Then, the main geotechnical structures affecting slope stability and presplitting will be discussed. Next, the use of rock mass classification (RMC) systems will be discussed for the application of presplit design. Furthermore, the RMC systems that are used at Kuusilampi open pit are introduced. Finally, the hydrogeological features are examined, that are of interest considering the slope stability at Kuusilampi open pit.

3.1 Rock types

There are four rock types at the kuusilampi open pit: black schist, mica schist, talc-tremolite schist and quartzite. The mineralization is hosted by the black schist which is the main rock type in the open pit. Mica schist is the second most common rock type in the open pit and it is found in the northern to north-eastern part of the open pit. The talc-tremolite schist is encountered only in the eastern part of the open pit in between the black schist and mica schist as a 1-10 meter wide zone (SRK 2020b). The quartzite is overlain by black schist and is rarely encountered in the open pit. No presplitting is done in the talc-tremolite schist and quartzite domains which is why these rock types will not be discussed further. Next, the mica schist and black schist strength parameters will be discussed further.

Table 1 shows the laboratory measurements of the strength parameters of the black schist and mica schist. These parameters have been obtained by tests completed by Helsinki University of technology in 2006 and 2004, and Sandvik in 2019. In addition to the strength parameters, the table also shows the coefficient of variation for each parameter which represents the scatter in the data and is calculated by dividing the standard deviation by the mean value. Mica schist has only one measurement of the Poisson's ratio which is why it does not have the coefficient of variation defined.

Both the mica schist and black schist have relatively high in situ strength, which can be seen in table 1. However, both of these rock types have anisotropic strength behaviour because of the foliated structure. Mica schist shows higher strength anisotropy than black schist. The high strenghts of the rock types mean that failures are typically controlled by geological structures.

Black schist is very prone to weathering, because of the high sulfide content, which has reduced its strength in areas where water has been in contact with the black schist. These areas are close to the surface at the top 30 to 40 meters of the deposit and at discontinuity surfaces especially faults where water has been flowing.

Mica schist has significantly higher tensile strength than black schist which suggests higher resistance towards fragmentation by blasting and fracturing by presplitting. However, black schist has higher elastic modulus than mica schist which indicates that black schist has higher resistance towards elastic deformation. Furthermore, mica schist has been observed to have more brittle failure type whereas black schist shows more ductile failure type. This means that black schist consumes more energy before a fracture is created when the elastic strength limit of the material is exceeded. This suggests that mica schist requires higher stress to fracture but black schist requires more energy to fracture.

Table 1: Rock strength parameters (SRK, 2020b).

Black schist		
Parameter	Mean value	Coefficient of variation
Elastic modulus [GPa]	59.5	28 %
UCS [MPa]	142	23 %
Poisson's ratio	0.23	13 %
UTS [MPa]	12.7	20 %
Mica schist		
Elastic modulus [GPa]	42.3	31 %
UCS [MPa]	148	24 %
Poisson's ratio	0.15	-
UTS [MPa]	19.6	15 %

SRK (2020b) summarized the joint conditions for the two different rock types as follows:

- Mica schist: Vary from undulating/rough to planar smooth with mostly no infill or higher strength infill
- Black schist: Full range of stepped/rough to polished/planar with mostly no infill or medium to fine harder infill materials.

A table showing the range of joint conditions is shown in appendix B. This summary means that, for mica schist the joint conditions vary from the medium strength joints to the second weakest joints and for black schist the joints vary from the strongest joints to the weakest joints based on planarity and roughness. This large variability in joint conditions for both rock types makes it difficult to evaluate if presplit blasting or blasting in general has caused a failure along a joint at a bench face or if the joint failed due to its inherent strength.

3.2 Geotechnical structures

Geotechnical structures control the failure mechanisms of the rock mass and significantly affect the blasting and presplitting functionality. At Kuusilampi open pit

tectonic deformation and medium–grade regional metamorphism has led to series of faults and fracture zones that are focussed along lithological contacts striking predominantly North West-South East. Furthermore, glacial unloading has created joint sets that are plentiful close to the ground surface but uncommon deeper in the rock mass. (SRK, 2020b).

Six joint sets have been identified through mapping and core logging in the Kuusilampi open pit by SRK (2020b). Table 2 shows the average dips, dip directions, persistences and spacings of the joint sets for the entire open pit. Joint sets J1 and J3 have been identified as the foliation and cleavage and J6 is the product of glacial unloading and is very common in the top 30 metres of the pit.

Table 2: Joint sets at the Kuusilampi open pit

Joint set	Dip	Dip direction	Persistence [m]	Spacing [m]
J1	71°	238°	7.0	3.6
J2	85°	205°	5.5	5.0
J3	56°	62°	9.6	4.2
J4	48°	208°	6.4	8.3
J5	54°	115°	10.1	8.8
J6	17°	264°	5.6	4.4

SRK (2020b) suggested that the open pit would be divided into seven design sectors (DS) according to the foliation trends and pushback designs. These sectors can be seen in figure 10. The yellow lines shown in figure 10 illustrate the main foliation trends within the sectors. Next, the pit will be divided into three sectors: North (DS2), East (DS3, 4 and 5) and West (DS6, 7 and 1), to discuss the structural geology in further detail.

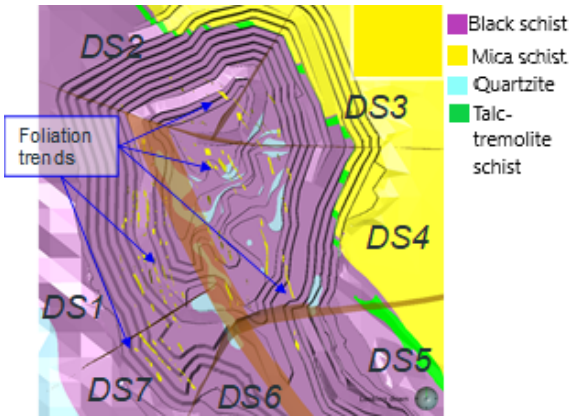

Figure 10: Geotechnical design sectors of Kuusilampi open pit (SRK, 2020b).

Figure 11a shows all joints mapped and logged from the northern black schist area and figure 11b shows the joint sets found in the mica schist areas. In the northern black schist area the main structures are a combination of J3 and J1 (foliation and cleavage), and J2 which create small scale wedge failures. Joint set J5 has been encountered mainly in core logging north of the pit walls. As can be seen from figure

11a, J1 and J3 have a large variation in the dip and dip direction but according to SRK (2020b) this does not affect stability significantly.

In the mica schist areas, J1 and J2 form small scale wedge failures. Joint set J3 is also found in the area but it is not as common in this area as in the black schist area. In addition joint sets J5 and J4 are found in some parts of the mica schist which results in a very blocky rock mass. (SRK, 2020b). The wall strike varies from 30° to 140° but is mainly 75° in the northern domain of the pit. In this area the dip of the bench face is 80°.

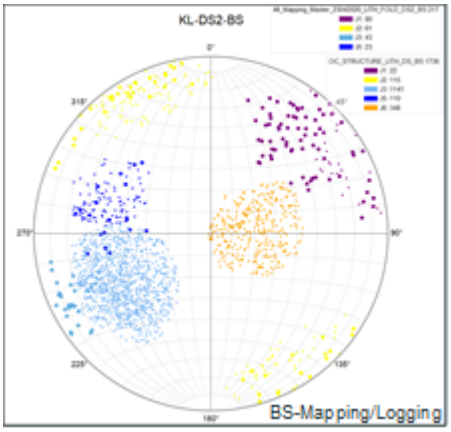

(a) Stereoplot from black schist joint sets in the north

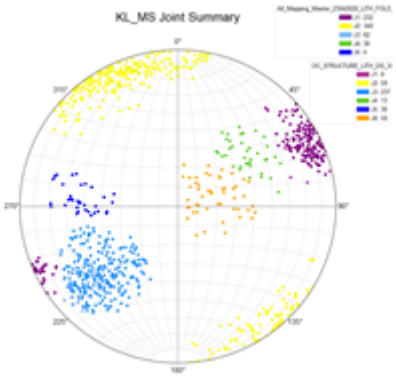

(b) Mica schist joint sets

Figure 11: Stereoplots from Northern part of the open pit. (J1 purple, J2 yellow, J3 light blue, J4 Green, J5 darker blue, J6 orange)(SRK, 2020b).

The joint sets found in the eastern black schist area are shown in figure 12. Joint sets J1 and J3, and J2 are the main joint sets in this area. J2 and J1 create small wedge failures. Although J1 has a very unfavourable direction towards the pit wall no larger failures have been recorded as J1 does not create large planes with the bench (SRK, 2020b). J3 is present in the bench faces but has caused no failures. The strike of the wall varies from 165° to 100° and is mostly around 160° in the eastern domain. In this area the dip of the bench face is 80°.

The western pit wall is currently the most unstable part of the open pit. This is because joint sets J3 and J2 have created bench scale wedge failures. Joint set J1 is also found in this area but it dips into the wall and has not caused any instability issues. The stereoplot of the western domain can be seen in figure 13. The figure shows that J4 and J6 are also found in the area but they only have a minor presence. Wall strike varies mainly from 300° to 365° but close to the interface between DS 6 and 7 the wall direction varies from 200° to 245°. In this domain the dip of the bench face is 70°.

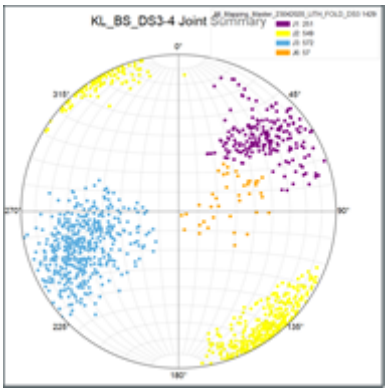

Figure 12: Stereoplot from black schist joint sets in the east (J1 purple, J2 yellow, J3 light blue, J4 Green, J5 darker blue, J6 orange)(SRK, 2020b).

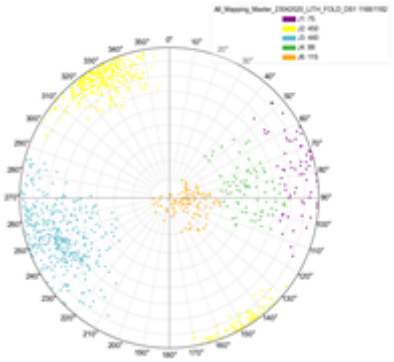

Figure 13: Stereoplot from black schist joint sets in the west (J1 purple, J2 yellow, J3 light blue, J4 Green, J5 darker blue, J6 orange)(SRK, 2020b).

3.3 Rock mass classification systems

RMC systems are widely used to evaluate the quality of the rock mass. However, they have received criticism for consistently failing to predict rock mass failure and producing too optimistic evaluations of the rock mass stability.

RMC systems cannot accurately predict the quality of the rock mass over different domains. However, open pit mines are generally divided into sections for the slope design. These sections group similar rock mass conditions together based on their stability. If suitable presplit designs are found for these design sectors, the presplit designs could be modified based on regional changes in the rock mass conditions.

The design sections of an open pit mine typically account for the discontinuity orientations towards the pit wall and strength parameters. However, the frequency and condition of discontinuities can change significantly within these sections. Thus, using a RMC system that quantifies these parameters could be used to define if a shorter presplit spacing is required or if the borehole pressure or powder factor should be decreased for a certain area.

RQD and Q' have been estimated from most of the geotechnical data at Kuusil-

ampi open pit and they have been interpolated into a geotechnical block model. Furthermore, GSI values have been converted from Q' values and have also been interpolated to the block model. This thesis will study the connection between the rock mass classification of the geotechnical block model and over- and underbreak in presplitting. More recently Laubscher's Mining rock mass rating (MRMR) was adopted by the mine, in addition to the previously used RQD and Q', to evaluate the rock mass quality more accurately.

Table 3 shows the MRMR and Q values for the different design sectors and rock types. Both the MRMR and Q values are in similar range. Although Q values show larger variation, this is expected as Q-system's values range from 0.001 to 1000 whereas RMR only ranges from 0 to 100. The values shown in table 3 suggests that the rock mass quality is better at the Northern to North-Eastern part (domains DS2 and 3) of the open pit than in other domains.

Table 3: Average rock mass quality classifications per design sector and rock type. DS means design sector, MS is mica schist and BS is black schist. (SRK, 2020b).

Domain	MRMR	Q
DS2-MS	55	67
DS3-MS	57	95
DS4-MS	47	13
DS1-BS	46	41
DS2-BS	51	65
DS3-BS	52	83
DS4-BS	44	12
DS5-BS	44	10
DS6-BS	42	9
DS7-BS	43	12

3.4 Hydrogeology

According to SRK's hydrogeological study, the rock mass can be divided into three zones based on hydraulic conductivity. The first zone starts at the bedrock surface and reaches down to 150 meter depth. This zone has the highest hydraulic conductivity and is characterized by higher fracture density and weathering of the rock mass. The second zone is located between 150 and 200 meter depth. This is an intermediate zone between the more highly fractured and weathered bedrock near the surface and the fresh bedrock that is located below 200 meters from the bedrock surface. (SRK, 2020a). These areas have not been observed to affect pit wall stability yet because the open pit currently reaches 180 meters depth at the deepest point.

In the first and second zone, hydraulic conductivity can be locally high because of geological structures and open foliations. In the third zone, water movement is only

associated with open faults and shears which typically have low permeability and are rarely connected. (SRK, 2020a).

SRK (2020a) concluded in the hydrogeological report that no active dewatering system is required at Kuusilampi open pit in the future. The pit water management should only focus on directing the surface waters away from the open pit.

Although slope stability does not require dewatering, the drilling and blasting would benefit from increased drainage because currently drilling is complicated by water on the production levels and borehole collapses occur partly due to the water seepage. Furthermore, blast damage caused by presplitting is increased because of water filled boreholes and production blast holes do not have entirely water resistant explosives which may cause misfires. The bulk emulsion explosive used in the production blast holes has high water resistance towards static water conditions, but dynamic water conditions can cause issues (Maxam blasting solutions, 2021b).

4 Review of previous practice in presplitting at Kuusilampi Open pit

This chapter introduces and discusses the previous practice in presplitting at Kuusilampi open pit. First, the different presplitting parameters that have been used will be introduced and discussed. Then, an attempt is made to find a connection between the rock mass quality, and over– and underbreak in presplitting.

4.1 Previous presplit designs

In 2008 when the mining commenced at the Kuusilampi open pit, presplitting was done with 89 millimeter diameter holes, and 1.0 and 1.2 meter hole spacings were used. The hole inclination used for the most part was 80°. The explosives that were used in presplitting were mainly Forcit's pipecharges. A photo showing an example of the presplit result with these parameters can be seen in figure 14.

When Terrafame took over the operation, the presplitting parameters were kept largely unchanged. However, the explosives were changed to Maxam's Riosplit Wf 32 mm cartridges. This change was at least partly due to the change in the explosives producer. However, there was also problems with unexploded charges when using the pipecharges, which have not been encountered with the current explosives cartridges.

Figure 14: Presplit face from 89 mm diameter presplit holes.

In 2016, Terrafame started utilising 165 mm diameter drill holes and 1.8 meter hole spacing to streamline the drill and blast process. This was the same diameter as the production holes which meant that the same drill rigs could drill the presplit holes

and production holes without any changes in the equipment. Furthermore, there were issues with hole collapses with the 89 mm boreholes, which were reduced with the change to 165 mm boreholes. Concurrently, the explosive cartridge diameter was changed from 32 mm to 45 mm because it was thought that the 32 mm cartridge could not produce sufficient borehole pressure with 165 mm boreholes.

Initially only 15 meter deep presplits were done even with 30 meter high benches. This resulted in a lip in the midpoint of the bench face because the lower part's presplit holes' drilling could not be started sufficiently close to the wall. This can be seen in figure 15a. To combat this, tests were made with 30 meter deep presplits which were largely successful as can be seen from figure 15b. These parameters have been used up to this date.

(a) Two times 15 meter deep presplit face (b) 30 meter deep presplit face

Figure 15: Presplit faces of 165 mm hole diameter and 1.8 meter spacing

All of these presplit designs have produced clean and stable pit walls in good quality rock mass. However, there are some advantages and disadvantages with the different designs. The problem with 89 mm diameter holes is that they bend more easily, because of the less robust drill rods, which reduces the drilling accuracy. Some hole bending can be seen in figure 14 which is a 15 meter high bench face. Compared to the figures 15a and 15b there is less hole bending with 165 mm holes. Thus the

89 mm holes may not be as suitable for 30 meter deep presplits as larger diameter boreholes.

Furthermore, the advantage of using 165 mm diameter presplit holes as described earlier was streamlining of the drill and blast process. This change also reduced drilling meters as the hole spacing was increased from 1.2 meters to 1.8 meters. The process was further improved by the change from two times 15 meter to 30 meter deep presplits. Consequently, the efficiency was improved and costs were reduced.

If we try to consider the difference in produced blast vibrations between the 89 mm diameter hole presplits (1.2 meter spacing and 32 mm Riosplit Wf explosive) and the 165 mm presplits (1.8 meter spacing and 45 mm Riosplit Wf explosive), the differences affecting blast vibrations between these design parameters are as follows

- Difference in borehole pressure 44% higher with 89 mm boreholes
- Charge weight per millisecond 24% lower with 89 mm boreholes
- Charge weight per borehole 49% lower with 89 mm boreholes

The borehole pressures were calculated with equations 4 and 5. The higher borehole pressure should result in higher blast vibrations according to Wang's (2018) findings. However, the lower charge weight per millisecond and per borehole should result in lower blast vibrations. Thus, it is impossible to say which presplit design produces lower blast vibrations as the joint effect of these differences is not known.

Wang (2018) also found that stress attenuation increases when decoupling ratio increases from one to two but decreases when decoupling ratio increases from two to four. Thus, 89 mm holes should result in slightly higher blast vibration attenuation.

4.2 Presplitting success and rock mass quality

4.2.1 Data collection

The rock mass quality will be estimated using a geotechnical block model made by Pöyry. The block model includes GSI, RQD and Q' values that have been interpolated using inverse distance squared method. The block model consists of $25 * 25 * 25m^3$ blocks. The data that was used for the interpolation was collected from core logging.

In order to estimate the presplitting success in different design sectors of the open pit, the amount of over- and underbreak is calculated from a total of 100 meters of presplit wall from each design sector. The method of calculating the deviation between the planned and final presplit face is the same as described in chapter five. The criteria used to select the evaluated presplit faces' are as follows:

- Production blast has been successful in front of the presplit
- No over- or underbreak resulting from failures of large scale geological structures
- Hole diameter 165 mm, spacing 1.8 meters

This criteria was chosen to limit the influence of other parameters to the final bench face and to compile representative data from the previous presplit success. Over- and underbreak due to large scale geological structures were delimited from this study as they can be considered statistically as outliers when considering the result of presplit blasting. Furthermore, the aim is to analyse typical presplit results from the different design sectors to evaluate the typical problems for the different domains.

4.2.2 Results

Figures 16a and 16b show scatter plots of the measured overbreak and underbreak plotted against the block model Q' values for the analysed areas. The overbreak and underbreak volumes are divided by the surface area of the analysed wall to normalise the values for comparison. The points in the plot are coloured based on the design sectors where the analysed walls are located. A further analysis on the selected presplit faces with figures can be found in appendix A. Figures 16a and 16b show that there is no clear correlation between the deviation from the planned bench face and block model's Q' values. There is no notable difference between the block model's Q', RQD and GSI values and no correlation was found between any of these values, and the underbreak or overbreak.

The red lines in figures 16a and 16b illustrate threshold values for overbreak and underbreak, which were determined based on the analysis of presplit faces. The threshold values for overbreak are 0.3 and 0.6 m^3/m^2. Values below 0.3 are presplit faces where there is minor to no overbreak. Values below 0.6 are intermediate values where there is some overbreak and points above 0.6 have major overbreak. The threshold values for underbreak are -0.5 and -1.0 m^3/m^2. Values above -0.5 have minor to no underbreak. Values above -1.0 have some underbreak and points below -1.0 have major underbreak. The presplit faces within the minor underbreak and overbreak range have been very successful. The presplit faces within the intermediate underbreak or overbreak range have been partly successful. The presplit faces within the major overbreak or underbreak range have not been successful.

Figure 16b shows that the underbreak remains largely constant throughout the different design sectors with the exception of design sector six. However, in design sector six only the upper bench part (15 meters) of the presplit wall was visible during this thesis, which may have caused the small amount of underbreak observed as most of the underbreak observed at the 30 meter high bench faces is located at the toe of the bench. This may also be the reason for the relatively large amount

of overbreak observed in design sector six, which can be seen in figure 16a because overbreak is mostly observed at the crests of the bench faces.

The amount of overbreak throughout the design sectors is mainly scattered between 0.1 and 0.4 m^3/m^2 with the exception of the western part of the open pit. In design sectors one and seven, there has been more instability issues and bench faces largely form along J3 foliation which has caused the larger amount of overbreak observed. In other design sectors, the overbreak is located at the crests of the walls and is mainly caused by blast damage.

Furthermore, the foliation has also caused the two largest measured underbreak in DS1 and DS7 shown in figure 16b. Comparing the amount of measured underbreak and overbreak, it can be seen that underbreak is larger in most of the design sectors. However, the amount of underbreak is overestimated in the measurements compared to overbreak, which is why the thresholds for underbreak are also higher. The underbreak values are overestimated compared to overbreak because loose material tends to compile at the toes of the bench faces.

Anyway, underbreak is a larger problem than overbreak at Kuusilampi open pit because most underbreak values are below the first threshold value whereas most overbreak values are located in the minor to no overbreak range (below the first threshold value).

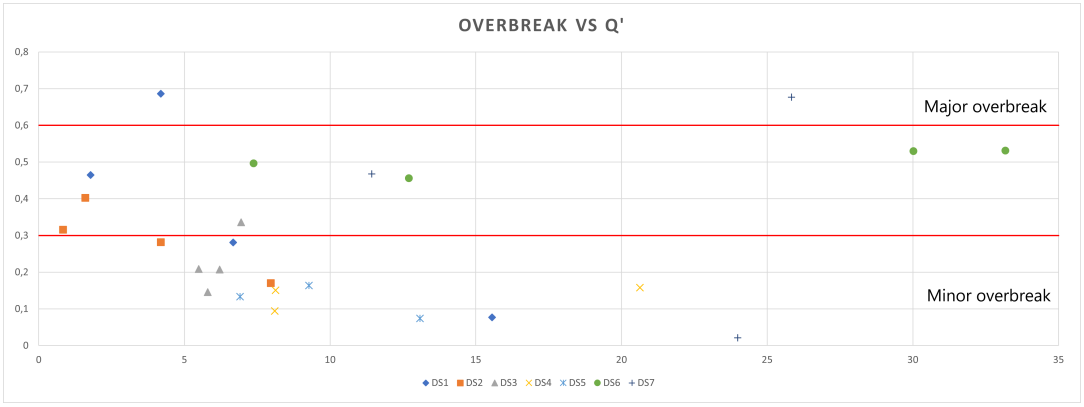

(a)

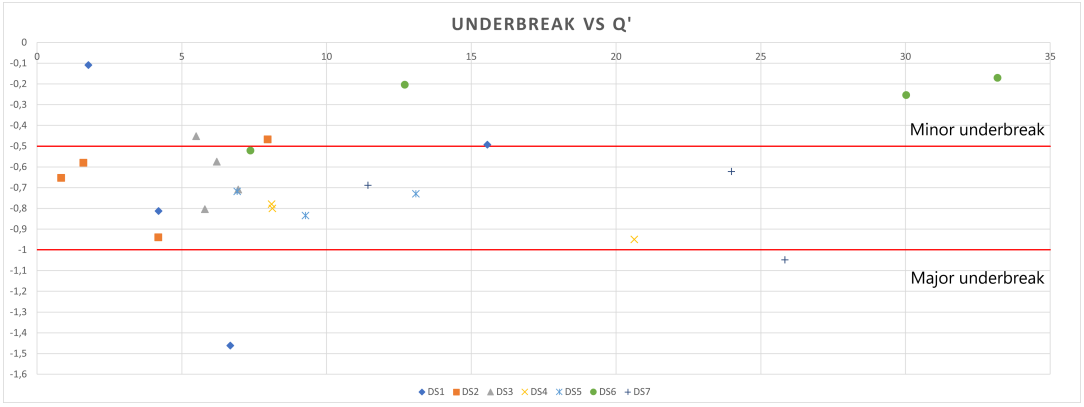

(b)

Figure 16: Scatterplots of the measured overbreak (a) and underbreak (b) (test presplit faces not included) vs block model Q' values. X-axis shows the block model's Q' values for the analysed presplit walls and Y-axis shows the deviation of the presplit wall from planned in m^3/m^2. Point symbols are given according to the design sector, where the wall is located. Red lines indicate threshold values that divide the overbreak and underbreak into minor, intermediate and major ranges.

5 Research materials and methods

This chapter introduces the presplit test process and the data that is gathered during the process. First, a general description of the presplit drill and blast process is given and the information that is documented during this process is introduced. Then, the presplit blast and buffer row parameters and calculated borehole pressures are discussed. Finally, the data analysing process is described in two parts. First, the process of borehole wall image logging is described. Then, the methods of analysing the presplit success are introduced.

5.1 Description of the presplit drill and blast process

The first step is to plan the presplit holes with Surpac mine planning software. This produces a file containing the planned boreholes, which is imported to the drill rig. The drill rig has a GPS positioning system that is used to accurately drill the holes at planned locations. However, most hole deviations from planned are due to surface conditions, that force the drill rig to start the holes from a slightly different position, or hole bending. After the holes have been drilled, some of the holes are surveyed by the drilling contractor to ensure that no major hole collapses have occurred.

Furthermore, the drill rigs record different parameters during drilling, such as penetration speed and applied pressure. This data, also know as Measured While Drilling data (MWD), can be used to estimate the rock mass quality along the borehole, which is done by Terrafame at the site for some of the holes. However, this data is not part of this thesis.

Next, boreholes selected for the video recording are flushed with flocculant mixed with water to ensure that clear images are produced of the recorded holes. The flocculant binds with the particles in the hole and makes them sink into the bottom or flow out with the water which results in a clear image of the walls of the hole.

The video recording of the holes is taken by lowering a camera into the hole with an automatic spool that keeps the speed constant. The depth of the camera is measured constantly and the depth is tied to the video footage. In the beginning the starting dip and azimuth are recorded which can then be used to calculate the orientation of detected joints and any borehole deviation from the planned. Furthermore, the collar position of the recorded holes are surveyed.

Finally, the holes are charged with explosives. The used explosives is Maxam's Riosplit WF, which consists of a detonating cord running inside 0.5 meter long cartridges. During the charging process, these cartridges are used to measure the approximate length of the holes to detect any hole collapses. Water is also detected in this phase as it causes some buoyancy to the explosive cartridges.

Once the presplit wall is visible, the wall is photographed with a drone before scaling and after scaling. Furthermore, the scaling time and used equipment is recorded. At the mine site scaling is done with an extended boom backhoe and impact hammer depending on the location and equipment availability.

The drone that was used for photographing the presplit wall was DJI Phantom 4 RTK. The drone has a 20 Mp camera with a mechanical shutter and a stabilizing gimbal. A 3D image of the presplit wall is constructed by following the steps below:

1. Create and execute a flight plan for the drone
2. Use Pix 4D mapper software to construct the 3D image
3. Tie the 3D figure to the correct location by georeference points

The first step is to define the borders of the area of interest and it is made with mine planning software. This border file is then uploaded to the drone. The drone automatically creates a flight plan according to the border file. This flight plan can be modified but the initial flight plan is generally sufficient.

The used flight plan consists of five flight routes. During the first route, the drone takes images looking directly down. The rest of the flight routes take images with the camera tilted 30° from the vertical. These routes take the images from four different directions, which are illustrated with the black arrows in figure 17. The images are taken so that there is 70 percent overlap between sequential images. Figure 17 illustrates the flight plan, which shows the camera locations for all images used to construct a 3D mesh of the presplit wall. The used flight plan had a flying height of 50 meters which according to the drone's manufacturer results in a 1.66 cm GSD (ground sample distance) in good lighting conditions (DJI, 2021). The 3D images used for the measurements in the historical review part utilized a less accurate flight plan with 100 meter flying height (2.7 cm GSD) and two flight routes: top view and a side view.

The 3D image is constructed using Pix 4D mapper software. All images taken during the flight plan are imported to the software which first does initial processing. During this step, the software finds keypoints from the images and matches these keypoints between images. Furthermore, the camera's parameters are calibrated and an initial geolocation of the model is done based on the drones location information. The photos taken with the drone include the location of the camera in the metadata. DJI states that this has an accuracy of 1.5 cm vertical accuracy and 1.0 cm horizontal accuracy (DJI, 2021).

When the initial processing is done, the surveyed georeference points are imported to the software and the model's geolocation is calibrated by selecting these points from several images. At least three georeference points are marked and numbered around the scanned area and their coordinates are surveyed. Next, the initial processing

step is run again, and a densified point cloud and a textured 3D mesh is created by the software. This 3D mesh can then be imported to Deswik for analysis.

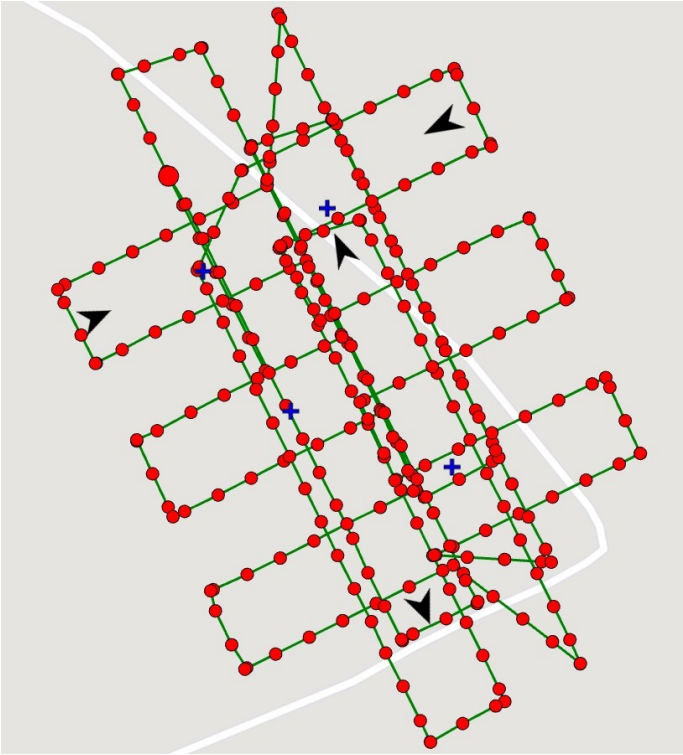

Figure 17: Flight plan from the second presplit test. The blue crosses are georeference points, red circles are camera locations for the images and black arrows indicate the direction of filming.

5.2 Presplit parameters

Four different borehole diameters were considered to be used in the presplit tests. The different diameters can be seen in table 4. These diameters were considered because the used drilling equipment can easily adapt to these without further modifications than a change of the drill bit.

The explosive cartridge used in these presplit tests is 32 mm for the most part. Previously, the mine has used 45 mm explosive cartridges in presplitting, which have been used in one test area as well. This change was made to try and limit the degree of unwanted blast damage the rock mass is subjected to. Table 4 also shows the estimated borehole pressure for the 165 mm borehole with 45 mm explosive cartridge. The rest of the estimated borehole pressures are calculated with a 32 mm explosive catridge parameters.

The presplit spacings that were used were determined mainly based on the powder factor and previous experience with presplitting at the mine. A spacing of 1.2 and 1.4 meters was mainly used in the tests.

The used hole inclinations were selected based on the desired bench face angle. Thus 80° was used for the northern mica schist tests and 70° was used for the western and southern black schist tests. Hole inclinations closer to 60° were considered to be used on the western pit wall because the foliation has a dip of around 60° into the pit in this area. Thus, this presplit inclination should help reduce failures along the foliation. However, drilling holes with such inclination is challenging which is why an inclination of less than 70° was not used.

No stemming is used in the presplit holes and for 15 meter deep presplits 0.5 meters is left uncharged from the collar of the hole. For the 30 meter deep presplits, the holes are charged up to the surface in the tests. Previously, one meter has been left uncharged from the collars of the holes with 30 meter deep presplits and 45 mm explosive cartridges.

The explosives are initiated by a detonating cord running along the presplit line. The detonating cord is typically initiated from both ends to ensure that all holes are detonated. The initiation is done from one end of the presplit and the other end is initiated with a delay so that it functions as a fail safe if there is a failure in the detonating cord. The detonating cord has a VOD of 7000 m/s, which means that with a hole spacing of 1.2 meters adjacent holes are detonated with a 0.17 ms delay which can be considered as simultaneous detonation.

Table 4 show the borehole pressures and spacings for the different borehole diameters that are tested. These values were calculated based on equations 4, 5, 6 and 7. The spacing is taken as two times the expected fracture length estimated by equation 7.

The fracture toughness of the different rock types have not been measured which is why the fracture toughness of the rock types were estimated based on an empirical relation shown in equation 9 (Zhang, 2016).

$$K_{lc} = \frac{1}{6.88} * \sigma_t \tag{9}$$

Where:

K_{lc} = Fracture toughness of rock in $Pa/\sqrt{m}$

σ_t = Tensile strength of rock in Pa

Explosive's parameters were retrieved from Maxam's website (2021a). Instead of the explosive heat the effective energy of the explosive was used to calculate the adiabatic expansion coefficient.

Sandvik (2019) measured the sonic velocities of 10 mica schist samples and 9 black schist samples which were used to calculate an average for the respective rock types. The averages were then used in equation 7. Furthermore, there were 16 measurements

of black schist's tensile strength (4 by Helsinki University of technology (2004) and 12 by Sandvik (2019)) and 11 measurements of mica schist's tensile strength (measured only by Sandvik (2019)), which were also used to calculate averages for the rock types.

Table 4: Borehole pressures and suggested spacings based on equations 4, 5, 6 and 7

Rock type	Borehole diameter [mm]	Coupling ratio	Borehole pressure [MPa]	Spacing [m]
Mica schist	115	0.28	350	1.19
	127	0.25	281	1.12
	140	0.23	227	1.06
	165	0.27	335	1.93
	165	0.19	158	0.97
Black schist	115	0.28	350	1.83
	127	0.25	281	1.73
	140	0.23	227	1.63
	165	0.27	335	2.98
	165	0.19	158	1.48

The difference between the computational spacings for the two rock types are substantial. The difference is mainly due to the difference in tensile strength. There is also a slight difference in the sonic velocities for the two rock types. However, this constitutes to only a minor difference.

The buffer row's hole collars are placed 3 meters away from the presplit. The buffer row is drilled with an inclination of 5° closer to vertical than the presplit holes. This way the burden between the presplit and buffer row at the toes of the holes is roughly 1.5 meters. This is done because the presplit blast has been observed to damage the rock mass at the top of the bench which increased hole collapses in the buffer row.

Otherwise, the used buffer row has the same parameters as the production blast holes. The spacing is typically 5 meters, hole diameter is 165 mm and stemming length is usually 2 meters. The explosive used in the production blast's is Maxam's Riomex 7000 which is an emulsion explosive.

5.3 Analysing the data

5.3.1 Borehole logging

The video recording of the boreholes is done by Astrock Oy. They process the video recording and create images of the borehole walls. They also provide a software that can be used to calculate joint dip and dip direction from the images.

The borehole wall images are used to calculate the RQD, and estimate the fracture

frequency per meter and the number of joint sets for every 3 meters of borehole. Furthermore, a description of the joint condition is also made to evaluate the probability of explosive gases venting into a joint.

The borehole wall images are compared to images of the borehole half-cores from the presplit wall. This is done to assess if blasting has opened some joints more than others. Furthermore, the effect of borehole diameter to the opening of joints is studied based on this data. The video recorded boreholes are surveyed so that they can be located on the scanned presplit surface. The structured 3D mesh allows for the borehole locations to be located on more accurate images of the presplit face which then allows for the comparison to the borehole wall images.

5.3.2 Analysing the presplit face

In this thesis only the upper 15 meters of the 30 meter deep presplits were analysed because the mine deepens approximately 30 meters per year and the schedule for this thesis is approximately half a year.

Using the drone scanned surface of the presplit face and a surface of the planned bench face made from the planned presplit holes, the over– and underbreak is calculated in Deswik CAD using the tool: Surface cut and fill volumes. This tool requires an upper and a lower surface to calculate the volume below the upper surface and the volume above the upper surface, which are the under- and overbreak respectively. These volumes are then divided by the surface area of the bench face to normalize the values for comparison.

The planned surface is digitized from the planned presplit holes and a horizontal part is included at the toe and at the crest of the wall. The horizontal parts are digitized based on the scanned surface's bench level 5 to 10 meters away from the wall, so that all of the overbreak and underbreak is covered by the planned surface and thus included in the calculations. The accuracy of the planned surface is the main source of error in the measurements. Mainly, the amount of overbreak resulting from the overlying bench's subdrilling results in overestimation of overbreak. The crest position can also vary from the measured due to loose material on the bench during drilling which can result in overestimation of the overbreak and underbreak. Furthermore, there is typically loose material left at the toe of the bench face which results in overestimation of underbreak.

Furthermore, Deswik's deviation coloring tool is used to visualize the over and underbreak areas. This tool measures the normal distance between the planned and resulting surface triangles and colours the surface accordingly. An example of such surface can be seen in figure 19.

HCF is calculated by measuring the visible drill hole half cores in Deswik. The sum of the visible borehole half-cores are divided by the borehole lengths observed during

charging of explosives. Thus, the total hole lengths do not account for the collapsed parts of the holes. Pictures are also used to help detect the locations of the visible half-cores. The hole lengths are rounded to half a meter accuracy.

6 Results

This chapter discusses the results obtained in the experimental part of this thesis. First, the test areas are described and each test is examined separately. Then, the test results are summarized. Figure 18 shows the locations of the test areas on a map of the open pit. Table 5 lists the presplit parameters used in the tests. The test column indicates the test location shown in figure 18 and part of the test area e.g. test MS 2.1 is the first part of the second mica schist test.

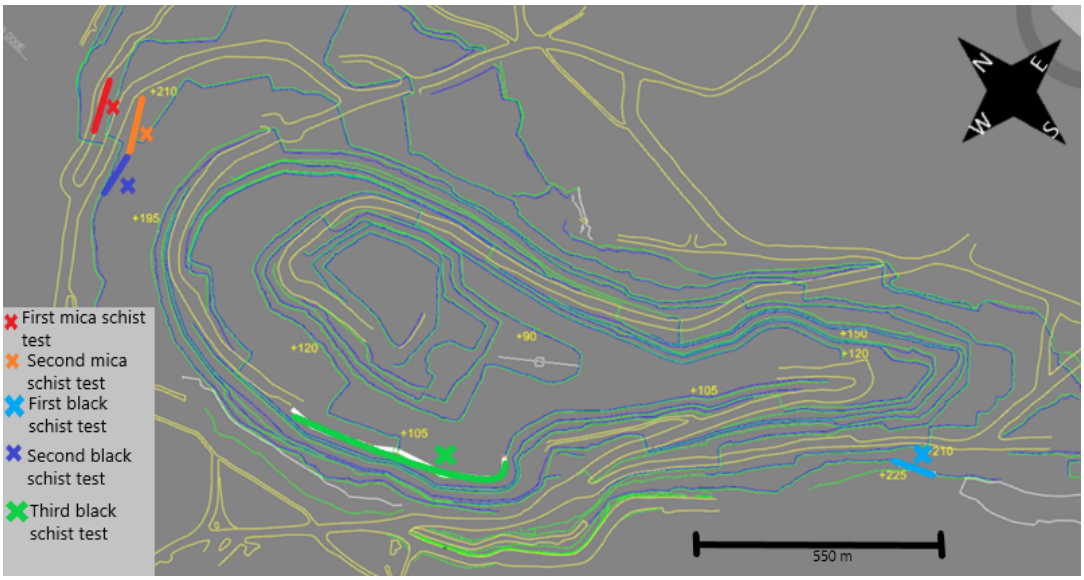

Figure 18: Map of the open pit showing the locations of the test areas. The numbers (e.g. +90) in the figure indicate the altitude in meters above sea level.

Table 5: Presplit test parameters

Test	Rock type	Borehole ⌀ [mm]	Spacing [m]	Inclination [°]	Explosive ⌀ [mm]
MS 1.1	Mica schist	115	1.2	80	32
MS 2.1	Mica schist	165	1.4	80	32
MS 2.2	Mica schist	165	1.2	80	32
BS 1.1	Black schist	115	1.2	70	32
BS 1.2	Black schist	127	1.2	70	32
BS 2.1	Black schist	165	1.4	80	32
BS 3.1	Black schist	165	1.2	70	32
BS 3.2	Black schist	165	1.2	70	32
BS 3.3	Black schist	165	1.8	70	45

6.1 Mica schist

6.1.1 First test

This presplit test was conducted in the northern mica schist domain (design sector 2) of the open pit near ground surface. The presplit was done to the side of a ramp which is why the wall height gradually increases from 3 meters to 15 meters. The analysed area was restricted to the part with a wall height of more than five meters. Thus, 30 meters of the presplit wall was left out of examination because in this area crest damage dominates the results and no representative result of the presplit exists. The presplit parameters used in this test are listed in table 5, row MS 1.1.

The rock mass in this area is good to very good according to the rock mechanical block model and the borehole video logging. Video recording was taken from ten boreholes in this presplit line. In this area J2 joint set is the most important for presplitting because the orientation of joint set J2 towards this presplit line is almost parallel.

Before scaling, very little overbreak was observed which is typical for mica schist in the Kuusilampi open pit. A presplit plane was created for the most part of the wall which could be seen in the wall before scaling. However, there were a lot of visibly loose blocks in the crest of the wall which came down during scaling and revealed some overbreak.

Figure 19 visualizes the overbreak and underbreak in the final wall after scaling. The first meter from the top of the wall has a lot of the overbreak, which can be accredited to subdrilling of the overlying bench blast. However, the area with the most overbreak, which can be seen in figure 19 at the black arrow, is the result of very blocky rock mass. This area can also be seen in figures 20a and 20b. Joints from J1, J2 and J5 joint sets were identified and also a J3 fault is in the final wall in this area. The lower rock mass quality in this area was not reflected in the rock mass classifications of the geotechnical block model.

The second area with the most overbreak resulted from joint J2 dipping into the pit with a dip of approximately 60°. This joint's strike is close to parallel to the wall. This area can be seen in figure 19 and in figures 22a and 22c, at the blue arrow in all figures. In this area a presplit plane was created in front of the discontinuity which can be seen in figure 22a. However, figures 22b and 22c show that the final wall after scaling merges to the J2 joints. Figure 22a also shows that the rock mass at the crest has moved relative to the rock mass below (boreholes are not aligned). The most probable cause for this movement is the production blast, which has caused some bulk movement damage in this area. However, it is unlikely that this plane failure could be prevented through more careful blasting because of the very unfavourable location and orientation of the joint plane.

Figure 21 shows an image of the borehole wall, where one of the joints that is seen in the presplit wall after scaling, can be seen. In the figure, a tightly spaced joint set can be seen. Furthermore, the yellowish line seen in the figure is most likely pyrite (and other sulfide minerals). The same joint set was identified in multiple boreholes and also a very similar joint set could be identified in other borehole images in this area, which can also be seen in the final wall before and after scaling. These joints have a very similar dip and strike to the presplit plane and these joints intersect multiple adjacent boreholes, which is the most probable reason why these joints form the final wall.

The area shown on the left side of figure 22c had no water in the holes during charging. In this area the presplit has also been very successful. The presplit success in this area could be partially due to the dry boreholes. However, it can also be because the rock mass quality is favourable and joint set J2 is not present in this area.

The area with the most underbreak in this presplit area can be seen on the right side of figure 19 at the red arrow. This area can also be seen in figures 22a and 22b. Most of the underbreak is focused in the toe of the wall. Some underbreak is also present in upper part of the wall in this area. The underbreak has been most likely caused by joints belonging to J1 joint set venting the gases from the production blast and the buffer row. It is difficult to determine if a presplit plane has been created in this section. However, visual inspection of the final wall suggests that the discontinuities have prevented the creation of the presplit. Especially densely located J2 jointing has probably vented the gases from the presplit blast which has caused the presplit to fail partly.

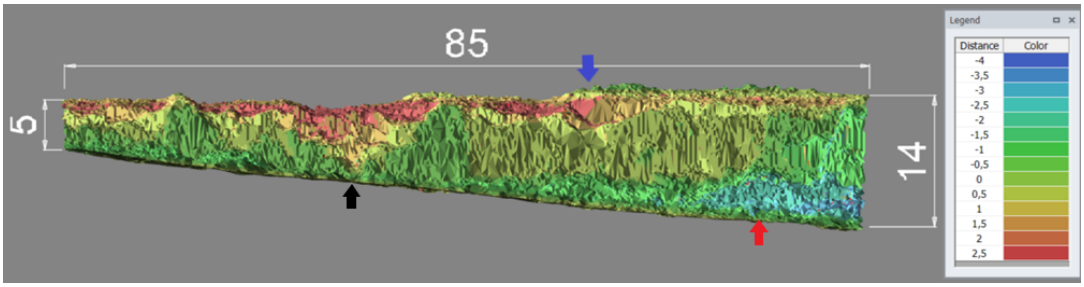

Figure 19: The first mica schist test presplit (MS 1.1) wall after scaling colored according to deviation from planned in meters. Negative numbers indicate underbreak and positive numbers overbreak. The height and length of the wall is shown in meters in the figure. The arrows are reference points for the different figures in this chapter.

In conclusion this presplit test was reasonably successful. The overbreak was mainly due to unpreventable jointing and blast damage from overlying bench blast. The underbreak was mainly due to the buffer row failing to provide sufficient breakage up to the presplit.

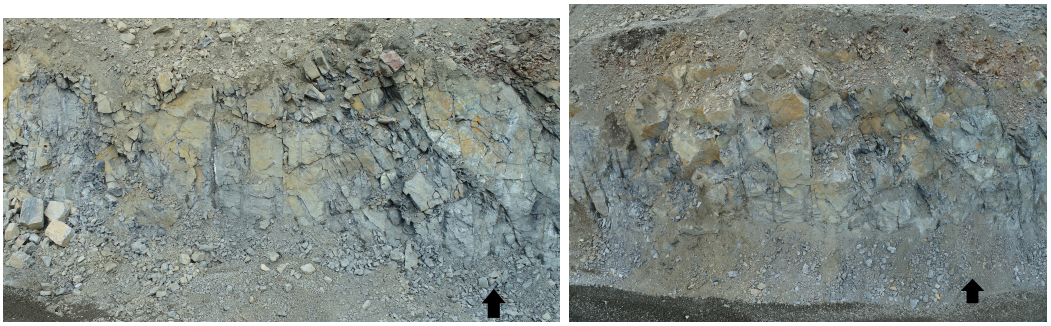

(a) (b)

Figure 20: Photos of the presplit wall before scaling (a) and after scaling (b) from the first mica schist test area (MS 1.1). The arrows are reference points between the figures in this chapter.

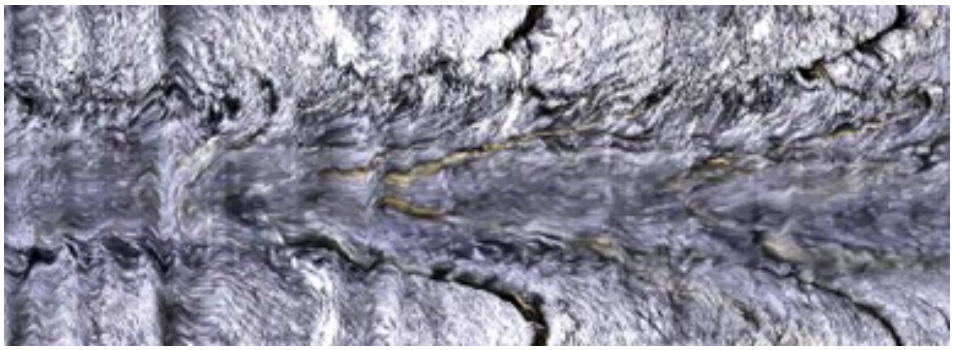

Figure 21: Borehole image from the first test in mica schist. This hole is located at the green arrow in figure 22c. The left side of the image is located at 3.9 meter depth from the hole collar and the right side at 4.9 meters. The y-axis in this figure ranges from 0° to 360° from the bottom to the top

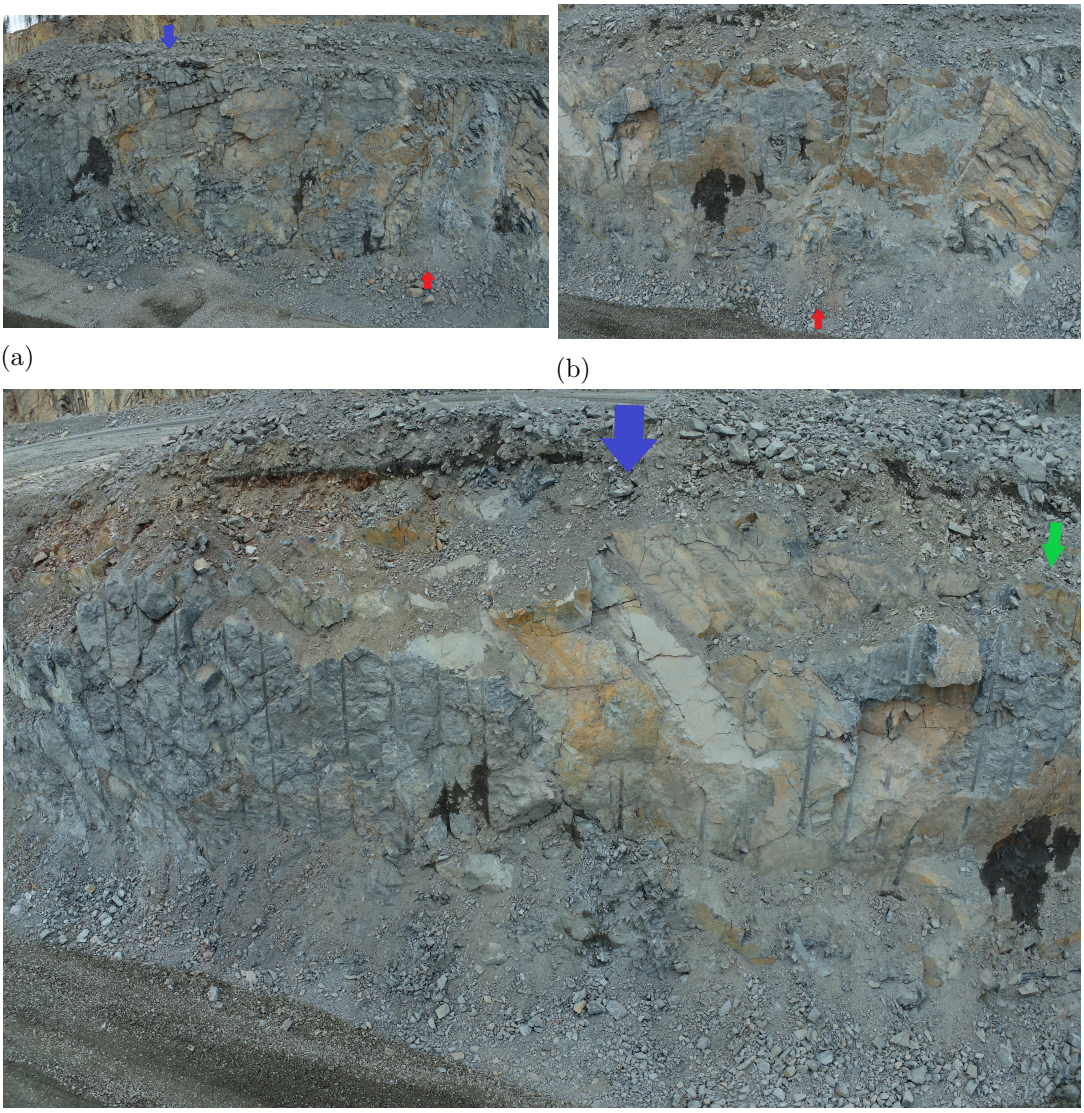

(a)

(b)

(c)

Figure 22: Photos of the presplit wall before scaling (a) and after scaling (b and c) from the first mica schist test area (MS 1.1). The different color arrows are reference points between the different figures displayed in this chapter except for the green arrow which shows the collar position for the borehole shown in figure 21.

6.1.2 Second test

This test presplit was located in the northern mica schist area (design sector 2) of the open pit. The presplit was 30 meters deep but only 15 meters of this was analysed because of schedule constraints. This presplit test area used two different borehole spacings. The first part of the presplit test, seen in figure 24a, used borehole spacing of 1.4 meters and the second part of the presplit test, seen in figure 24b, used borehole spacing of 1.2 meters. All the presplit parameters used in this area are listed in table 5, rows MS 2.1 and MS 2.2. Furthermore, an overview of this test area is provided in figure 23.

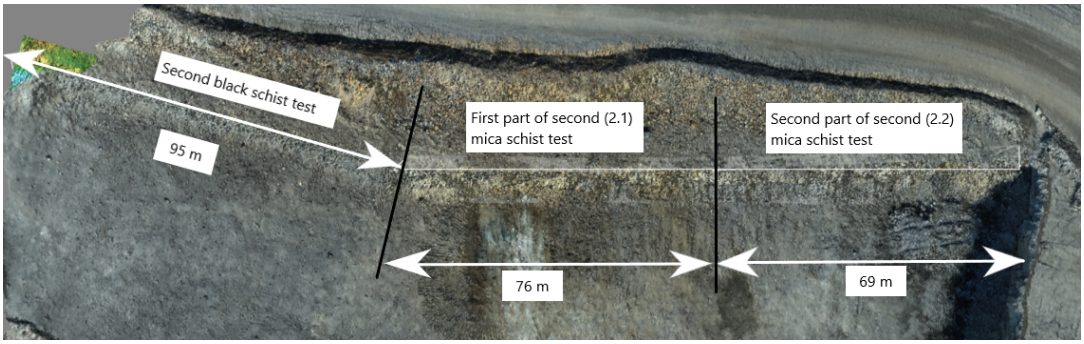

Figure 23: Top view of the second mica schist test area (MS 2.1 and 2.2). Second black schist area (BS 2.1) is also shown in the figure.

The rock mass quality in this area according to the geotechnical block model is good. The rock mass quality based on visual appearance of the presplit face is generally good as well. There are two areas where the rock mass is more densely jointed and thus has lower quality based on the visual appearance of the wall. The first area is on the left side of figure 25 at the mica schist-black schist contact, where there is also the talc-tremolite schist domain. The second area is on the right side of figure 25 and figure 24a, where there is some overbreak at the crest of the wall and slightly more underbreak at the toe of the wall. Joints belonging to J3, J2 and J1 joint sets can be identified from the presplit face in this test area. Borehole video material could not be obtained from this presplit area due to tight production schedule.

The overbreak and underbreak after scaling, in the first part of this presplit test, are visualised in figure 24a. Furthermore, figure 25 shows a picture of this presplit face after scaling. These figures show that the presplit has been successful for the most part as the borehole half cores are largely visible and for the most part the wall does not deviate a lot from the planned. There is some underbreak at the toe of the wall for almost the entire length of the wall, which is most likely caused by the buffer row. However, there is little overbreak in this area, which is only located at the crest of the wall and is partially caused by the subdrilling of the overlying bench blast. There was no significant need for scaling at this presplit face. However, some scaling was done to the wall on the right side of figure 25, where there was some underbreak at the wall after blasting.

Figures 24a and 25 show that there is slight overbreak at the contact between mica schist and black schist. However, the talc-tremolite schist has not affected the presplit quality adversely although the talc-tremolite schist has significantly lower strength than black schist or mica schist. The mica schist is also more densely fractured at the contact which has caused most of the overbreak in this area.

In figure 25, it can be seen that J2 joints, that have a very similar dip and dip direction to the wall, are present in this area of the wall. However, no significant failures have been caused by this jointing, which suggests that the presplit has done very little damage to the remaining rock mass. However, the joints could also have higher strength or small persistencies, which would have prevented any larger rock mass failures.

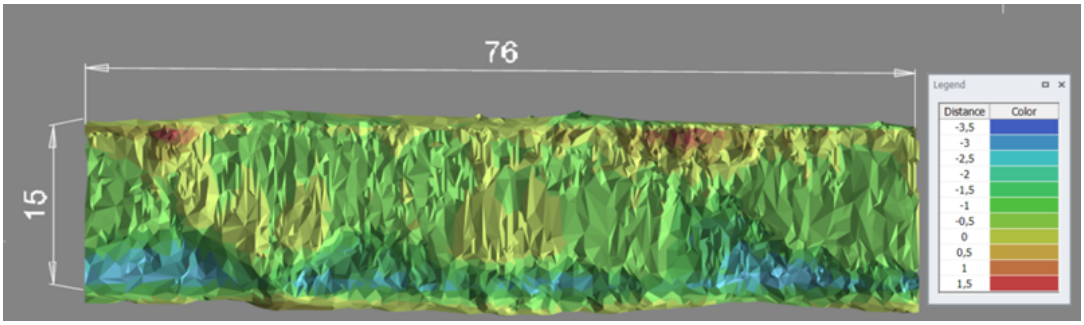

(a)

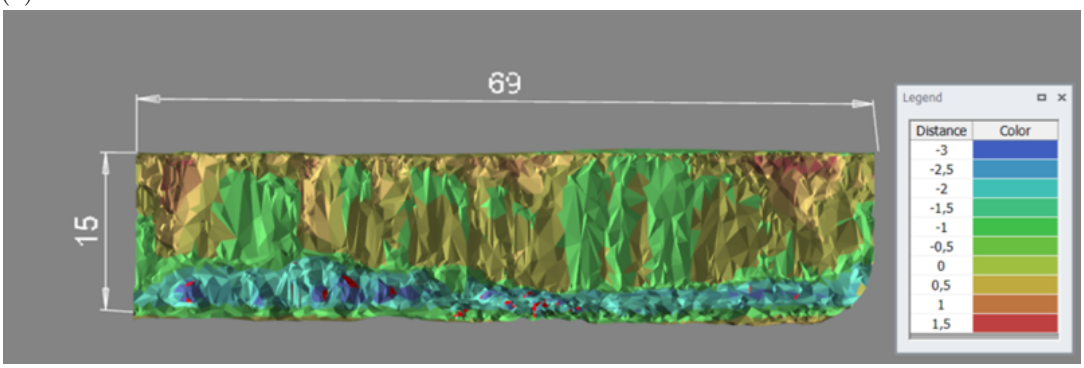

(b)

Figure 24: The second mica schist test presplit wall after scaling colored according to deviation from planned in meters. Figure a shows the first part of the presplit blast (MS 2.1) and figure b shows the second part of the presplit blast (MS 2.2). Negative numbers indicate underbreak and positive numbers overbreak. The height and length of the wall is shown in meters in the figure.

Figure 26a shows an area of the presplit wall where five out of eight presplit holes, that were drilled in this area, collapsed at the collar and were not charged with explosives. Furthermore, four of these collapsed holes were adjacent and thus the spacing between the charged presplit holes was seven meters. It is very unlikely that a presplit plane could be created in this area because of these hole collapses. However, in this area there is very little overbreak or underbreak and even some presplit borehole half cores can be seen in the wall. Figure 26b shows an area where

Figure 25: First part of the presplit test after scaling (MS 2.1).

the presplit has been successful for comparison to figure 26a. There is a difference in the visual appearance of the wall between these figures. The successful presplit face has a cleaner visual appearance than the area with the collapsed boreholes. However, the wall area in figure 26b has more underbreak. This highlights the effect of the buffer row on the observed presplitting success as the failed presplit is better according to deviation from planned in this case.

(a) (b)

Figure 26: A comparison between a successful presplit face (b) and a failed presplit face (a) in the second mica schist presplit test area (MS 2.1). Figure a shows an area where 5 out of 8 boreholes (drilled in this area of the wall) collapsed at the collar and were not charged with explosives. Figure b shows an image of a successful presplit for comparison.

The second presplit blast in this test area produced a clean presplit wall, which can be seen in figure 27b. However, the presplit wall was not visible after blasting and

required a significant amount of scaling. Most of the presplit wall was revealed after scaling with a backhoe. However, a hydraulic hammer was also used to remove some underbreak that was left at the wall after the scaling with the backhoe. Figure 27a shows a picture of the wall before scaling, where it can be seen that there is a lot of underbreak at the face and the rock mass is very broken at the face. Thus, the buffer row has not functioned sufficiently well in this area. It has broken the rock mass up to the presplit plane, which is indicated by the fact that most of the presplit face was revealed by scaling with a backhoe. However, the buffer row did not remove the rock from the presplit. This may have been caused by too high confinement which would have been the result of the production blast not providing sufficient throw to the rock mass. This theory is supported by observations made during loading of the rock from this blast. It was observed that the rock mass was tightly packed and difficult to load with the backhoe.

The underbreak and overbreak after scaling, in the second part of the presplit, is visualised in figure 24b. The figure shows that there is some overbreak at the crest of the wall which has been caused by subdrilling of the overlying bench blast. Furthermore, there is some overbreak that has been caused by wedge failures from J2 and J1 jointing, which can also be seen in figure 27b. One of the wedge failures is caused by J2 and J3 jointing. Figure 27b also shows that there is potential for larger failures along the J2 jointing as traces of the J2 jointing can be seen to continue further than the failures that are currently seen.

Figure 24b also shows that there is some underbreak at the toe of the wall for the entire length of the wall. However it can be seen in figure 27b that the underbreak is overestimated on the right side of the figure as there is some loose material at the toe of the wall.

In conclusion, this presplit test was very successful. There was very little overbreak observed in this presplit face. Furthermore, presplit borehole half cores are visible for the most part at the bench face. In addition, the underbreak and required scaling was due to the buffer row that was unsuccessful.

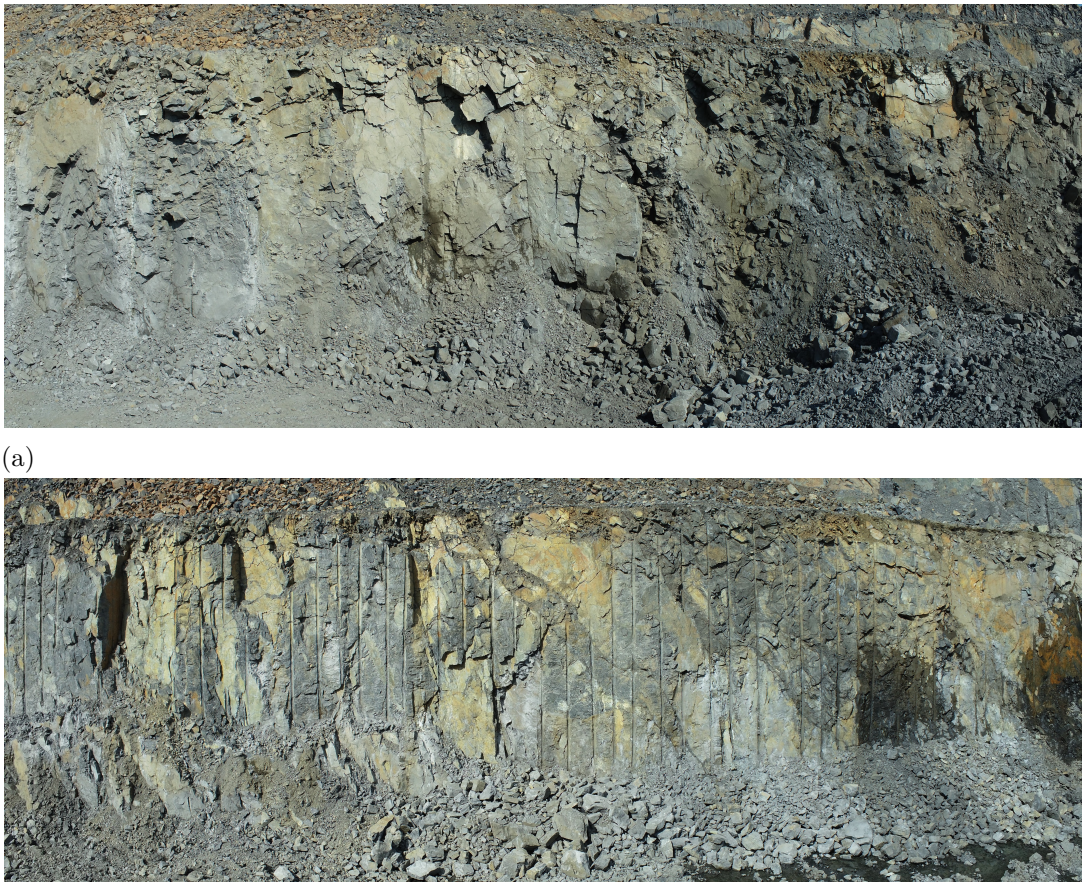

(a)

(b)

Figure 27: Second part of the presplit test before scaling (a) and after scaling (b) (MS 2.2).

6.2 Black schist

6.2.1 First test

This presplit test was located in the south-eastern part of the open pit in design sector 6 at the bedrock surface. The presplit height was 15 meters. Presplit parameters used in this test are listed in table 5, rows BS 1.1 and BS 1.2. The planned presplit holes can be seen in figure 28. The blue line in figure 28 shows where the hole diameter changes from 115 mm to 127 mm (on the left side of the line hole diameter is 115 mm). The presplit was blasted in two parts and the black line in the figure shows where the first blast ended and second started (the presplit was blasted from left to right). Furthermore, the bright green lines are located above the boreholes that were video recorded. In total 16 holes were recorded from this presplit. The overbreak, underbreak and HCF percentage was calculated separately for the first and second presplit blast.

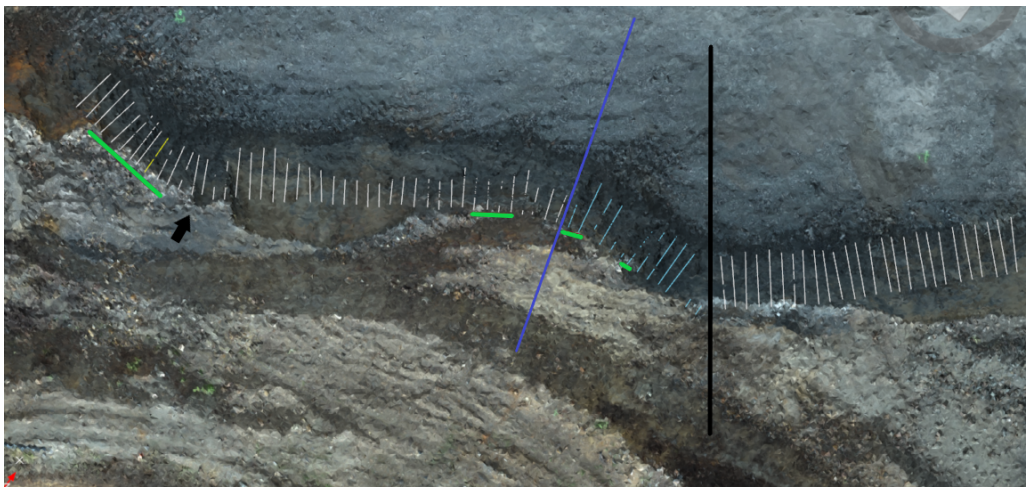

Figure 28: Top view of the the first black schist presplit test (BS 1.1 and 1.2). White lines illustrate designed presplit holes (115 mm holes left of the blue line and 127 mm holes right of the blue line, black line shows the border between blast one and two). The black arrow functions as a reference point between figures 29 and 30.

The rock mass quality in this area according to the rock mechanical block model is fair. However, there was very little information of the rock mass quality close to this area. According to the borehole video logging the rock mass is fairly competent and not highly fractured. However, there are two faults that were detected in the borehole wall images (one of which is shown in figure 32b) and the rock mass in this area is weathered to some degree. Furthermore, the rock mass quality in the second presplit blast area was very poor with highly weathered rock mass and tightly spaced J3 foliation. This change was not reflected in the geotechnical block model's rock mass classification.

The overbreak and underbreak observed in the first part of the presplit is visualized in figure 33a. The overbreak was the result of J3 and J2 joints that created one

larger wedge failure (red area in figure 33a) and two smaller wedge failures (yellow areas on the right side in figure 33a. These failures are largely unpreventable through improved blasting and will most likely happen without rock bolting. This area of the presplit face can also be seen in figure 29.

Figure 29: Photo showing an overview of the first part of the presplit wall in the first test in black schist (BS 1.1). The black arrow functions as a reference point between figures 28 and 30.

There is only one area with underbreak in this presplit face which is in the first part of the presplit and is located at the toe of the wall. In this area the bench face has been created along the foliation. This presplit face did not require scaling because of the small amount of underbreak observed.

On the left side of figure 28 the boreholes (right side of figure 33a) have smaller spacing at the toe, because of the shape of the wall, which shows signs of too high explosive charging in the presplit face in this area, which can be seen in figure 30. This is partly caused by J2 joints that are also present in this area as well and can be seen in the figure 30 especially in the lower part.

Furthermore, in this area of the presplit wall, free face was too close to the presplit which caused the blast wave from the presplit blast to reflect back as a tensile wave which resulted in some spalling from the bench face. Furthermore, one joint was opened during the presplit blast which made the production bench drilling more difficult. This joint and some spalling can be seen on the right side of figure 30.

Figures 32a and 32b show an image of a joint before blasting (figure 32b (a borehole wall image)) and after blasting (figure 32a (presplit wall image)). This joint has a similar dip and dip direction to the joint plane that has caused the large wedge failure on this presplit face. Furthermore, from the borehole image it can be seen that the joint looks very open (the joint opening has a length of 15 cm). However, this joint has not caused failure as of yet. Furthermore, a clean presplit face has been created in this area of the wall, which suggests that this joint did not vent the explosive gases from the presplit blast. Although, it could be expected that this joint

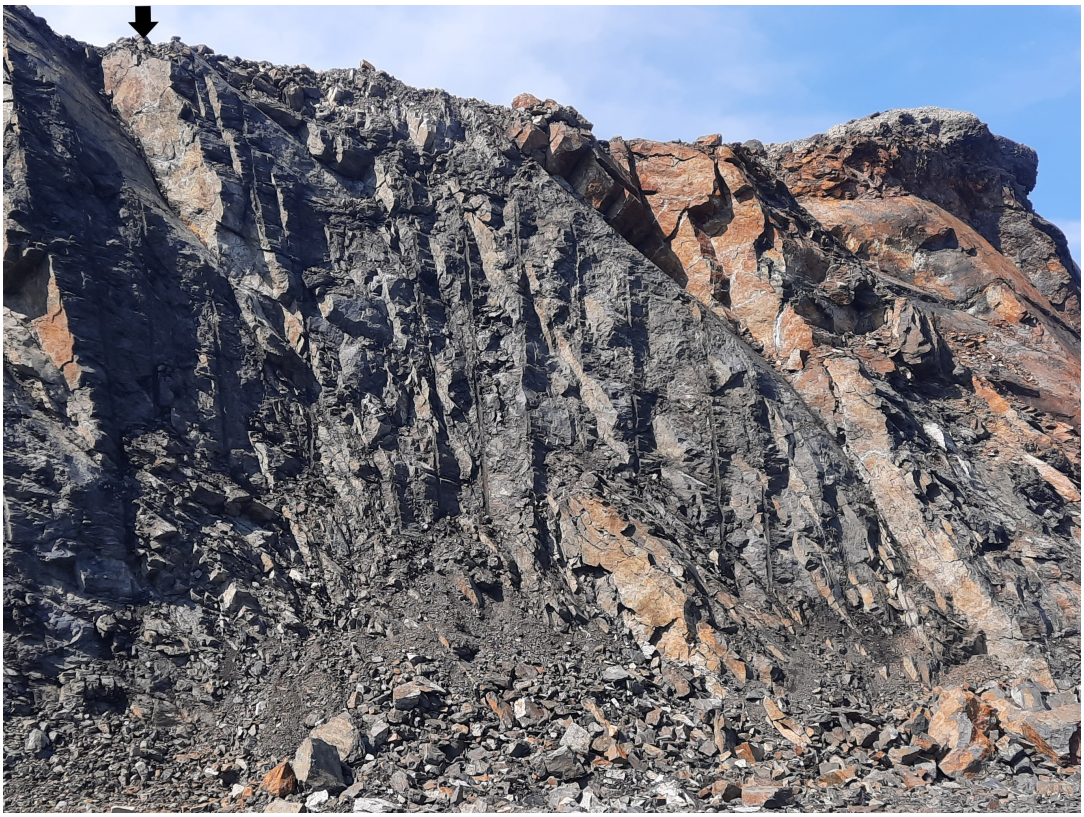

Figure 30: A more detailed photo of the presplit face from the left side of figure 28. The black arrow functions as a reference point between figures 28 and 29.

would provide the path of least resistance for the explosive gases.

In the second part of the presplit, there was practically no underbreak because the bench face adhered to J3 jointing which resulted in overbreak. This is illustrated in figure 33b. On the right side of the figure 33b, there were a few borehole half-cores visible but already in this part the bench face mostly merged with the foliation. On the left side of the figure 33b, the rock mass quality is significantly lower because of very frequent J3 foliation and weathering which are the main causes for the overbreak. A photo of this area can be seen in figure 31. Due to the large amount of overbreak and the wall adhering to the foliation no scaling was required at this bench face.

Although there is a significant difference in overbreak between the 127 mm hole and 115 mm hole presplit areas, the cause for this is the rock mass quality and not the hole diameter. Thus, no difference in the presplit result could be found between 115 mm holes and 127 mm holes.

Figure 31: Photo showing an overview of the second part of the presplit wall in the first test in black schist (BS 1.2).

(a) (b)

Figure 32: Comparison of a joint in an image of the presplit wall (a) and in a borehole image (b) in the first part of the first test in black schist (BS 1.1). Figure a, red arrow shows the starting location of the recorded borehole shown on the right. The red circle highlights the joint shown in the borehole image. Figure b, top of the image starts from 4.3 meters and bottom of the image is at 5.3 meters from the top of the bench. The x-axis in figure b ranges from 0° to 360° from the left to the right.

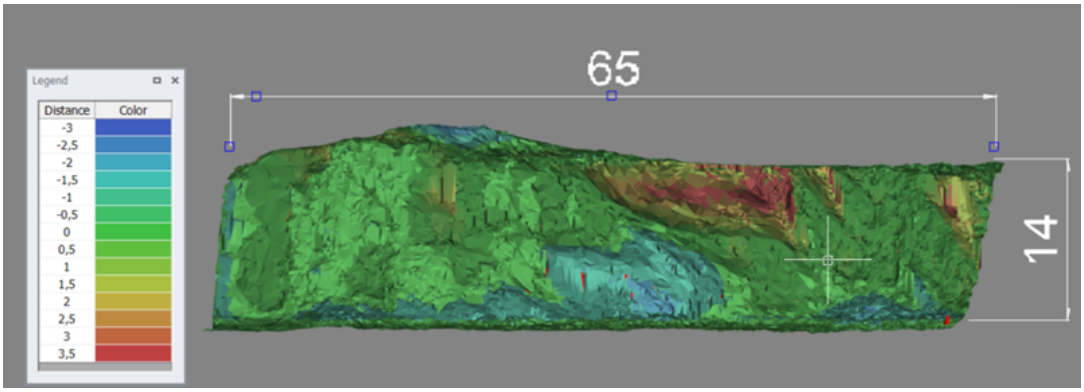

(a)

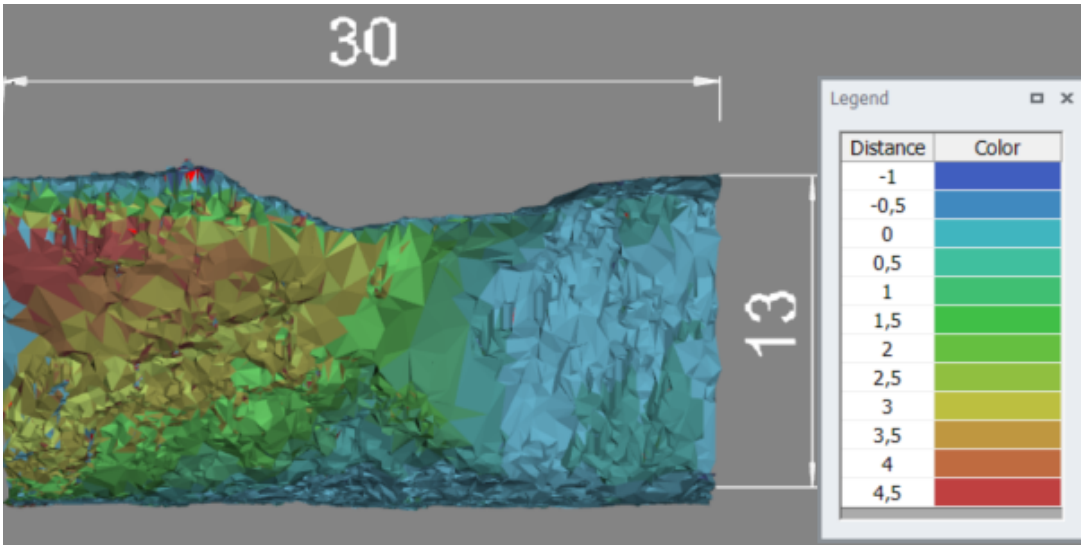

(b)

Figure 33: The first black schist test presplit wall colored according to deviation from planned. Figure a shows the first part (BS 1.1) and figure b shows the second part (BS 1.2). Negative numbers indicate underbreak and positive numbers represent overbreak in the color scale. The length and height of the wall is shown above and next to the wall in meters

6.2.2 Second test

This presplit test was located in the northern part of the pit in design sector 2. A 30 meter high presplit was made but only 15 meter (i.e. the first bench) was analysed in this thesis due to schedule constraints. The presplit parameters used are shown in table 5, row BS 2.1.

The rock mass quality in this area according to the rock mechanical block model is fair to good. Borehole image logging is not available from this area due to a tight production schedule. The contact between black schist and mica schist is located very close to this presplit face on the eastern side (right side of figures 34 and 35). Talc-tremolite schist that is found in the contact between mica schist and black schist can be seen on the right side of figure 35 (the white powdery material).

Joints belonging to joint sets J1, J3 and J6 can be seen in the presplit face. These joints are favourably oriented in relation to the bench face and have not caused any issues for the blasting. Furthermore, these joints are closed which is why these joints have only caused some surface roughness to the bench face.

Joints belonging to J2 joint set, which causes the most overbreak in this area of the open pit, can be found only in the western part of this bench face. In this area, there is minor overbreak as can be seen in figure 34 (red area on the left side of the figure). The overbreak is also partly due to the shape of the wall which can be seen in figure 35. There is a sharp corner at the end of this bench face, which cannot be expected to stay intact after blasting. Otherwise, no overbreak can be found in the presplit face apart from minor crest damage.

In this presplit face, underbreak can be found mainly at the western and eastern ends of the presplit face (left and right ends of figures 34 and 35 respectively). At the western end (left side of the figures) of the presplit the underbreak is only at the toe of the wall and is probably due to the buffer row. The buffer row has most likely vented the explosive gases through the side of the bench along the J2 joints.

At the eastern side (right side of the figures) of the presplit the underbreak has been most likely caused by the talc-tremolite schist which can be seen in figure 35 (the white powdery rock). The talc-tremolite schist has probably vented the gases from the production blast holes and thus caused the underbreak.

The presplit has been very succesful in this test. A presplit plane seems to have been created along the entire bench face. Furthermore, it seems that the talc-tremolite schist has not affected the presplit blast greatly and a presplit plane has been created in this area as well. Furthermore, this presplit face did not require scaling because the presplit face was sufficiently clean.

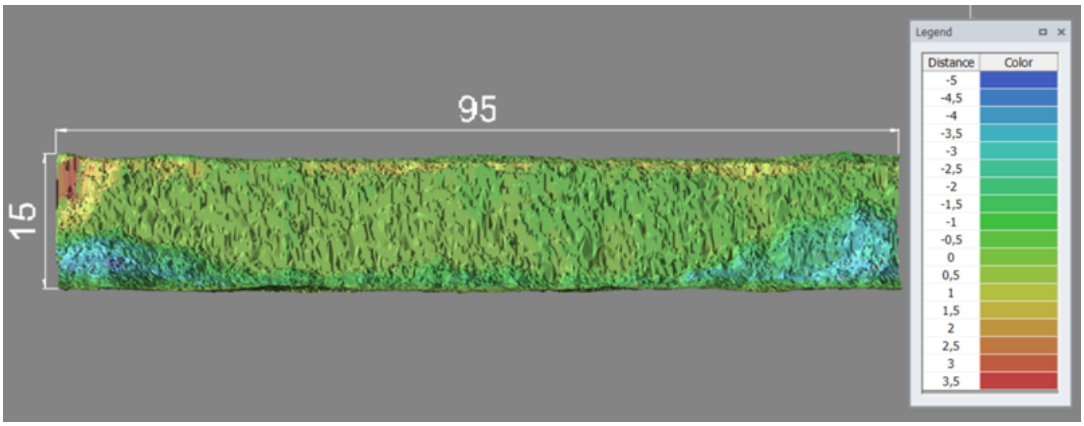

Figure 34: The second black schist test presplit (BS 2.1) wall colored according to deviation from planned in meters. Negative numbers indicate underbreak and positive numbers overbreak. The length and height of the wall are shown above and next to the wall.

Figure 35: Photo of the second black schist test presplit face (BS 2.1).

6.2.3 Third test

This presplit test area is located at the western pit wall (in design sectors 1 and seven). A 30 meter deep presplit was made but only the upper bench part was analysed in this thesis due to schedule constraints. This presplit test area is divided into three parts for analysis, which are shown in figure 36. The black lines in figure 36 delimit the different parts of the test area. The first area is on the right side (south side) of figure 36. The presplit parameters used in the parts can be found in table 5, rows BS 3.1, BS 3.2 and BS 3.3.

The rock mass quality varies from very poor to good according to the geotechnical block model's Q' values, but the rock mass quality is mainly fair to good based on the block model. Based on visual appearance of the presplit face the rock mass quality is challenging for the most part. There are areas with low quality rock mass i.e. densely fractured with mainly J3 and J2 jointing, in some areas J6 jointing can also be identified. Furthermore, in areas where the rock mass is not densely fractured based on the appearance of the bench face, there is J3 jointing that produces overbreak and underbreak to the presplit face. In this presplit test area, the borehole video recording failed due to hole collapses during washing of the holes and tight production

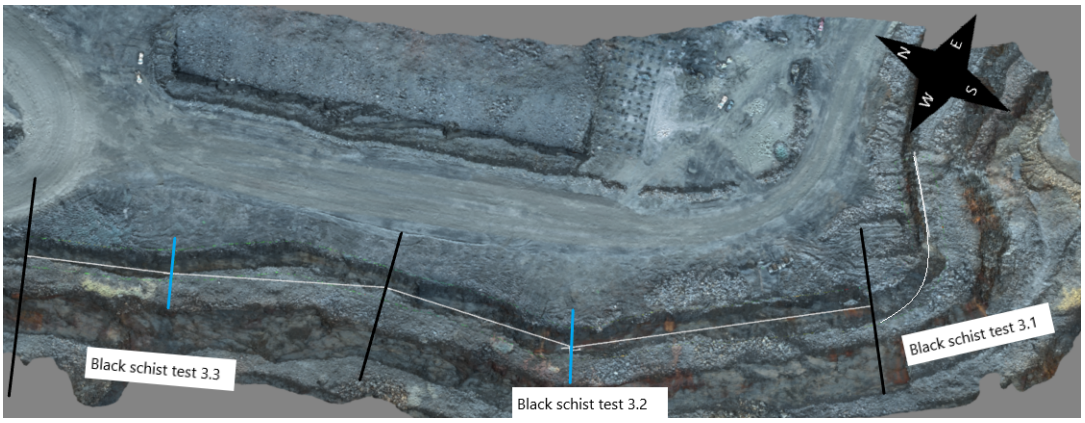

Figure 36: Top view of the third presplit test area. Black lines in the figure outline the different parts of this test area. The first part is located on the right side of the figure. Blue lines illustrate the contact between figures 38a and 38b, and figures 39a and 39b.

schedule.

The first presplit part is shown in figure 41a and figure 37, which shows the deviation of the bench face from planned. It can be seen in these figures that the presplit has been very successful on the left side of the figures. This successful area has a very different wall dip direction compared to the rest of this presplit test area as can be seen in figure 36. The wall dip direction is more favourable towards the J3 jointing, which is one of the reasons for the presplit success in this part. However, this wall dip direction is nearly parallel to J2 jointing and a J2 joint plane can be seen in figure 41a, where there is minor underbreak. However, the J2 jointing has not reduced the presplit face quality significantly most likely because it is not present in this particular area abundantly.

The rest of the first presplit part has not been successful. There is a significant amount of overbreak from the crest of the wall. However, there is practically no underbreak contrary to figure 37. This underbreak is actually loose material left at the toe of the wall as can be seen in figure 41a. The overbreak in this presplit part is a result of mainly two factors. The first factor is the shape of the wall, which would be challenging to achieve even in good quality rock mass because the confinement of the production blast increases as the blast holes close to the corner only have approximately a 90° angle, where it can discharge the rock, contrary to a 180° angle a normal blast hole has at a straight part of the wall. Thus, the blast holes at the corner of the wall are prone to cause more unwanted blast damage. The second factor is the dense J3 jointing, which can be seen in figure 41a, where traces of J3 joint planes can be seen.

The second presplit part can be seen in figures 41b, 41c, 38a and 38b. Figures 38a and 38b show the deviation of the bench face from the planned. The part of the wall shown in figures 38a and 41b has a lot of crest failures along J3 foliation, which strikes nearly parallel to the wall in this area. Preventing such failures may be practically

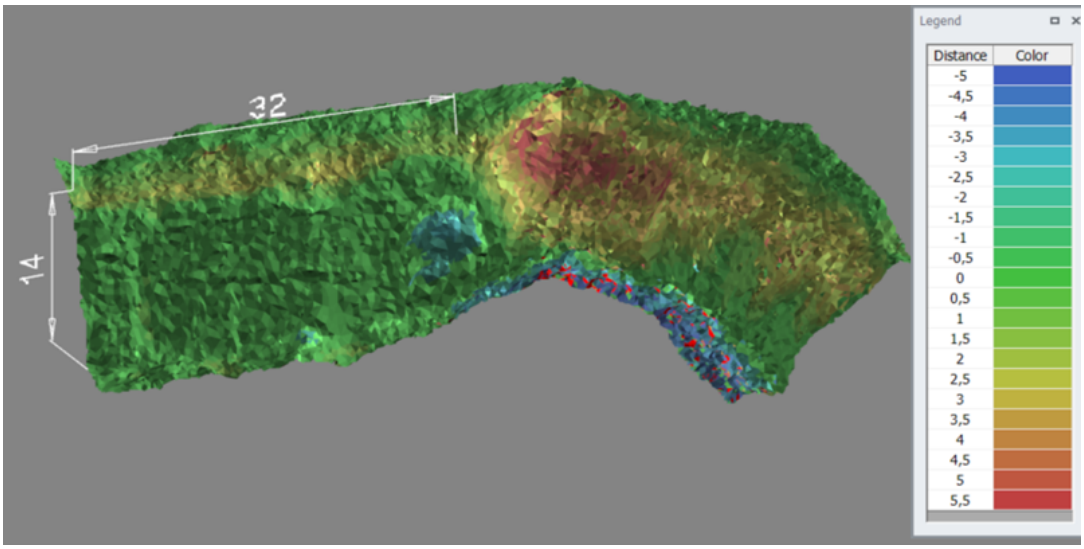

Figure 37: The first part of the third black schist test (BS 3.1) presplit wall colored according to deviation from planned. Negative numbers indicate underbreak and positive numbers represent overbreak. The length and height of the wall is shown above and next to the wall in meters

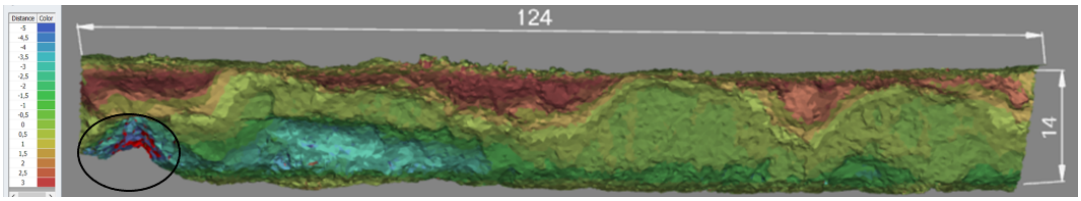

(a)

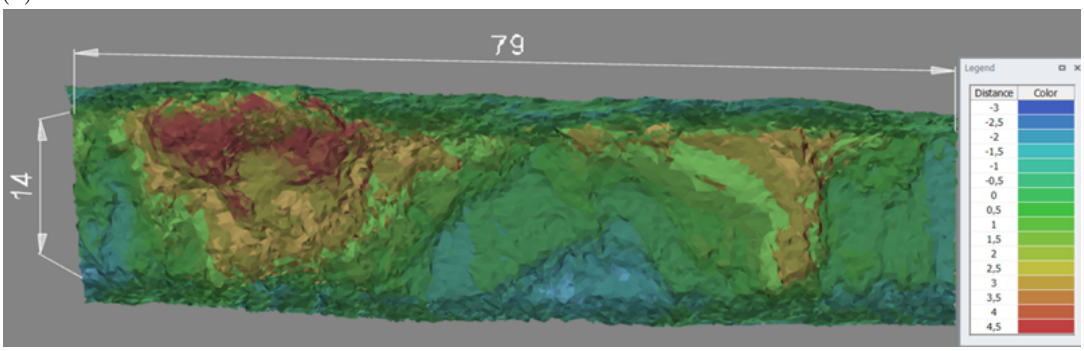

(b)

Figure 38: The second part of the third black schist test (BS 3.2) presplit wall colored according to deviation from planned. Figure a shows the southern section of this part of the test and figure b shows the northern section. In figure a, the area within the black circle is not actual underbreak but loose material left at the toe of the wall.

impossible due to the inherent strength of the discontinuities. Furthermore, there is some underbreak at the toe of the wall, which is most likely caused by the buffer row not breaking the rock up to the presplit. However, the underbreak circled in figure 38a is in reality loose material.

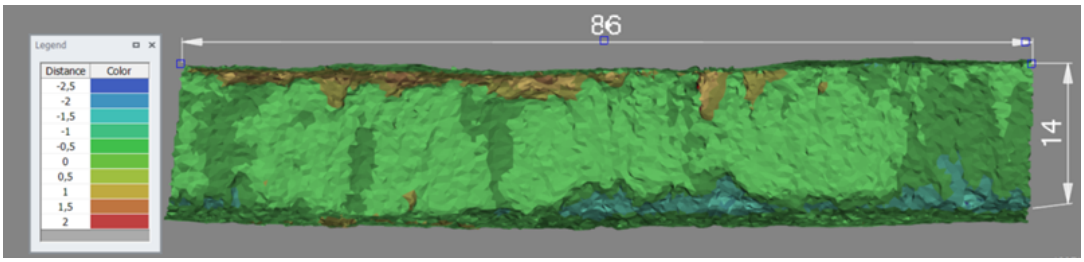

(a)

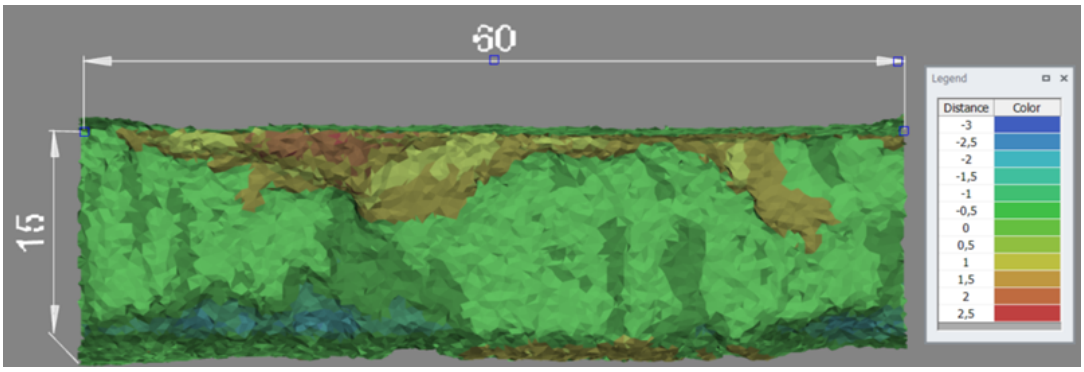

(b)

Figure 39: The third part of the third black schist test (BS 3.3) presplit wall colored according to deviation from planned. Figure a shows the southern section of this part of the presplit test and figure b shows the northern section.

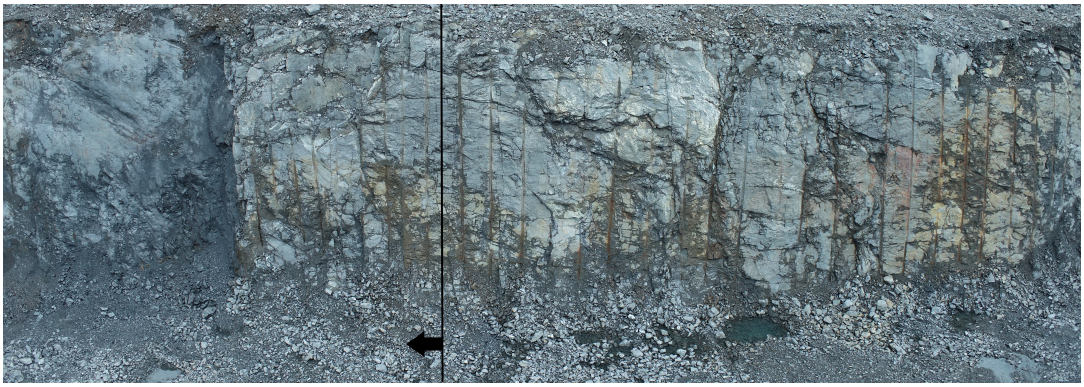

Figure 40: Photo of the area where the presplit parameters change. The black line shows where the presplit parameters change and the arrows show the direction where the second presplit (BS 3.2) part is.

The part of the presplit wall shown in figures 41c and 38b show that the presplit result is poor. There is significant overbreak on the left side of the figures, where the wall's strike direction changes, which is shown in figure 36 (at the southern blue line). The overbreak is most likely caused in this area by the increased confinement of the production and buffer blast holes as was with the first part of this presplit test area. The rock mass quality is also challenging in this area, but the roughness of the surface in the overbreak area suggests that it has been caused by blast damage. There is also one wedge failure from this wall area which has been caused by J2 and

J3 jointing and may be practically unpreventable. There is only minor underbreak in this wall area which can be seen in the middle part of figures 41c and 38b.

The third part of this presplit test area can be seen in figures 41d, 39a and 39b. Figures 39a and 39b show the deviation of the bench face from planned. As can be seen from the figures this presplit part has been very successful. There is only minor overbreak at the crest of the wall and also very little underbreak at the toe of the wall. However, this part of the presplit wall required some scaling after blasting to reveal the presplit plane.

The third part of this presplit test area seems to have better rock mass quality. The central part of figure 41d has an area of dense J6 jointing that has not reduced the presplit quality significantly because of the favourable orientation of this jointing towards the wall. Furthermore, only two areas show J3 foliation in the wall in this presplit test part, which can be seen in figure 39b (the two areas with overbreak). One of these areas, with J3 jointing, can also be seen on the right side of figure 41d.

The first and second part of this presplit test area show no significant improvement compared to the bench faces directly above the test area. The same structures cause overbreak and similar underbreak can also be observed. However, the third part of this presplit test area shows some improvement compared to the bench face above this area. Although, the presplit parameters that were used in this area were the same as previously used. Furthermore, figure 40 shows the area, where the presplit parameters change (interface between part two and three of the presplit test). There is no major difference between the visual appearance of the wall where the presplit parameters change.

It was observed from the presplit face in this test area that there are several presplit holes drilled with incorrect azimuth. However, this has not affected the presplit result significantly on the upper bench level. Furthermore, the collapsed and partially collapsed holes in this presplit area have not had a significant effect on the result either. However, these might affect the lower level's presplit result especially because the partially collapsed holes were mostly more than 15 meters deep.

In conclusion, the bench face quality seems to be controlled by rock mass structures especially in the first and second part of this presplit test. The rock mass in the third part of this presplit seems to have less J3 jointing, which has resulted in a good presplit result.

(a)

(b)

(c)

(d)

Figure 41: Photos of the third black schist presplit test. The photos advance from south (figure a) to north (figure d). Figure a shows the BS 3.1 test part, figure b and c show the BS 3.2 test part and figure d shows the BS 3.3 part.

6.3 Summary

All the presplit test parameters have been observed to produce a presplit crack between the boreholes at least in some areas of the bench faces. Thus, all the tests have been successful or at least no complete failures due to the presplit parameters were observed.

The mica schist test areas were located close to each other which can be seen in figure 18. The rock mass quality between the test areas is very similar with the second test area having a slightly better quality rock mass due to less abundant J5 jointing. However, there is a significant difference in the amount of overbreak observed at the presplit faces between these tests as can be seen from figure 42. The first mica schist test is the grey point with 25 % HCF. The first test area has more overbreak that has occurred along J2 joints. However, the second test area also has similar J2 jointing, but the presplit face has not failed along these joints as much as in the first test. This might be due to the lower borehole pressure used in the second test presplit.

Furthermore, based on the HCF:s the lower borehole pressures used in the second test area has produced a cleaner presplit face. The over- and underbreak plotted against the HCFs can be seen in figure 42. The second part of the second test produced the highest HCF. This indicates that the low borehole pressure and the smaller spacing compared to the first part of the second test would produce the best results. Although, there is little evidence to support this based on visual appearances of the presplit faces and the measured overbreak and underbreak are also very similar for the different parts of the second test. Furthermore, the amount of test data is too limited to draw such conclusions as there are multiple uncontrollable variables involved that can affect the result especially in mica schist, where the presplitting experience is currently limited to the tests made in this thesis.

The variation of the results can be seen in the black schist test results shown in figure 42. The second, third and fourth highest overbreaks and lowest HCFs have used the same presplit parameters (i.e. the 165 mm borehole and 32 mm explosive) as the highest HCF presplit test. Although, these test results differed in the borehole spacing and inclination, it was expected that the results would be similar. However, the results could be predicted by observing the bench faces close to the test areas. The changes in the presplit parameters did not change the resulting bench face quality significantly compared to other bench faces close to the test areas. The only exception is the first black schist test, where the presplit face seems more rough in some areas, which maybe because of too high explosive energy in the presplit caused by the high borehole pressure relative to the used presplit spacing.

Furthermore, no significant differences were observed between the visual appearance of the presplit test faces, where they were visible. In addition to this, on the western pit wall it was expected that some improvements could be made to the bench face

quality, by using the lower borehole pressure (165 mm hole and 32 mm explosive) and lower spacing, compared to the overlying bench faces on the western pit wall. However, this was not the case and the same structures that caused failures on the upper levels' bench faces have caused failures on the test face. Thus, either the discontinuities causing the failures are so weak that their failure cannot be prevented through more careful blasting or the buffer row and/or the production blast damage the discontinuities which cause the failure.

Red lines in figures 42 and 43 are threshold values for underbreak and overbreak determined based on the analysis of previous presplit faces. The values in the minor overbreak and underbreak range have little to no overbreak or underbreak and presplitting has been very successful with the points in this range. The values between the two red lines are intermediate values that have some underbreak or overbreak and presplitting has been partly successful with the points in this range. The final range of values have significant overbreak or underbreak and presplitting has not been successful with the points in this range.

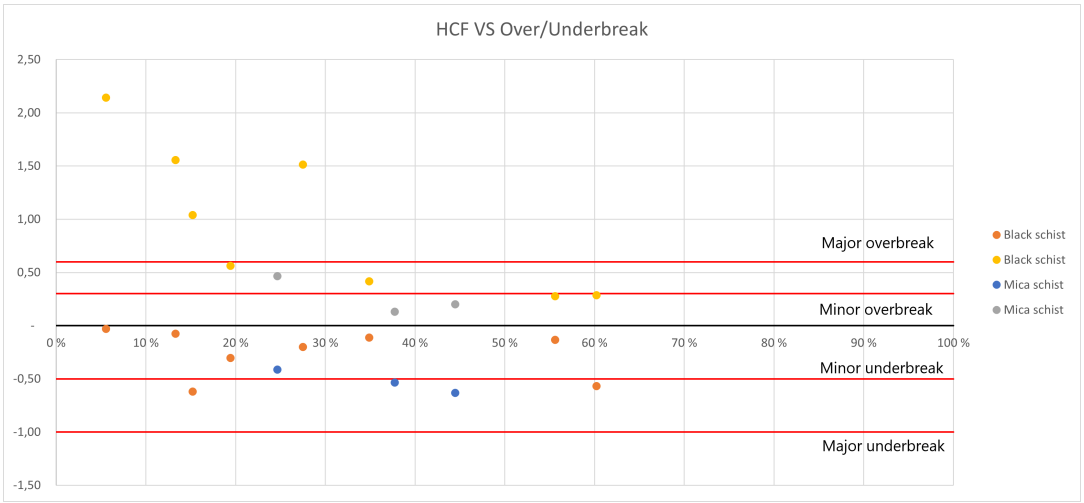

Figure 42: A scatterplot of measured underbreak and overbreak plotted against measured HCF (data from only test presplits). Red lines indicate threshold values that divide the underbreak and overbreak into major, intermediate and minor ranges.

Figure 43 shows a graph of the deviation (i.e. overbreak and underbreak) from planned plotted against the presplit wall direction and the point markers are given according to the used presplit parameter. The "1st" point marker represents the deviation with the previously used presplit parameter (165 mm, 45 mm and 1.8 m) and the others are presplit parameters used in the tests. It can be seen from the figure that most of the points are grouped up close to each other, which indicates that the test presplits have not resulted in a significant improvement regarding the deviation of the bench face from planned.

However, there are a few outliers: the three "5th" points, which are from the first and second part of the third black schist test (BS 3.1 and 3.2), and the "3rd" point which is from the second part of the first black schist test (BS 1.2). Although, the third

black schist test showed very similar results to the previously blasted presplits in the same area, the points from the test stand out from the data because the selection of analysed areas for the historical review part omitted areas with larger failures and focused on the more successful presplit areas. Furthermore, only the first 15 meters of the test presplit faces was analysed, which increases the relative amount of overbreak as overbreak mainly occurs from the crest of the wall.

Figure 43 also shows a slight trend of decreasing overbreak when the presplit wall direction angle increases. The trend is also observable visually in the open pit and the trend may be explained through the orientation of the wall towards J3 and J2 jointing, which cause the majority of the overbreak in Kuusilampi open pit. Furthermore, there seems to be a very slight trend of increasing underbreak when the presplit wall direction angle increases. However, this might be due to random variance in the data and is considered to have little relevance.

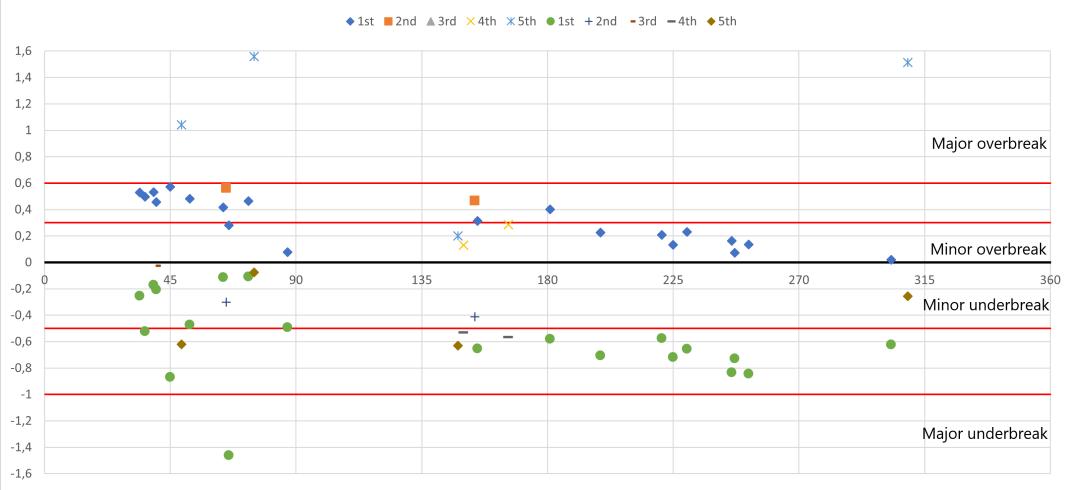

Figure 43: Graph of overbreak and underbreak (Y-axis) plotted against presplit wall dip direction(X-axis). The points are coloured based on the used presplit parameters. 1st = 165/45 mm, 1.8 m; 2nd = 115/32 mm, 1.2 m; 3rd = 127/32 mm, 1.2 m; 4th = 165/32 mm, 1.4 m and 5th = 165/32 mm, 1.2 m (borehole diameter/explosive diameter, spacing). Red lines indicate threshold values that divide the underbreak and overbreak into major, intermediate and minor ranges.

In conclusion, the presplit test results do not differ greatly from the previous presplitting practice. Thus, the greatest improvements to the bench face quality should be searched from other blast parameters more specifically the buffer row parameters should be examined more carefully.

7 Discussion and Recommendations

This chapter analyses the results introduced in the previous chapter, discusses the validity of the obtained results and provides recommendations of further study areas. First, the results from the attempt to find a connection between rock mass quality estimates and presplitting are discussed. Then, the used presplitting parameters are discussed and recommendations are made for future presplit tests. Next, the effect of the buffer row is discussed and recommendations for modifying the buffer row parameters are made. Finally, the accuracy and relevance of the measurements made to evaluate presplitting success are discussed.

7.1 Rock mass classification and presplitting

This thesis studied the connection between a geotechnical block model's rock mass quality estimates and presplitting success, but no clear correlation was found. However, the data set that was gathered during this thesis is not exhaustive and the selection of analysed areas might have incorporated some bias into the data set. Thus it cannot be determined with certainty that there is no correlation between these variables. However, it was also found that the block model's rock mass quality estimates accuracy is questionable for few reasons. The first reason is that the accuracy of the logging data used for the interpolation has some errors or inconsistencies which were found by SRK (2020b). The second reason is that the data points used for the interpolation are too sparse for the block model to reflect the rock mass quality with sufficient resolution.

Previous studies and the analysis of the presplit faces made in this study show that there is a connection between rock mass quality and presplitting success e.g. figure 20b, where the quality of the presplit face has been greatly reduced by the higher fracture frequency and number of joint sets in the area. However, higher fracture frequency alone does not seem to affect presplit quality adversely as can be seen from figures 25, where there is abundant J2 jointing, and 41d, where there is an area with tightly spaced J6 jointing. In these areas the higher fracture frequency has not affected the presplit quality significantly as the borehole half cores are largely visible and the location of the bench face does not deviate significantly from the planned. Thus, a RMC method such as RQD or fracture frequency may not be very suitable to predict presplit success. A RMC method, such as Q' or RMR, may be more suitable as these consider multiple rock mass quality parameters.

However, the problem in trying to use rock mass quality estimations to guide presplit designs is acquiring accurate data with a sufficient resolution. MWD data could be used in theory, but once the data is available the presplit holes have already been designed and drilled. Thus, it does not help in presplit design, but maybe the buffer row design could be modified based on the MWD data acquired from drilling presplit

holes. Although, the charging of presplit holes could be modified based on the MWD data by using decking or air decking. However, this has not been studied previously and could result in a worse presplit result.

In conclusion, modifying presplit designs based on RMC methods' rock mass quality estimates is currently very challenging and it is suggested that different presplit designs are made for different design sectors or rock mass quality domains, that are identified at a given site. Furthermore, it is questionable if the added complexity incorporated into the design process by modifying presplit designs based on estimated rock mass quality, would be justifiable through improved presplit results.

This thesis also utilised borehole video logging data that was obtained from two presplit test areas. The borehole video recording could not be obtained from the other areas due to the production schedule and borehole collapses during washing of the holes, which was done to get a clear image of the hole walls. Very little could be deduced from this data largely because it was only obtained from two areas. The lack of data and the variability of rock mass makes it impossible to conclude anything based on this data. If there was more of this data available, some connection between the logged values from this data and presplitting success might be made. Furthermore, some connection might be found between the joint properties identified from the borehole wall images and rock mass failures from the presplit face.

7.2 Presplitting parameters

Equations 4, 5, 6 and 7 that were used to calculate the borehole pressures and suggested spacings shown in table 4 cannot be considered very accurate due to multiple reasons. The first reason is that in Ouchterlony's (1997) study, where he developed the equations, there were two outliers in the data set. The common factor with these outliers was that both of the outliers' explosives had high VODs. The explosive used in this thesis' tests has an even higher VOD. The second reason for possible inaccuracy with the equations is that in Ouchterlony's tests the coupling ratios were similar but the hole and cartridge diameters were significantly smaller, which can make a difference. The final reason is that the rock strength parameter used to estimate the minimum required crack pressure may not be the correct parameter (Ouchterlony, 1997). Furthermore, the measurements that have been made of the rock strength parameters are very limited and are used to represent very large amounts of rock mass. Thus, it is questionable how well these values represent the rock mass. It would be beneficial to develop Ouchterlony's equations further so that they could be utilised in initial presplit designs more reliably in an open pit mine.

The inaccuracy of the estimated crack lengths can be seen when comparing the suggested spacings shown in table 4 to the test results. The calculated spacing for mica schist with 165 mm borehole and 32 mm explosive was 0.97 meters, but a successful presplit was created with 1.4 meter spacing in the second mica schist test.

However, if only the effect of the coupling ratio on the crack lengths predicted with equations 4, 5, 6 and 7 is considered, the equations can be reduced down to equation 10, where a is the power clause found in equation 7. The effect of the VOD and seismic velocity that are included in the power clause can be considered minor. Thus, the effect of the coupling ratio on the expected crack lengths can be calculated and related to the previously used presplitting parameters, which has been done and the result is shown in figure 44.

$$R_c = (constant * \frac{d_e^{2.2}}{d_h^{1,7}})^a * 0.5 * d_h \tag{10}$$

Where:

R_c = Crack radius in m,

d_e = Explosive diameter in m,

d_h = Borehole diameter in m,

$Constant$ = Explosive's properties and rock strength properties from equations 4, 5, 6 and 7,

a = Power clause from equation 7.

Figure 44 shows a plot comparing the predicted crack lengths for the different borehole diameters and different explosive cartridges relative to the 165 mm borehole and 45 mm explosive cartridge. There is less than one percentage difference between the values obtained from equation 10 for black schist and for mica schist. This difference results from the seismic velocity that is included in the constant a. Although, there are several uncertainties with these equations as described above. This plot in figure 44 could be used as a guideline to optimise the presplitting practices in the future.

The predicted crack lengths can also be considered to represent the relative amount of blast damage each coupling ratio inflicts on the rock mass. Thus, using a higher coupling ratio (smaller borehole or larger explosive) should enable using a larger borehole spacing as well. If the spacing cannot be increased due to the rock mass quality, using a higher coupling ratio would increase the amount of unwanted blast damage.

All the presplit tests, conducted in this thesis, can be considered successful. A presplit crack was created in every test with the different parameters based on the visual observations. Furthermore, no considerable differences were found between the different presplit design parameters nor the different rock types. Although, there is considerable difference between blasting results in mica schist and black schist, the presplit results did not differ significantly based on the visual observations.

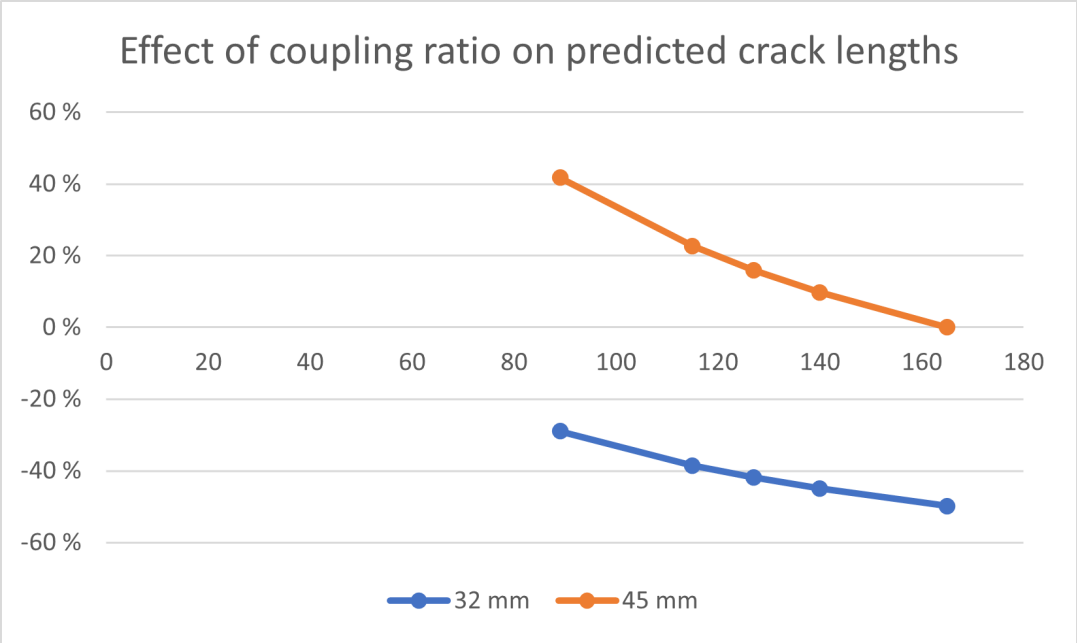

Figure 44: The effect of coupling ratio on predicted crack lengths in presplitting. X-axis shows different borehole diameters and Y-axis shows the difference in predicted crack lengths compared to the 165 mm hole and 45 mm explosive cartridge.

Based on the test results and theory discussed above, it can be recommended that the following presplit parameters should be used to improve the slope stability at the western pit wall. The suggested presplit spacing is not definite and should be tested further because the test results show that both 1.2 meter and 1.4 meter spacings functioned well and the maximum spacing, that produces a clean presplit face, was not found.

- Borehole diameter 165 mm
- Explosive diameter 32 mm
- Borehole spacing 1.2–1.5 meters

Although, these parameters did not improve the presplit result on the western pit wall compared to the previous presplit practice, these parameters should minimise the blast vibrations created by the presplit because of the low borehole pressure resulting from the low coupling ratio. Thus, it is recommended that this presplit design is used at the western pit wall close to the large scale structures that have been identified. Furthermore, it can be said that the previous presplit design parameters (listed below) produce good results in good quality rock mass and as such there is no need to change them.

- Borehole diameter 165 mm

- Explosive diameter 45 mm
- Borehole spacing 1.8 meters

However, there is room for optimisation with the presplit parameters and the following strategy is suggested for further testing to find the optimum presplit parameters for mica schist areas, northern and eastern domains of the open pit.

  - Test with four different coupling ratios
- Borehole diameters 165 mm and 115 mm
- Explosive diameters 45 mm and 32 mm
- Increase the borehole spacings with the different coupling ratios until the presplit fails

This way the maximum presplit spacings can be found for the different coupling ratios and it can be seen if the maximum borehole spacings for the different coupling ratios follow roughly the theoretical relation shown in figure 44. If the results do not follow the theory at all, the borehole spacing is most likely also constrained by the quality of the rock mass. In this case the optimum presplit design, considering slope stability, is the one with the lowest coupling ratio and highest borehole spacing. Otherwise, the optimum presplit design parameters can be considered based on other factors, such as the drilling efficiency and costs.

However, this test strategy does not consider the vibration attenuation properties of the presplit. The attenuation properties may be different with different presplit parameters even if based on visual observation there is very little difference between the presplit parameters' results. It is recommended that a further study is conducted where the presplit's attenuation properties are measured. Furthermore, the same blast vibration data obtained in the attenuation study coupled with slope stability radar's measurements of movements in the large scale structures at the western pit wall could be used to determine PPV ranges that induce movements in large scale structures in the pit walls. A similar study was conducted by Rajmeny and Shrimali (2019) at an open pit mine.

Based on the test results no changes in the presplit hole inclination are required. However, on the western pit wall there have been a few plane failures where a successful presplit face, based on visual observation (borehole half cores visible), has fallen down along the foliation. The probability of these failures could be reduced by using a presplit inclination closer to 60° because this way the presplit would be nearly parallel to the foliation. However, this would also reduce the drilling efficiency and it might increase borehole collapses. Furthermore, such slope failures are also partly induced by blast vibrations and water percolation through the joints. Thus,

the probability of failures can also be reduced by reducing these. It can be tested if a larger hole inclination would produce improved slope stability at the western pit wall. However, it is thought that no great improvements can be achieved through this change.

No stemming has been used in the presplit holes and the presplit holes have mostly been charged up to the surface (this was described more detailed in chapter 5.2). This has most likely been a partial cause to some of the overbreak at the crests of the walls. Thus it is suggested that the uncharged lengths in presplit holes are increased to 1.5–2 meters from the surface. The suitable length is expected to be within this range. However, the suitable uncharged length can be found through testing.

Water can have an effect on presplitting results as was discussed previously and the presence of water in the presplit holes in the tests was documented. Nearly all presplit holes contained some water, which may have resulted in increased blast damage. However, based on the visual observations from the test presplit faces, the water in the presplit holes has not had a significant effect on the presplit result.

Figures 45a and 45b show box plots of measured overbreak and underbreak, in m^3/m^2, sorted according to the analysed bench face height. Thus, the figures show the differences in underbreak and overbreak between single and double benching. Figure 45a shows that single benching results in more overbreak relative to double benching as was expected based on the theory introduced in chapter 2.5. Furthermore, figure 45b shows that single benching results in relatively less underbreak than double benching. This is because the presplits have been almost equally successful with single and double benching, which is illustrated by figure 45c. Thus, single benching will have more overbreak and less underbreak than double benching.

However, reducing underbreak maybe more straightforward than reducing overbreak because overbreak is largely caused by geological structures. Thus, preventing or reducing overbreak may be impossible or impracticable because the structures may have so low inherent strength that they will fail from the slightest blast damage. Although underbreak is also influenced by geological structures, this influence may be easier to mitigate by modifying the blast designs. Furthermore, double benching requires less preparation work as the presplit is drilled and blasted at once for two bench levels whereas in single benching the presplit is drilled and blasted before each bench blast. Thus, double bench presplitting can be considered better than single bench presplitting.

However, the differences in overbreak and underbreak may be exaggerated because the 30 meter bench faces comprise of selected previous presplit faces and 15 meter bench faces are mostly test presplit faces. The selection may have incorporated some bias into the data set. Furthermore, the influence of the selection criteria can be seen in figure 45c, where the 30 meter bench faces have smaller variability in the deviation than the 15 meter bench faces. This is because the selection focused on more successful presplit faces, which is most likely the main reason for the reduced

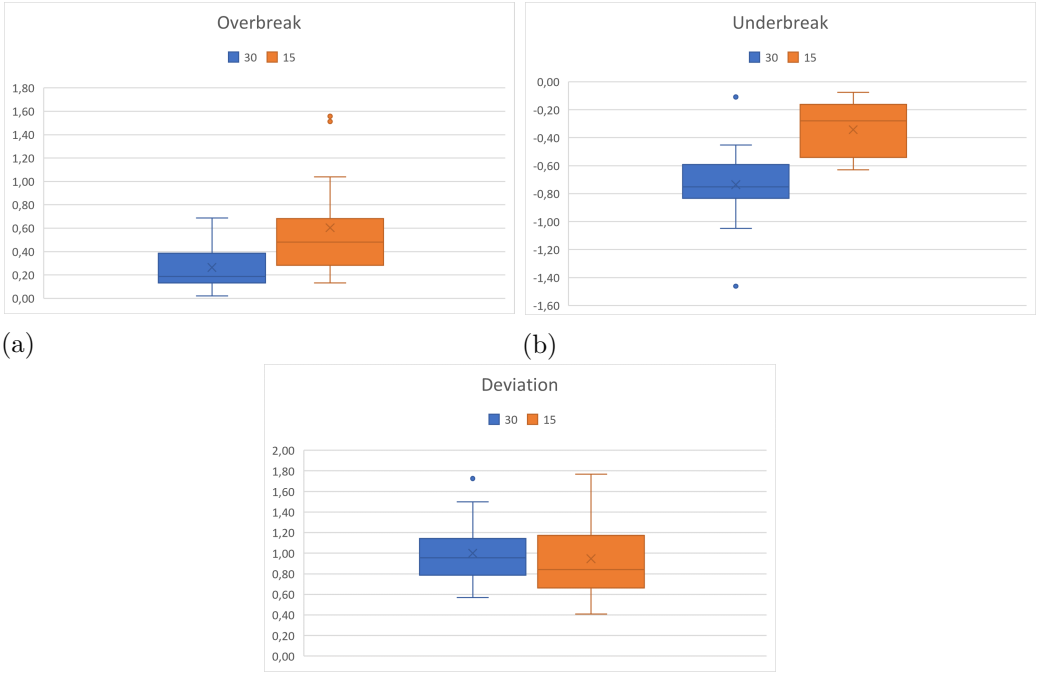

Figure 45: Box plots of overbreak (a), underbreak (b) and deviation (c), which is the sum of overbreak and underbreak. Blue box comprises of the data from 30 meter high bench faces and orange box comprises of the data from 15 meter high bench faces. The box represents the second and third quartile, the X is the mean value and the line within the box is the median. The lines outside the box represent the first and fourth quartile of the data and points are outlier values.

variability.

This thesis did not examine the effect of the production blast on the observed presplit success. Although, it can have a detrimental effect on the result. However, the production blasts have been reasonably successful at Kuusilampi open pit and thus it can be considered that the production blasts have not had a major effect on the results apart from the buffer row, which was examined more carefully and its effect is discussed more in depth in the following chapter.

7.3 Buffer row

The analysis of the previous presplit faces and test areas suggest that the largest improvements for achieving the planned bench faces would result from modifications to the buffer row. Most of the bench faces have overbreak at the crest of the wall which results mainly from subdrilling on the overlying bench blast, for which changes have already been implemented at the mine, and joints that dip into the pit. However, the buffer row may also have damaged the rock mass at the crest and joints, that dip into the pit, which has resulted in overbreak. Furthermore, underbreak is found

at the toes of the walls at almost all analysed areas, which could be reduced with improvements in the buffer row. The following changes are suggested to the buffer row.

- Hole inclination 80°
- Buffer row's distance from the presplit = 1.5–2.5 meters

The suggested hole inclination is the same inclination that is used for the production blast holes. Using the same inclination should help reduce the underbreak at the toe of the wall because with the same inclination the buffer row's burden would remain constant regardless of the depth. Furthermore, this change requires that the buffer row's distance from the presplit is changed. The suitable distance should be between 1.5 and 2.5 meters based on previous experience. Previously, it has been observed that the buffer row's holes are more prone to collapse at the collar, when placed closer to the presplit than 3 meters. In order to reduce the hole collapses, it is suggested that a longer uncharged length is left at the collars' of the presplit holes. A suitable uncharged length that does not affect the presplit result but reduces the breakage at the collar should be tested on but two meters is suggested as a starting point.

However, on the western pit wall using this inclination is not viable as the presplit and bench face inclination is 70°. The buffer row's hole collars would have to be approximately 3 meters away from the presplit when using an inclination of 80°. Otherwise, the buffer row would intersect the presplit plane. Thus, it is suggested that the buffer row inclination in this area is maintained at 75° as changes in the buffer row inclination would require further changes in either the production blast holes or the presplit holes which are not deemed necessary at this point. However, modifications to the inclination and distance of the buffer row from the presplit in this area should be reconsidered if the following suggestions do not remove the underbreak at the toes of the bench faces.

The above-mentioned changes should be sufficient in the eastern and northern black schist domains of the open pit where there have not been any major problems with blasting and the planned bench faces are already achieved with sufficient accuracy. Further changes are suggested for the more challenging areas, where planned bench faces are more rarely achieved and significant amount of scaling is required after blasting.

- Hole spacing = 0.5 * production hole spacing
- Hole diameter 115 mm
- Stemming between 6 to 4 meters

In the western domain of the open pit, it is further suggested that the buffer row's hole spacing is reduced to half of the spacing used for the production holes. This change should reduce the control of geological structures on the blasting result, which seems to be the main issue in this area. However, the reduced spacing increases the powder factor which would most likely result in increased blast damage. Thus, the reduction in borehole diameter and increase in stemming length are suggested. The increased stemming length should also help reduce the crest damage as the explosive energy is reduced at the crest. However, the lower bench of a double bench high presplit face can most likely utilise smaller stemming length than the top bench because typically overbreak does not occur in the lower bench area at the site. Experiments should be made to find the correct stemming length, such that the planned wall crest position is achieved as a too long stemming length will result in a lip at the crest of the wall.

These changes might also be necessary for the mica schist areas of the open pit because in the tests it was observed that significant amount of scaling was required to remove loose blocks from the bench face and to reveal the presplit plane. However, based on only two tests in the mica schist areas it is impossible to say if these changes are required and it is suggested that further mica schist presplit tests are made before major changes to the buffer row. If the presplit faces require significant amount of scaling in the future as well, the above-mentioned changes in the buffer row should be considered.

7.4 Measurements

This thesis measured the presplitting success by measuring the amount of overbreak and underbreak, and HCF, which are all based on visual observations of the bench face. These measurements are not a direct measure of presplitting success because they are highly dependent on the success of the buffer row, which in turn is dependent on the bench blast.

The overbreak and underbreak were measured relative to the planned presplit holes. Thus, it is also dependent on the drilling accuracy. However, based on observations made during this thesis project, the drilling accuracy at Kuusilampi open pit is on a sufficiently high level that it does not have a significant effect on these measurements. The main errors in these measurements result from the deviations of the crest and toe bench levels. At the crest level, there is typically some loose material, which is calculated as underbreak, and there is also some overbreak from subdrilling of the overlying bench blast. At the toe level there may be some loose material which typically results in overestimation of underbreak. The accuracy of the 3D surfaces used in analysis incorporate some random error to the data. However, this error is very minor compared to the above-mentioned error sources. Anyway, the accuracy of the measurements is considered to be at a sufficiently high level regarding the scale of the operation.

It was found in the presplit tests that measuring the overbreak and underbreak may actually represent more the success of the buffer row than presplit success. HCF may be a more direct method of presplitting success than overbreak and underbreak. However, it is also highly dependent on the buffer row and it may be considered that HCF is only a measurement of how well the buffer row has revealed the presplit holes. However, it may also be considered that a successful presplit blast provides a free face for the buffer row to act on and break the rock up to the presplit, which then results in a high HCF. Anyway, HCF does measure the blast damage inflicted on the remaining rock mass by the presplit and production blast.

Furthermore, it has been observed at the western pit wall in Kuusilampi open pit, that failures typically occur from bench faces where the presplit borehole half cores have been visible. Thus, the successful presplit faces fail more often than the areas where the bench face is formed along the foliation. Thus, the used measurement methods do not measure accurately the stability of the pit walls either. Presplitting will never remove the risk of such failures. It only reduces the probability of the failures by reducing the blast damage to the remaining rock mass. Although, the successful presplit faces may seem riskier as the failures have occurred in such areas, they increase safety by ensuring that the planned catch benches are achieved.

Thus, the measurement methods measure the safety of the pit walls in a way by determining how well the planned catch berms are achieved as underbreak typically reduces the catch bench width from the toe of the wall and overbreak reduces the catch bench width from the crest of the wall. Thus, a successful presplit with low under- and overbreak will have sufficient catch bench widths to prevent rock mass failures from risking the safety of the operation.

Currently, there does not seem to be a robust method for measuring presplitting success because the visible result is highly dependent on the buffer row, the production blast and rock mass quality. Thus, it is very problematic to try and study presplitting in isolation of other blast parameters. A statistical analysis, with large amount of data, could be used to distinguish the effects of the presplit parameters and the different variables involved in presplitting. However, such study was outside the scope of this thesis.

Currently, the most accurate method for measuring presplitting success, based on previous studies, is measuring blast vibrations next to the production bench and behind the presplit to see if the vibrations are attenuated by the presplit. However, this measurement method is also prone to errors caused by the heterogeneity of rock mass, which can also be combatted with statistical analysis that incorporates large amount of data.

8 Conclusion

This thesis aimed to improve the slope stability at Kuusilampi open pit by improving the presplit blasting practices. Previously, the slope stability had been on a generally good level. However, there was one area of the open pit which had had problems with achieving the planned bench faces. Furthermore, the mine is deepening and expanding to an area where a new rock type (mica schist) will comprise the permanent and semi-permanent bench faces.

The mine had planned presplitting tests with smaller diameter explosive, different hole diameters and borehole spacings and this thesis was conducted as a part of these tests. The main aim of this study was to discover suitable to near optimal presplit designs for the different areas of the open pit. However, the optimality of the presplit designs were considered mainly based on slope stability and the economical point of view was not considered. Furthermore, the connection between a geotechnical block model's rock mass classification (RMC) estimates and presplitting success was studied based on the test presplits and historical presplits. The connection between these parameters was studied in an attempt to create a tool for designing presplits.

This study consists of the presplit tests that were made and a historical review into the used presplit designs. The presplit parameters that were mainly studied were the coupling ratio (i.e. the borehole diameter and explosive diameter), borehole spacing and inclination, other presplit parameters were not changed during the tests. Furthermore, the effect of the buffer row on presplitting was considered as it can have a large impact on the observed presplitting result. However, the effect of the production blast was not considered in this thesis. Although, it can also have a detrimental effect on the observed presplitting result.

In this thesis it was found that the geotechnical block model's RMC estimates and presplitting success did not have any significant correlation. Although, the data gathered in this thesis was insufficient to conclude that there is no correlation between the parameters. The block model was found to not have the sufficient accuracy nor resolution to represent the rock mass quality with such accuracy that it could be used as a tool for presplit design.

Furthermore, the test results indicated that a high fracture frequency alone does not reduce presplitting quality adversely, which is why a RMC method, such as RQD may not be suitable to predict presplit success. Other rock mass quality parameters, such as joint condition and number of joint sets, influence presplitting success adversely, which is why using a RMC method, such as Q' or RMR, may be more suitable to predict presplit success. However, it was concluded that currently it is not viable to modify presplit designs based on rock mass quality estimates at the mine.

It was also found that suitable, but sub-optimal, presplit designs for the different areas of the mine would be

  - Northern and Eastern domains of the open pit
    - Borehole diameter 165 mm
    - Explosive diameter 45 mm
    - Spacing 1.8 meters
  - Western domain and mica schist area
    - Borehole diameter 165 mm
    - Explosive diameter 32 mm
    - Spacing 1.2–1.4 meters.

The northern and eastern domains have more favourable rock mass conditions which results in good quality presplit faces even with a larger explosive and a larger spacing. In the western domain of the open pit, there are large-scale geological structures whose failures are promoted by blast vibrations. Thus, using a smaller explosive, which should reduce the blast vibrations from the presplit blast, is recommended and using a smaller explosive requires a smaller borehole spacing. In the mica schist area, the presplitting experience is currently limited to the tests made in this study, where it was found that the above-mentioned parameters produced the best results.

These presplit designs were found to produce clean and stable bench faces. However, they are not optimal and further tests were suggested to find optimal presplit designs. The suggested presplit tests used four different coupling ratios with 165 mm and 115 mm hole diameters and 32 mm and 45 mm explosive cartridge diameters. The goal of these tests would be to find the maximum hole spacing that still produces a stable presplit face. This information could then be used to select the optimal solution for the mine.

It was also concluded that using double bench presplitting is better compared to single bench presplitting because double bench presplitting requires less preparation work and thus improves the production schedule. Additionally, double benching results in relatively less overbreak than single benching. Although, double benching was also observed to result in relatively higher underbreak compared to single benching. It is though that underbreak may be easier to reduce than overbreak through modifying blast designs.

Furthermore, it was found in this thesis that the buffer row has a very large influence on the observed overbreak and underbreak. It was concluded in this thesis that the greatest improvements to slope stability at Kuusilampi open pit could be achieved with modifications in the buffer row parameters and recommendations on these modifications were provided.

In conclusion, it was found in this thesis that modifications to the presplit parameters did not change the quality of the resulting bench face compared to previously made bench faces in the neighbouring areas. Thus, improvements to bench face quality should be searched from other blasting parameter and more specifically the buffer row.

9 References

Adamson, W. R. 2012. *Reflections on the functionality of pre-split blasting for wall control in surface mining.* In: Singh, P.K. and Sinha, A. Rock fragmentation by blasting Fragblast 10: proceedings of the 10th International Symposium on Rock Fragmentation by Blasting. New Delhi, India. 26–29. November 2012. London, England. Taylor & Francis group. pp. 697-–705. ISBN 978-0-203-38767-2.

Bauer, A. 1982. *Wall control blasting in open pits.* CIM Special Volume 30. In 14th Canadian rock mechanics symposium.

Birhane, M. 2014. *Presplitting at Aitik mine.* [Online]. Master thesis. Luleå University of Technology, Department of Civil, Environmental and Natural Resources Engineering. Luleå. Sweden. Available from: https://www.diva-portal.org/smash/get/diva2:1018948/FULLTEXT02

Blair, D.P. 2018. *Vibration modelling and mechanisms for wall control blasting.* In: eds. Schunnesson, H. and Johansson, D. 12TH international symposium on rock fragmentation by blasting. Luleå, Sweden. 11.-–13. June 2018. Luleå University of Technology. ISBN: 978-91-7790-134-1.

Blastershouse Oy. 2020. *Tärinämittausraportti Terrafame Oy.* Blast vibration study at Kuusilampi open pit.

Calder, P. 1977. *Pit slope manual.* Chapter 7. Perimeter blasting. CANMET, Energy, Mines and Resources Canada. Report 77–14. p 82.

Chiappetta, R. F. 2001. *The importance of pre-splitting and field controls to maintain stable high walls, eliminate coal damage and over break.* Proc. 10th High-tech Seminar on State of the art, blasting technology, instrumentation and explosives application. GI-48. Nashville, Tennessee, USA. July 22–26.

Chiappetta, R.F. 1991. *Pre-splitting and controlled blasting techniques including air decks and dimension stone criteria.* In: Chiappetta RF (ed) Proc blast technology instrumentation and explosives applications seminar. San Diego.

Danell, R.E., Lewandowski, T. and Luan Mai, V.K. 1997. *Influence of discontinuities on presplitting effectiveness.* Fragblast International journal for blasting and fragmentation, [Online journal]. vol. 1, issue 1, pp. 27–39. Available from: https://doi.org/10.1080/13855149709408388 ISSN: 1385-514X (print). ISSN: 1744-4977 (online).

Dindarloo, S.R., Askarnejad, N.A. and Ataei, M. 2015. *Design of controlled blasting (pre-splitting) in Golegohar iron ore mine, Iran.* Mining technology, [Online journal]. vol. 124, issue 1. pp. 64–68. Available from: https://doi.org/10.1179/1743286314Y.0000000077.

DJI. 2021. *Phantom 4 RTK specs.* [Website]. Available from: https://www.dji.com/fi/phantom-4-rtk/info#specs

Helsinki University of technology. 2006. *Test report.* Test report from laboratory strength measurements on drill core samples from Kuusilampi open pit.

Helsinki University of technology. 2004. *Test report.* Test report from laboratory strength measurements on drill core samples from Kuusilampi open pit.

Hustrulid, W. 1999. *Blasting principles for open pit mining. Volume 1, General design concepts.* Rotterdam: Balkema.

Langefors, U and Kihlström, B. 1967. *The modern technique of rock blasting.* 2nd ed. Stockholm: Almqvist & Wiksell; ´ Langefors, U. nad Kihlström, B. 1978. *The modern technique of rock blasting.* 3rd ed. Halsted Press, New York. ISBN 0-470-99282-4

Ma, G. 2010. *Analysis of Blast Wave Interaction with a Rock Joint.* Rock mechanics and rock engineering. Rock mechanics and rock engineering. [Online journal].vol. 43, issue 6.pp. 777–787. Available from: https://doi.org/10.1007/s00603-009-0062-0

Maxam blasting solutions. 2021a *Riosplit Wf.* [Website]. Available from: https://www.maxamcorp.com/en/blasting-solutions/products/products-list/riosplit-wf

Maxam blasting solutions. 2021b. *Riomex 7000.* [Website]. Available from: https://www.maxamcorp.com/en/blasting-solutions/products/products-list/riomex-7000

McKenzie, C.K. 2013. *Limits blast design: Controlling vibration, gas pressure & fragmentation.* In: Singh, P.K. and Sinha, A. Rock fragmentation by blasting Fragblast 10: proceedings of the 10th International Symposium on Rock Fragmentation by Blasting. New Delhi, India. 26–29. November 2012. London, England. Taylor & Francis group. pp. 85–94. ISBN 978-0-203-38767-2.

Ouchterlony, F. 1997 *Prediction of crack lengths in rock after cautious blasting with zero inter-hole delay.* Fragblast International journal for blasting and fragmentation, [Online journal]. vol. 1, issue 4. pp. 417–444. Available from: https://doi.org/10.1080/13855149709408388 ISSN: 1385-514X (print). ISSN: 1744-4977 (online).

Raina, A.K. 2019. *Influence of joint conditions and blast design on pre-split blasting using response surface analysis.* Rock mechanics and rock engineering. [Online journal]. vol. 52, issue 10, pp. 4057–4070. Available from: https://doi.org/10.1007/s00603-019-01822-8

Rajmeny, P. and Shrimali, R. 2019. *Use of radar technology to establish threshold*

values of blast vibrations triggering sliding of geological faults at a lead-zinc open pit mine. International journal of rock mechanics and mining sciences. [Online]. vol. 113. pp. 142–149. ISSN 1365-1609.

Rorke, A. 2011 *Limiting blast induced damage on final pit walls.* From: Birhane, M. 2014.

Sanden, B.H. 1974. *Pre-split blasting.* M.Sc. Dissertation. Queen's University.

Sandvik Mining and Construction. 2019. *Summary of mechanical rock testing.* Test report from laboratory strength measurements on drill core samples from Kuusilampi open pit.

Singh, P.K., Roy, S. K. and Sinha, A. 2003. *A new blast damage index for the safety of underground coal mine openings.* Mining technology, [Online journal]. vol. 112, issue 2. pp. 97-104, Available from: https://doi.org/10.1179/037178403225001638

Singh, S.P. 2005. *Blast damage control in jointed rock mass.* Fragblast International journal for blasting and fragmentation, [Online journal]., Vol. 9, issue 3, Available from: https://doi.org/10.1080/13855140500293280 ISSN: 1385-514X (print). ISSN: 1744-4977 (online).

Singh, P. K. Sirveiya, A. K. Babu, K. N. Roy, M. P. and Singh, C. V. 2006. *Evolution of effective charge weight per delay for prediction of ground vibrations generated from blasting in a limestone mine.* International Journal of Surface Mining, Reclamation and Environment. vol 20, issue 1. pp. 4-19, Available from: https://doi.org/10.1080/13895260500286050.

Singh, P. and Narendrula, R. 2007. *The influence of rock mass quality in controlled blasting.* In: Peng, S. S., Mark, C. and Finfinger, G. 26th International conference on ground control in mining. Morgantown, WV (United States). 31. July– 2. August, 2007. ISBN: 9780978938321.

Singh, P.K., Roy, M.P. and Paswan, R. K. 2014. *Controlled blasting for long term stability of pit-walls.* International journal of rock mechanics and mining sciences. Volume 70. pp. 388–399. Available from: https://doi.org/10.1016/j.ijrmms.2014.05.006. ISSN: 1365-1609.

Singh, P.K., Roy, M.P., Himanshu, V.K., Paswan, R.K. and Kumar, S. 2018. *Pre-split blasting techniques at dragline benches for stable bench with improved fragmentation level.* In: eds. Schunnesson, H. and Johansson, D. 12TH international symposium on rock fragmentation by blasting. Luleå, Sweden. 11.–13. June 2018. Luleå University of Technology. ISBN: 978-91-7790-134-1.

SRK Consulting (UK) Limited. 2020a. *Pit water management study for the Terrafame mine in the Kainuu region of Finland.* Hydrogeological study of Kuusilampi open pit.

SRK Consulting (Finland) Oy. 2020b. *Kuusilampi geotechnical assesment and slope design update.* Geotechnical study of Kuusilampi open pit.

Stacey, P. and Read, J. 2009. *Guidelines for Open Pit Slope Design.* Australia. CRC Press Imprint.

Tariq, S. M. and Worsey, P.N. 1996. *Investigation into the effect of varying joint aperture and nature of surface on pre-splitting.* In: Proceedings of the 12th Symposium on Explosives and Blasting Research.

Vuolio, R. and Halonen, T. 2012 *Räjäytystyöt.* 2. ed. Helsinki: Suomen Rakennusmedia. ISBN : 978-952-269-072-2.

Wang, Y. 2018. *Visualizing the blast-induced stress wave and blasting gas action effects using digital image correlation.* International journal of rock mechanics and mining sciences. [Online]. vol. 112. pp. 47–54. ISSN 1365-1609.

Worsey, P. 1981 *Geotechnical factors affecting the application of pre-split blasting to rock slopes.* [Online]. PhD thesis. University of Newcastle, Department of mining engineering. Newcastle, England. Available from:
http://theses.ncl.ac.uk/jspui/handle/10443/3613

Yang, L., Wang, Q., Xu, L., Yang, R., J. and Chao, Y.J. 2020. *Fracture path of cracks emigrating from two circular holes under blasting load.* Theoretical and Applied Fracture Mechanics, Volume 108. Available from:
https://doi.org/10.1016/j.tafmec.2020.102559. ISSN 0167-8442.

Yu, T.R., Vongpaisal S. 1996. *New blast damage criteria for underground blasting.* CIM, vol. 89 No. 998. pp. 139–145.

Zhang, Z. 2016. *Rock fracture and blasting: Theory and applications.* Butterworth-Heinemann. ISBN 9780128026885.

Zou, D. 2017. *Theory and technology of rock excavation for civil engineering.* Singapore: Springer Singapore Pte. Limited. ISBN: 978-981-10-1989-0.

A Analysis of previous presplit faces

This chapter introduces and analyses the presplit faces from the different design sectors that were analysed for the historical review part. The analysed presplit faces from design sector one colored according to the deviation from planned can be seen in figures A1a, A1b, A1c and A1d. In the first two figures the final wall is formed along a J3 joint with a dip of approximately 60°. This can be seen from the figures as there is significant overbreak at the crest and significant underbreak at the toe. In the third and fourth figure, the final wall is formed fairly well along the presplit plane with only minor overbreak at the crest and minor underbreak at the toe of the wall. In figure A1d there is also some overbreak on the left side of the figure, which has been caused by a discontinuity.

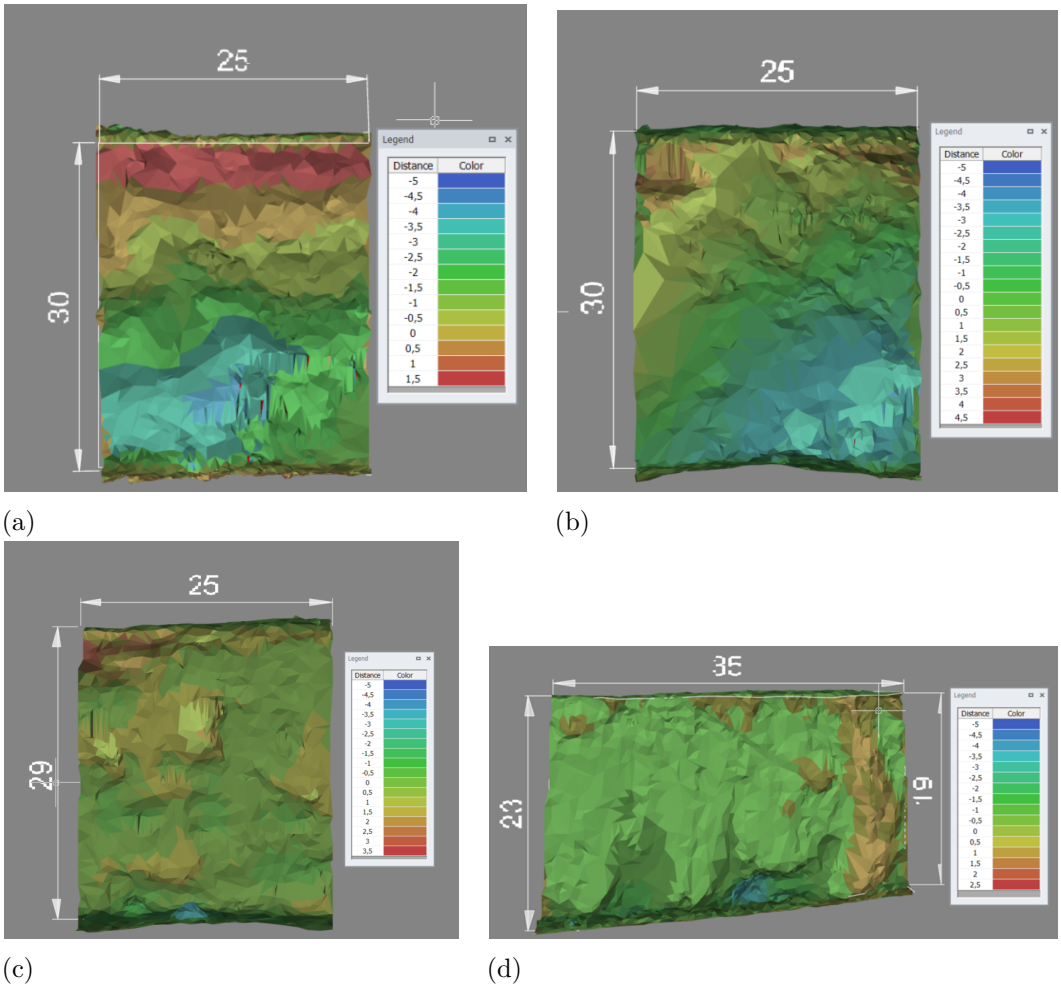

Figure A1: Presplit faces from design sector 1 colored according to the deviation from planned. The scale shows deviation from planned in meters, negative numbers indicate underbreak and positive numbers represent overbreak. The length and height of the wall is shown above and next to the wall in meters.

The analysed presplit faces from design sector two colored according to the deviation

from planned can be seen in figures A2a, A2b, A2c and A2d. The figures show that there is some overbreak at the crest of the wall. Furthermore, there is significant underbreak at the toe of the wall. In the middle part of the bench faces there is only slight deviations from the planned and in these parts most of the presplit borehole half cores are visible in the face. At these presplit faces the buffer row was not very successful and significant scaling was required to achieve the final faces.

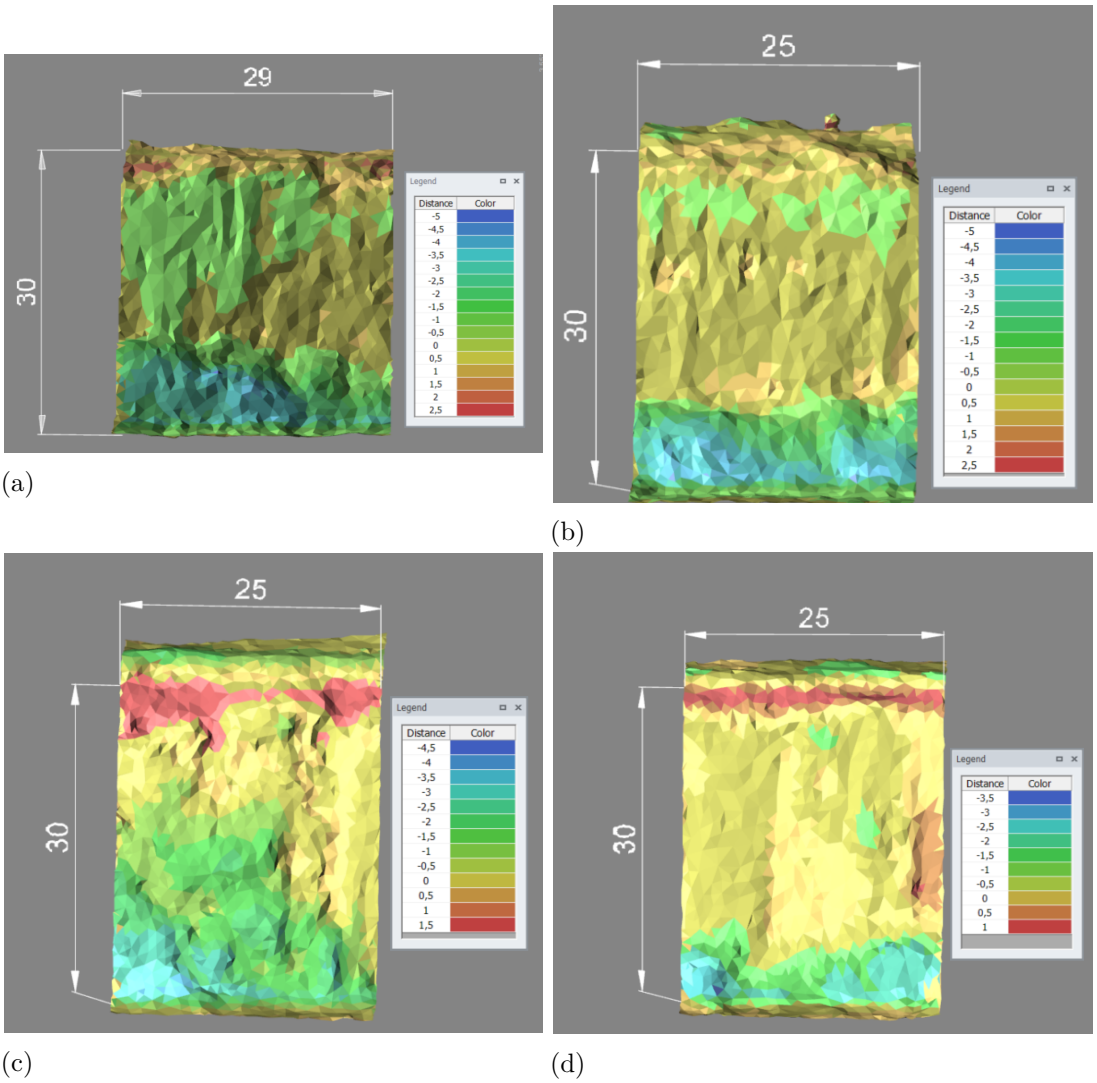

(a) (b) (c) (d)

Figure A2: Presplit faces from design sector 2 colored according to the deviation from planned.

The analysed presplit faces from design sector three colored according to the deviation from planned can be seen in figures A3a, A3b, A3c and A3d. The figures show that there is very minor overbreak at the crest of the wall and for the most part of these presplit faces the presplit borehole half cores are visible in the wall. However, there is significant amount of underbreak at the toe of the wall. Furthermore, this area's presplit faces also required significant amount of scaling to achieve the final faces, which indicates that the buffer row was not successful.

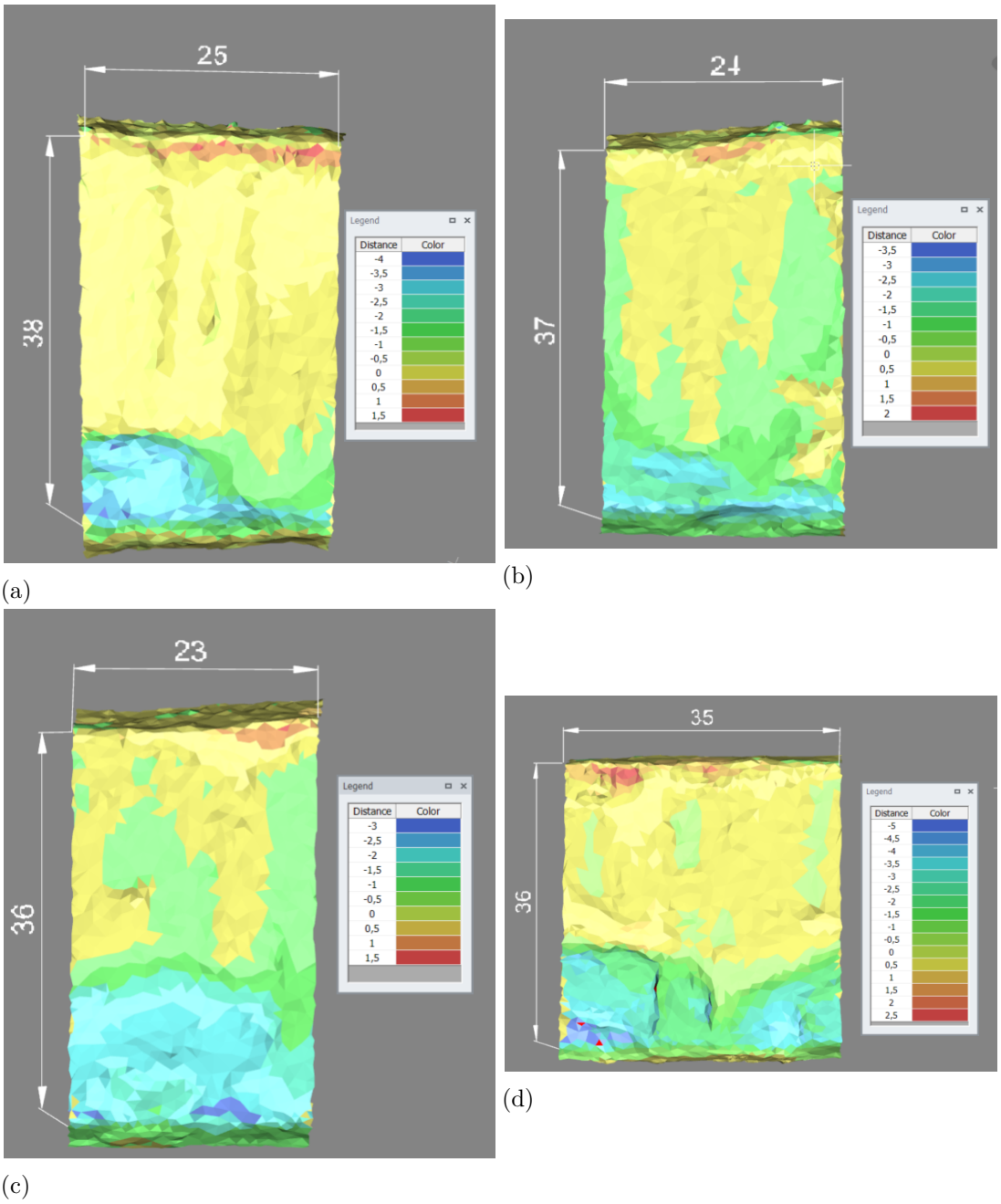

Figure A3: Presplit faces from design sector 3 colored according to the deviation from planned.

The analysed presplit face from design sector 4 can be seen in figure A4. This presplit face was analysed in three parts which are illustrated with the wall length scales seen in the figure. In this area presplitting has been reasonably successful with only minor overbreak at the crest of the wall and minor underbreak at the toe. This presplit wall can be considered as an example of a sufficiently successful presplit wall at Kuusilampi open pit.

The analysed presplit face from design sector 5 can be seen in figure A5. This presplit

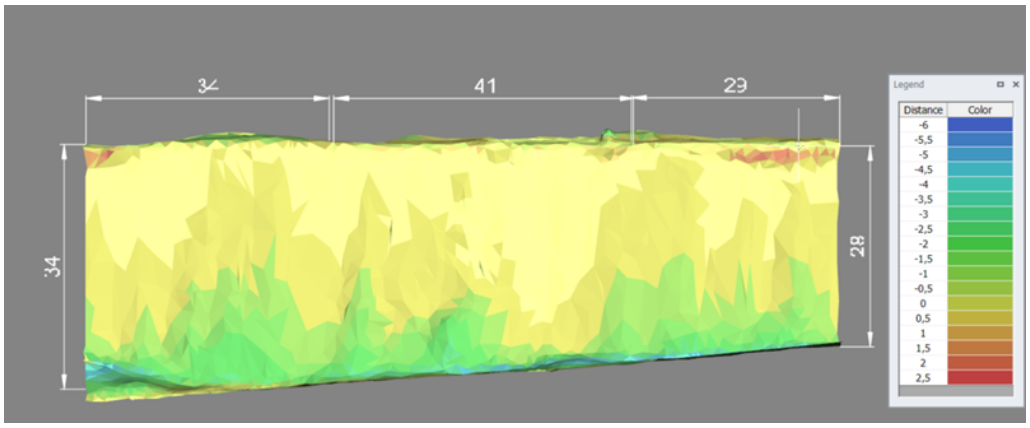

Figure A4: Presplit face from design sector 4 colored based on deviation from planned in meters.

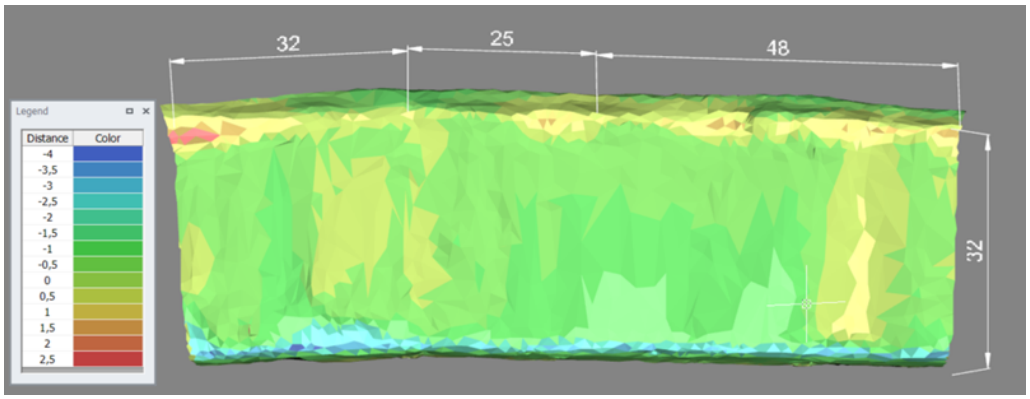

Figure A5: Presplit face from design sector 5 colored based on deviation from planned in meters.

face was analysed in three different parts which are illustrated with the wall length scales shown in the figure. In this design sector presplitting has been very successful overall. There is only minor overbreak at the crest of the wall and minor underbreak at the toe of the wall, which can be seen from the figure. Most of the presplit borehole half cores are visible in the final wall and the deviations from planned seen in the figure are caused by the drilling accuracy. However, this difference between planned and drilled hole locations have not affected the stability of the bench face. This presplit wall can also be considered as an example of a sufficiently successful presplit wall at Kuusilampi open pit.

The analysed presplit walls from design sector 6 can be seen in figures A6a, A6b, A6d and A6c. In this design sector 200 meter long bench face was analysed because the analysed wall height is only 15 meters. The total presplit height in the analysed location is 30 meters but only the height of the first production bench was visible at the time of this thesis. The fact that only half of the bench is analysed may result in a smaller amount of underbreak compared to other analysed bench faces as most of the underbreak at the bench faces is typically located at the toe and at the lower production benches area. However, this is partly caused by scaling because the

underbreak at the toe of the upper bench is typically removed during scaling.

As can be seen from the figures the bench faces are fairly smooth with minor underbreak at the toe of the wall and overbreak at the crest of the wall only. In figure A6a the lower bench level is very uneven, which will cause some overestimation of the underbreak and overbreak.

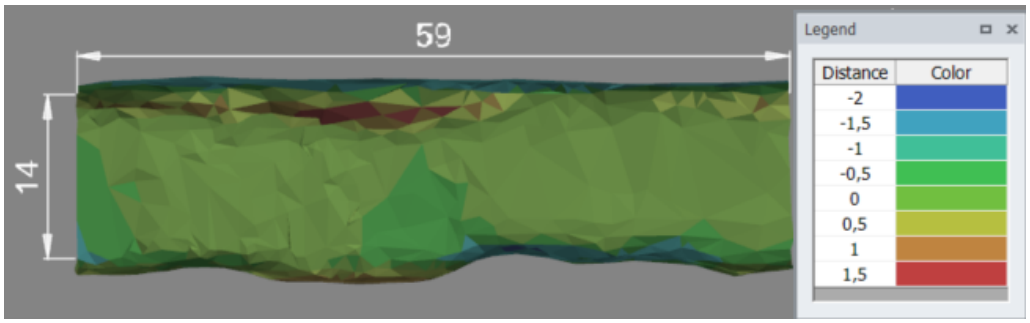

(a)

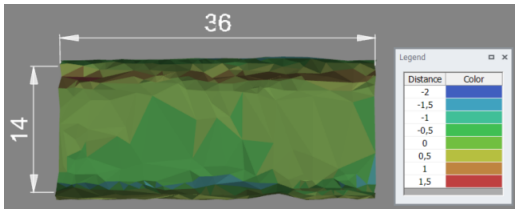

(b)

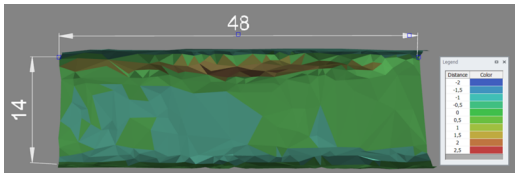

(c)

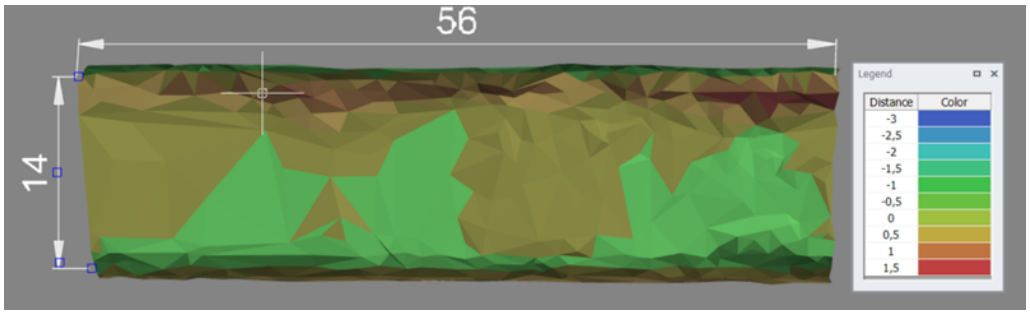

(d)

Figure A6: Presplit faces from design sector 6 colored based on deviation from planned in meters.

The analysed presplit walls from design sector 7 can be seen in figures A7a and A7b. The presplit face seen in figure A7a was analysed in two parts which are illustrated with the wall length scales. This presplit face has some overbreak at the crest of the wall which was caused by a J3 joint. Furthermore, this presplit face has significant underbreak at the toe of the wall where the bench face adheres to J3 jointing. The presplit face seen in figure A7b has practically no overbreak. However, there is a typical amount of underbreak compared to other bench faces. This part of the wall is oriented very differently compared to the wall in figure A7a. The wall is strikes in the same direction as the first part of the third black schist test, which is shown in figure 37 and in figure 18. The more favourable direction of the wall towards the

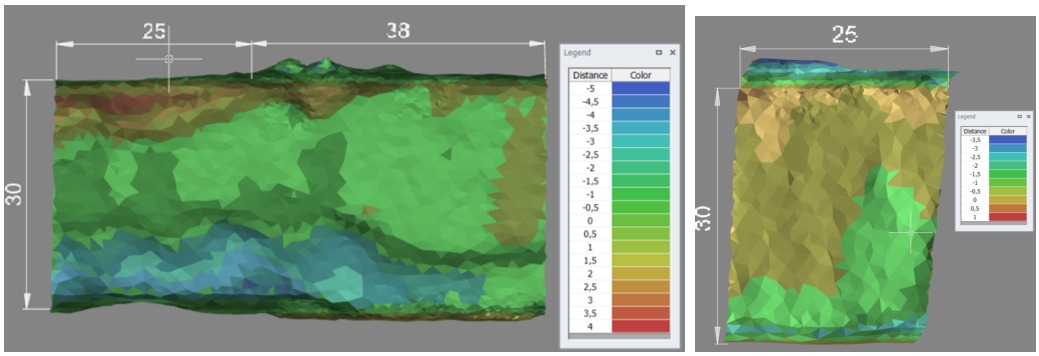

(a) (b)

Figure A7: Presplit faces from design sector 7 colored based on deviation from planned in meters.

discontinuities is the most probable reason for the low amount of overbreak at this bench face.

As can be seen from the figures included in this chapter, the toe positions of the surfaces undulate and do not adhere to the planned surfaces in some areas. This deviation is mostly due to loose material located on the lower level's berm and is not actual underbreak, which results in an overestimation of the underbreak.

B Joint condition parameters

Table B1: Joint condition parameters (SRK, 2020b)

Strength	Planarity and roughness	Joint infill
Strongest	Rough stepped	None
	Smooth stepped	Staining
	Slickensided stepped	Non-softening coarse
	Rough Undulating	Non-softening medium
	Smooth undulating	Non-softening fine
	Slickensided undulating	Soft sheared coarse
	Rough planar	Soft sheared medium
	Smooth planar	Soft sheared fine
	Polished planar	Gouge < amplitude
Weakest		Gouge > amplitude